中国颗粒学会第十一届学术年会

暨海峡两岸颗粒技术研讨会

会议摘要集

第

一

分

会

场

中国·厦门

二〇二〇年十月

目 录

论文编号：01–001

高铁车厢空气质量现状及控制技术

徐峻[1]，赵金龙[2]，于佳轩[3]

[1]中车长春轨道客车股份有限公司，吉林省-长春市-绿园区-长客路 2001 号，130000

[2]中车长春轨道客车股份有限公司，吉林省-长春市-绿园区-长客路 2001 号，130000

[3]中车长春轨道客车股份有限公司，吉林省-长春市-绿园区-长客路 2001 号，130000

*Email: xujun@cccar.com.cn; zhaojinlong@cccar.com.cn; yujiaxuan@cccar.com.cn

摘要正文：

动车组作为公共交通的主要运输载体，承载着数以千万计人员的流动，动车组车厢具有封闭性强、人员密集、流动性大等特点，车厢内的空气质量对旅客的健康情况影响重大。

高铁车厢内空气中主要有粉尘、甲醛、TVOC、细菌及病毒等有毒有害物质，粉尘主要来自于车外空气，车内顶板、座椅、地板布等内装件是甲醛、TVOC等污染物的主要释放源，旅客易携带细菌及病毒，通过气溶胶飞沫及扶手接触等途径传播。高铁车厢内的气流组织形式决定了各种空气颗粒物的传播扩散途径。

当前新冠肺炎疫情常态下，动车组科学防治、精准施策的防疫措施显得尤为重要，目前车辆上已采取加大新风量、调整顶送风模式、增加空气消杀设备等措施抑制病毒传播，已经将病毒传播的风险降到最低。

未来中国高铁车厢内部的空气质量控制体系将继续发展和完善，逐步建立提升车厢内空气品质的技术方法，有效阻断附着细菌、病毒的颗粒物气体流经旅客呼吸区域，开发车载小型空气病毒实时监控装置研制技术，形成满足旅客列车防疫安全性的车厢空气质量控制技术规范。

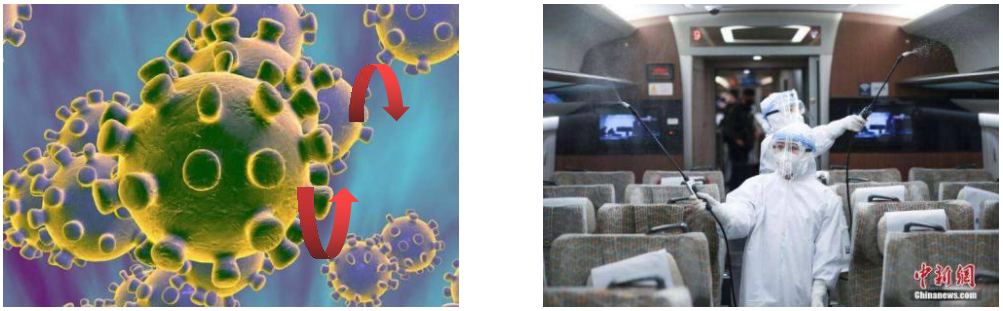

图1 病毒在车厢内传播图示

关键词：空气颗粒物；气流组织；过滤拦截；换气频次；病毒消杀

论文编号：01–002

兼具空气净化及抗菌灭毒功能的纳米催化氧化技术研发

黄宇[1,*]，李荣[1]，王震宇[1]，崔龙[1]，曹军骥[1]

[1] 中国科学院地球环境研究所，中科院气溶胶化学与物理重点实验室，陕西省西安市雁塔区雁翔路 97 号，710075

*Email: huangyu@ieecas.cn

摘要正文：

针对新型冠状病毒（SARS-CoV-2）的传播方式，世界卫生组织和我国国家卫健委在综合评估了新近的一系列研究和证据后，明确了新型冠状病毒存在空气（气溶胶）传播这一重要新途径。最新的研究更是指出，气溶胶化的新型冠状病毒在空气中存活长达3小时之久[1-2]。因此，新型冠状病毒的空气传播途径对空气净化技术提出了更进一步的要求，即在满足颗粒物及气态污染物的去除要求之外，还应实现高效的灭活细菌及病毒性能。

过滤、辐射等物理抗菌灭毒技术能在一定程度降低病毒传播风险，但存在杀灭不彻底或臭氧等二次污染物生成的问题；无机酸碱、重金属等化学杀毒灭菌技术虽然初次效果较好，但存在持久性差、腐蚀性强和对人体毒性较高等问题。此外，上述技术也难以兼顾颗粒物与气态污染物的净化。相比之下，纳米催化氧化技术可通过环境友好型催化剂解离空气中的氧气产生活性氧物种（·OH、$\cdot O_2^-$、H_2O_2等）起到抗菌灭毒与空气净化作用。一方面，纳米催化氧化技术能直接破坏病毒的蛋白质衣壳甚至核苷酸（RNA/DNA）结构阻断其基因表达，以及破坏细胞的细胞壁和细胞膜使其失活，从而达到高效抗菌杀毒目的，具有作用快而强、广谱抗菌灭毒（对细菌、霉菌、病毒和芽孢均有效）等特点；另一方面，纳米催化氧化技术也能在常温下将甲醛、一氧化碳等气态污染物完全降解。进一步地，将纳米催化材料负载到滤材上，可将过滤截留的生物气溶胶灭活。因此，纳米催化氧化技术是目前净化空气和抗菌灭毒的理想手段。

本研究利用液相法，通过调控Cu离子的价态和配位位点，合成出纳米Cu-MOF常温催化材料，在常温下吸附氧气产生活性氧物种，并结合Cu离子的缓释作用，对大肠杆菌可产生100%的杀灭效果（图1）。本研究还应用壳聚糖的成膜延展性结合TiO_2纳米溶胶工艺，可控制备出TiO_2/壳聚糖复合纳米薄膜材料，其对H3N2流感病毒和大肠杆菌的灭活率分别为100.0%和99.6%，并且该薄膜材料具有制备工艺易于量产、使用过程对人体无健康风险的优点。将所研发的纳米催化杀毒灭菌材料与高效滤材相结合，可应用于防护用品（如口罩、防护服等）、空气净化系统（空调、空气净化器等），有望为封闭/半封闭空间空气净化及控制细菌和病毒的气溶胶传播途径提供强有力的技术支撑。

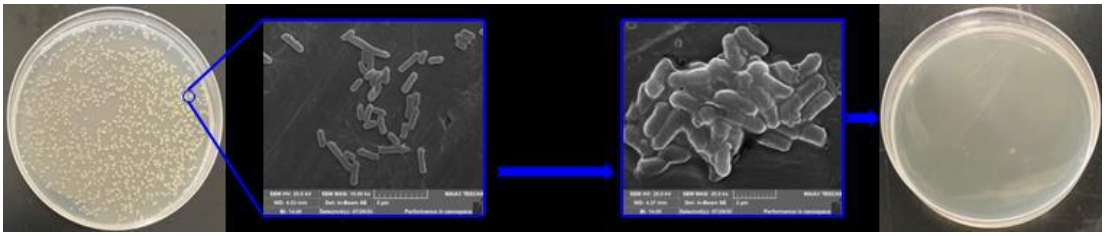

Fig. 1 The antibacterial results of Cu-MOF nano-catalyst at room temperature

关键词：COVID-19；气溶胶传播；空气净化；纳米催化

参考文献

[1] L. Morawska and J. Cao, Airborne transmission of SARS-CoV-2: The world should face the reality. Environment International. 2020, 139: 105730.

[2] N. Doremalen，D. Morris，M. Holbrook，et al，Aerosol and Surface Stability of SARS-CoV-2 as Compared with SARS-CoV-1. The New England Journal of Medicine，2020, 382: 1564-1567.

论文编号：01–003

Enhanced secondary pollution offset reduction of primary emissions during COVID-19 lockdown in China

Xin Huang[1], Aijun Ding[1], Jian Gao[2], Bo Zheng[3], Bo Zheng[3], Qiang Zhang[3]

Email: xinhuang@nju.edu.cn

[1]School of Atmospheric Sciences, Nanjing University, Nanjing 210023, China

[2]Chinese Research Academy of Environmental Sciences, Beijing 100012, China

[3]Department of Earth System Science, Tsinghua University, Beijing 100084, China

Abstract：

To control the spread of the 2019 novel coronavirus (COVID-19), China imposed nationwide restrictions on the movement of its population (lockdown) after the Chinese New Year of 2020, leading to large reductions in economic activities and associated emissions. Despite such large decreases in primary pollution, there were nonetheless several periods of heavy haze pollution in East China, raising questions about the well-established relationship between human activities and air quality. Here, using comprehensive measurements and modeling, we show the haze during the COVID lockdown were driven by enhancements of secondary pollution. In particular, large decreases in NO_x emissions from transportation increased ozone and nighttime NO_3 radical formation, and these increases in atmospheric oxidizing capacity in turn facilitated the formation of secondary particulate matter. Our results, afforded by the tragic natural experiment of the COVID-19 pandemic, indicate that haze mitigation depends upon a coordinated and balanced strategy for controlling multiple pollutants.

论文编号：01–004

新冠疫情对我国西南地区空气质量的影响

陈阳[1,*]，张蜀敏[2]

[1]中国科学院重庆绿色智能技术研究院，重庆，400714

[2]川北医学院，四川南充，637007

*Email: chenyang@cigit.ac.cn

摘要正文：

新型冠状病毒导致的疫情为我国人民的身体健康和生产生活带来了巨大的影响，同时也反应在空气质量和污染物的化学组成上。自2020年1月底疫情爆发以来，多数省份启动了应对重大突发公共卫生事件（RMPHE）的一级响应。根据中华人民共和国《传染病防治法》的规定，一级响应要求禁止社会性聚集，关闭学校、工业、企业和不必要的交通（民航、私家车和公共汽车）。上述措施在显著压缩了社会的生产生活，影响了大气、水、土壤等污染的现状。本研究聚焦疫情及防控对西南地区大气污染的影响，探究极端关停条件下空气质量改善的机制和成本，为今后的污染管控和可持续发展提供科学支持。研究表明，在一级响应期间，西南地区各主要污染物包括$PM_{2.5}$、PM_{10}、SO_2、NO_x 和 黑碳气溶胶与疫情之前相比减少了 30–50%；由于西南地区位于VOCs控制区，氮氧化物的减少导致O_3上升了130%。颗粒物光学性质方面，在370nm 到950 nm波长范围内，气溶胶吸光系数（b_{abs}）降低了约50%， AAE下降约20%，且棕色酸的吸收效应占比为54%，远高于正常情况下的10-20%。黑碳气溶胶源解析表明，一级响应期间，黑碳气溶胶来自于化石燃料的贡献仅为43%，远低于全面复工后的63%。研究同时还讨论了管控措施对$PM_{2.5}$化学组成的影响。本研究对空气质量管理和可持续发展存在一定的启示意义。

关键词：疫情；空气质量；颗粒物化学组分；来源

论文编号：01–005

上海新冠疫情期间隔离措施对$PM_{2.5}$化学组分的影响

陈晖[1]，霍俊涛[2]，伏晴艳[2]，段玉森[2]，肖航[3]，陈建民[1,*]

[1]复旦大学，环境科学与工程系，上海，200438

[2]上海环境监测中心，上海，200235

[3]中科院城市环境研究所，厦门，361021

*Email: jmchen@fudan.edu.cn

摘要正文：

利用高时间分辨率气溶胶飞行质谱（Tof-ACSM）在复旦大学江湾校区进行的观测表明，疫情期间$PM_{2.5}$的降低主要归因于硝酸盐和一次气溶胶的降低。隔离期之前没有减排的情况下，硝酸盐占难熔$PM_{2.5}$的37%。在隔离期间，由于氮氧化物的降低，硝酸盐浓度降低了约60%。铵盐作为主要的平衡阳离子，浓度同时降低了约45%。来自一次排放的氯盐和碳氢有机气溶胶（HOA）的浓度也有所下降。相比之下，硫酸盐和含氧有机气溶胶（OOA）的浓度略有下降，在隔离期间，它们的贡献分别增加到27%和18%，共同引发了两次$PM_{2.5}$超过100微克/立方米的污染事。基于大气氧化剂（$O_x = O_3 + NO_2$）和氮/硫氧化比（NOR/SOR）来表述大气氧化能力，研究发现随着二次气溶胶的贡献增加，较低的NO_x和硝酸盐浓度并不能完全避免上海在疫情期间出现雾霾。

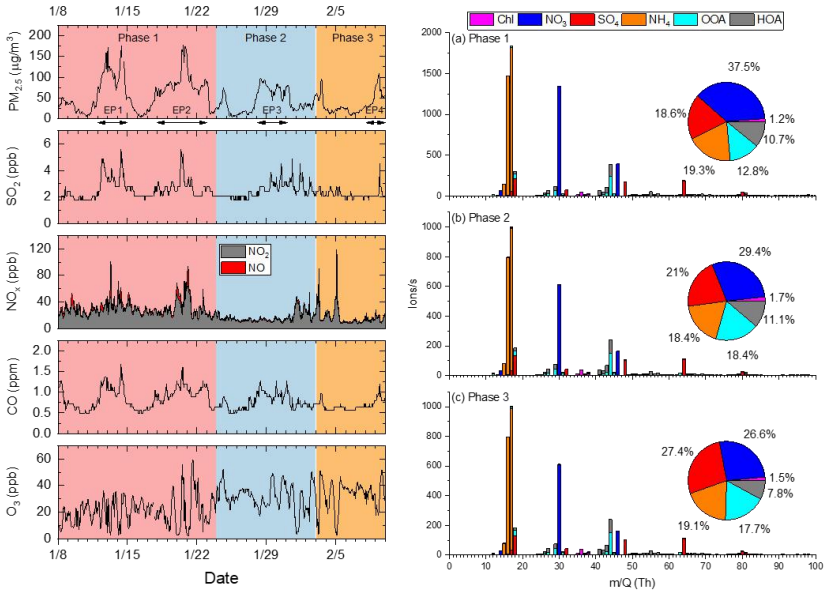

图 1 观测期间主要污染物时间变化趋势与平均谱图

关键词：新冠；$PM_{2.5}$；化学组分；隔离措施

论文编号：01–006

新型冠状病毒气溶胶与物体表面空间分布规律研究

王中一[1]，李京京[1]，程洪亮[1]，付莹莹[1]，李佳明[1]，陆兵[1,*]

[1]军事科学院军事医学研究院生物工程研究所，北京市丰台区东大街20号院，100071

*Email: 13693506666@163.com

摘要正文：

自2019年12月新型冠状病毒肺炎爆发以来，短短三个月已波及全球200余国家，造成超75万人感染，给各国医疗卫生体系造成沉重的负担。其传播范围之广、传播速度之快，引起了国内外对于新冠病毒多种传播方式的广泛关注。本研究团队深入武汉火神山医院病房诊疗一线，开展医护人员诊疗全流程气溶胶和物体表面暴露风险评估研究。该研究有三项重要发现：第一，在收治确诊病人的ICU及普通感染病房内，新型冠状病毒核酸广泛分布与空气和物体表面。第二，ICU内暴露风险高于普通感染病区。第三，即使在新风系统正常运行的 ICU内，病毒气溶胶仍然被检测到，最远传播距离可达4米。

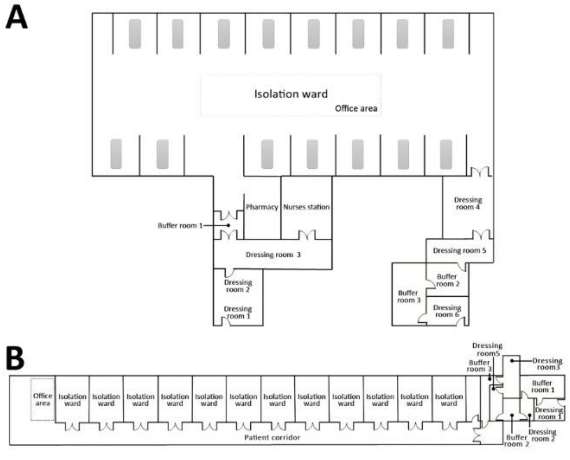

Fig. 1 Layout of the ICU and general ward

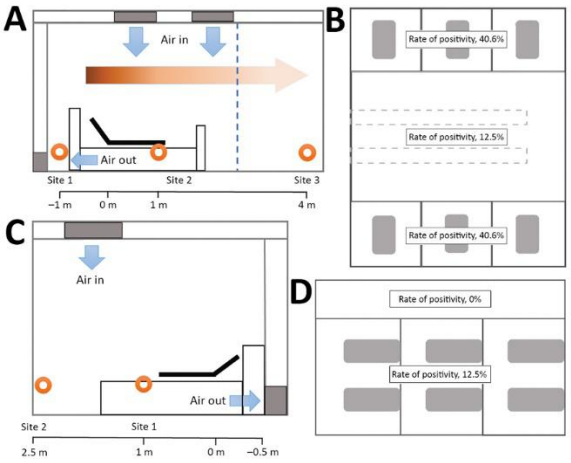

Fig. 2 Spatial distribution of SARS-CoV-2 aerosols

关键词：新型冠状病毒；气溶胶；物体表面；空间分布规律；诊疗全流程

参考文献

[1] World Health Organization. Coronavirus disease 2019 (COVID-19) situation report-71 [cited 2020 Mar 30]. https://www.who.int/emergencies/diseases/novel-coronavirus-2019/situation-reports

[2] Remuzzi A, Remuzzi G. COVID-19 and Italy: what next? Lancet. 2020 March 13 [Epub ahead of print]. https://doi.org/10.1016/S0140–6736(20):30627–9

[3] Peng X, Xu X, Li Y, Cheng L, Zhou X, Ren B. Transmission routes of 2019-nCoV and controls in dental practice. Int J Oral Sci. 2020;12:9. https://doi.org/10.1038/s41368-020-0075-9

[4] Ong SWX, Tan YK, Chia PY, Lee TH, Ng OT, Wong MSY, et al. Air, surface environmental, and personal protective equipment contamination by severe acute respiratory syndrome coronavirus 2 (SARS-CoV-2) from a symptomatic patient. JAMA. 2020 Mar 4 [Epub ahead of print]. https://doi.org/10.1001/jama.2020.3227

[5] Zhang Y, Gong Y, Wang C, Liu W, Wang Z, Xia Z, et al. Rapid deployment of a mobile biosafety level-3 laboratory in Sierra Leone during the 2014 Ebola virus epidemic. PLoS Negl Trop Dis. 2017;11:e0005622. https://doi.org/10.1371/journal.pntd.0005622

[6] Huang R, Xia J, Chen Y, Shan C, Wu C. A family cluster of SARS-CoV-2 infection involving 11 patients in Nanjing, China. Lancet Infect Dis. 2020 Feb 28 [Epub ahead of print]. https://doi.org/10.1016/S1473–3099(20)30147-X.

论文编号：01–006

Aerosol and Surface Distribution of Severe Acute Respiratory Syndrome Coronavirus 2 in Hospital Wards, Wuhan, China, 2020

Zhongyi Wang[1], Jingjing Li[1], Hongliang Cheng [1], Yingying Fu[1], Jiaming Li, Bing Lu[1,*]

[1]Institute of Biotechnology, Academy of Military Medical Sciences, Academy of Military Sciences, No.20 Dongdajie Road, Beijing, China, 100071

*Email: 13693506666@163.com

Abstracts:

As of March 30, 2020, approximately 750,000 cases of coronavirus disease (COVID-19) had been reported globally since December 2019, severely burdening the healthcare system. The extremely fast transmission capability of severe acute respiratory syndrome coronavirus 2 (SARS-CoV-2) has aroused concern about its various transmission routes. To determine distribution of severe acute respiratory syndrome coronavirus 2 in hospital wards in Wuhan, China, we tested air and surface samples. This study led to 3 conclusions. First, SARS-CoV-2 was widely distributed in the air and on object surfaces in both the ICU and GW, implying a potentially high infection risk for medical staff and other close contacts. Second, the environmental contamination was greater in the ICU than in the GW; thus, stricter protective measures should be taken by medical staff working in the ICU. Third, the SARS-CoV-2 aerosol distribution characteristics in the ICU indicate that the transmission distance of SARS-CoV-2 might be 4 m.

论文编号：01–007

新冠疫情防控下我国城市地区气溶胶一次排放和二次形成对空气污染的影响

田杰[1]，王启元[1,*]，张勇[1]，曹军骥[1,*]

[1]中国科学院地球环境研究所，陕西省西安市雁塔区雁翔路97号，710061

*Email: wangqy@ieecas.cn, and cao@loess.llqg.ac.cn.

摘要正文：

为应对2019年新冠病毒（The Coronavirus Disease, COVID-19）的爆发，我国在城市地区启动公共卫生事件一级响应，提供了一次独特的机会去探讨人为源排放对空气质量的影响。本研究在COVID-19防控期前后开展高分辨率的加强集中观测，表征我国代表性城市地区气溶胶一次排放和二次形成的变化。与正常时期相比，COVID-19防控期亚微米气溶胶（PM_1）及其主要化学组分的质量浓度下降了32–51%。作为PM_1最主要的贡献部分，有机气溶胶（OA）进一步利用混合环境受体模型（HERM）分解为四类一次排放OA（POA），包括烃类OA（HOA）、烹饪源OA（COA）、生物质燃烧源OA（BBOA）和燃煤源OA（CCOA），以及两类二次氧化OA（OOA），包括低氧化性OOA（LO-OOA）和高氧化性OOA（MO-OOA）。在COVID-19防控政策下，POAs特别是HOA的质量浓度下降（34–48%）高于OOAs（(21–28%），OOAs对OA的贡献则有明显上升。二次气溶胶与O_x和气溶胶液态含水量的相关性表明光化学氧化和液相反应是二次气溶胶形成的重要途径，其中光化学氧化对硝酸盐和OOAs的形成作用强于硫酸盐；液相反应在不同相对湿度条件下对二次气溶胶生成有更为复杂的影响。由于O_3和NO_3自由基的增加，大气氧化环境在COVID-19防控期有所增强，通过对比COVID-19防控期前后的污染事件，OOAs特别是LO-OOA对防控期内空气污染的形成具有重要作用。

关键词：新冠病毒；亚微米气溶胶；来源解析；二次形成

论文编号：01–008

人为排放影响下中国三个典型城市站点异戊二烯二次有机气溶胶生成的观测研究

张宇晴[1,2]，丁翔[1,*]，王新明[1]

1 中国科学院广州地球化学研究所，广东省广州市天河区科华街511号，510640

2 中国科学院大学，北京市石景山区玉泉路19号，100049

*Email: xiangd@gig.ac.cn

摘要正文：

二次有机气溶胶（SOA）对全球有机气溶胶（OA）的贡献率可超过50%，在中国城市灰霾天气时甚至可占OA的70%以上。SOA对地球辐射平衡、区域空气质量和人体健康都有重要影响，因此SOA是大气OA的重要组成部分。全球范围内自然源挥发性有机化合物（BVOCs）的排放量远高于人为源VOCs（AVOCs），其中异戊二烯的排放量最高，是BVOCs的主要组成部分。近期的研究表明异戊二烯SOA的生成会受到人为污染物（SO_2, NO_x等）排放的影响，但其具体机制与影响的大小尚不清楚。本研究于2013年11月至2014年11月在北京、合肥和昆明三个典型城市站点进行了为期一年的野外观测，共收集76个大气$PM_{2.5}$样品，并利用配备了电喷雾电离源（ESI-）的高效液相色谱-质谱（HPLC-MS/MS）及气相色谱-质谱（GC-MS）对10种异戊二烯SOA（iSOA）标志物的空间分布和季节变化进行了分析。

研究结果表明我国三个典型城市站点异戊二烯SOA含氧标志物（iOTs）的浓度在0.51～103 ng m^{-3}之间，有机硫酸酯（iOSs）浓度在0.43～12.6 ng m^{-3}之间，异戊二烯High-NO_x产物浓度在0.59～23 ng m^{-3}之间，异戊二烯Low-NO_x产物浓度在0.74～137 ng m^{-3}之间。iSOA浓度昆明浓度最高，合肥次之，北京浓度较低，三个城市的高值均出现在夏秋季，冬季浓度最低，表明iSOA时空分布主要受排放影响。三个站点异戊二烯有机硫酸酯与含氧标志物的比值（iOSs/iOTs）在冬季较高，夏季较低，且与异戊二烯与硫酸根及液相水反应速率的比值（$k_{aqSO42-}/k_{aq,H2O}$）呈正相关。这表明环氧中间体与水和硫酸根的反应速率是影响异戊二烯SOA组成的关键因素。三个站点iOSs/iOTs及$k_{aqSO42-}/k_{aq,H2O}$比值均小于1，表明异戊二烯相比于硫酸根更易与液相水发生酸催化开环反应。但北京站点冬季部分样品iOSs/iOTs比值可高于1，表明在某些条件下异戊二烯也可能更易与硫酸根反应生成SOA。异戊二烯SOA的High-NO_x与Low-NO_x产物的比值呈现冬季高夏季低的趋势，其季节变化主要受NO_x浓度以及异戊二烯环氧中间体反应性摄取速率影响。

关键词：异戊二烯；二次有机标志物；人为源排放；液相/非均相反应；反应速率

论文编号：01–009

大气气溶胶中长寿命自由基的理化性质

陈庆彩[1,*]

[1]陕西科技大学，西安市未央大学园区，710021

*Email: chenqingcai@sust.edu.cn

摘要正文：

作为大气气溶胶中的新型污染物-长寿命自由基（EPFRs）近年来备受关注，它的寿命长达数年之久，并可能通过产生活性氧进而对人体产生不利影响。本研究系统介绍了大气气溶胶中长寿命自由基的理化性质，包括：分析方法、类型、寿命、潜在来源和可能形成机制，并对将来的研究课题提出了展望。研究首先开发了针对大气颗粒物中EPFRs的仪器检测方法和数据处理软件，实现了准确检测，研究报道了西安市、临汾市大气颗粒物中EPFRs的浓度水平和季节变化特征、粒径分布特征；其次，对实际大气颗粒物和不同燃烧来源颗粒物样品中EPFRs的寿命进行了长时间分析，并依据寿命和g因子等信息划分了类别，发现EPFRs的寿命可长至数年；第三，针对实际大气颗粒物中EPFRs，进行了化学组分分析并利用因子模型解析了EPFRs的来源，发现燃烧源是大气EPFRs的最主要来源，不过沙尘来源也不可忽视，二次来源潜在来源较小；最后，提出了实际大气颗粒物中EPFRs的形成机制，指出氧化石墨烯结构可能是实际大气颗粒物中EPFRs的最主要形成本质，并对光化学二次形成过程和机制也进行了讨论，发现HULIS是大气气溶胶中光化学生成二次EPFRs最主要成分，然而这些二次EPFRs的寿命非常短暂。

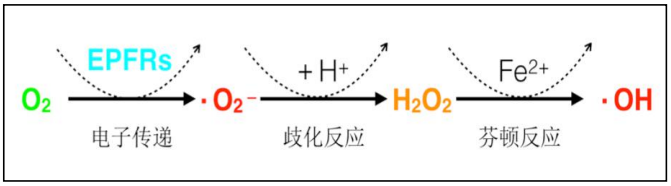

Fig. 1 EPFRs的潜在危害机制.

关键词：气溶胶；长寿命自由基；活性氧

参考文献

[1] Q. Chen, H. Sun, Ma. Wang, et al. Environmentally Persistent Free Radical (EPFR) Formation by Visible-Light Illumination of the Organic Matter in Atmospheric Particles. Environ. Sci. Technol. 2019, 53(17), 10053−10061.

[2] Q. Chen, M. Wang, H. Sun, et al. Enhanced health risks from exposure to environmentally persistent free radicals and the oxidative stress of PM2.5 from Asian dust storms in Erenhot, Zhangbei and Jinan, China. Environment International, 2018, 121(1), 260–268.

[3] Q. Chen, H. Sun, M. Wang, et al. Dominant Fraction of EPFRs from Nonsolvent-Extractable Organic Matter in Fine Particulates over Xi’an, China. Environ. Sci. Technol. 2018, 52(17), 9646-9655.

[4] Q. Chen, H. Sun, J. Wang, et al. Long-life type — The dominant fraction of EPFRs in combustion sources and ambient fine particles in Xi'an. Atmospheric Environment. 2019, 219, 117059.

[5] Q. Chen, H. Sun, Z. Mu, et al. Characteristics of environmentally persistent free radicals in PM2.5: Concentrations, species and sources in Xi'an, Northwestern China. Environmental Pollution. 2019, 247, 18-26.

论文编号：01–010

广州城区大气老化过程中黑碳吸光增强特性研究

吴晟[1,2*]，孙嘉胤[1,2]，吴兑[1,2,3*]，李梅[1,2]，邓涛[3]，杨闻达[1,2]，程鹏[1,2]，梁粤[1,2]，谭健[1,2]，何国文[1,2]，成春雷[1,2]，李磊[1,2]，周振[1,2]

[1]暨南大学质谱仪器与大气环境研究所，广东广州，510632；

[2]广东省大气污染在线源解析系统工程技术研究中心，广东广州，510632；

[3]中国气象局广州热带海洋气象研究所，广东广州，510640

*Email: wucheng.vip@foxmail.com

摘要正文：

本研究运用最小相关系数法(MRS),使用元素碳(EC)作为示踪物,得到一次排放的质量吸光效率(MAE_p),结合黑碳仪(AE33)和有机碳/元素碳分析仪获得实测的质量吸光效率MAE_t,进而通过MAE_t/MAE_p的比值得出吸光增强系数(E_{abs}).采样站点位于广州市城区暨南大学大气超级监测站,采样时间涵盖了干季(2017年11月15日~1月15日)和湿季(2017年7月31日~9月10日).对广州市城区的黑碳气溶胶及其光学特征进行分析,EC在干季的平均浓度(2.81±2.01)μgC/m^{3}高于湿季(1.94±0.93)μgC/m^3,而E_{abs520}在干季的均值(1.29±0.28)低于湿季(1.51±0.50).E_{abs520}在干湿季的日变化差异明显,但有机碳(OC)、EC、OC/EC、波长指数($AAE_{470-660}$)均为干季高于湿季.分析发现气溶胶负载补偿参数k值与E_{abs520}在湿季呈现出较好的相关性,而在干季相关性较差,可能与生物质燃烧的影响有关;此外也探讨了干湿季温度和SOC/OC对E_{abs520}的影响。

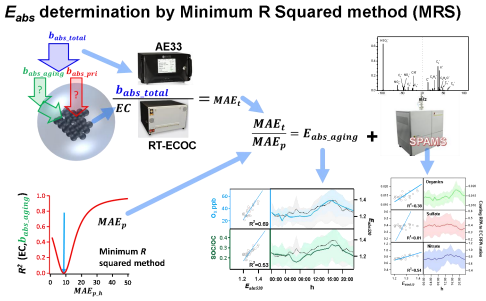

Fig. 1 Light absorption enhancement factor (E_{abs}) determination by minimum R squared (MRS) method.

关键词：黑碳；吸光增强；日变化；季节变化

参考文献

[1] Sun, J. Y., Wu, C.*, Wu, D.*, Cheng, C., Li, M., Li, L., Deng, T., Yu, J. Z., Li, Y. J., Zhou, Q., Liang, Y., Sun, T., Song, L., Cheng, P., Yang, W., Pei, C., Chen, Y., Cen, Y., Nian, H., and Zhou, Z.*: Amplification of black carbon light absorption induced by atmospheric aging: temporal variation at seasonal and diel scales in urban Guangzhou, Atmos. Chem. Phys., 20, 2445-2470, doi: 10.5194/acp-20-2445-2020, 2020.

[2] 孙嘉胤，吴晟*，吴兑*，李梅，邓涛，杨闻达，程鹏，梁粤，谭健，何国文，成春雷，李磊，周振. 广州城区黑碳气溶胶吸光特性研究. [J]. 中国环境科学. 2020, 40(10)

论文编号：01–011

Black carbon emission and wet scavenging from surface to the top of boundary layer over Beijing region

Dantong Liu[1, *], Shuo Din[1]

[1]Department of Atmospheric Sciences, School of Earth Sciences, Zhejiang University, Hangzhou, China

*Email: dantongliu@zju.edu.cn

Abstract：

The heating impacts caused by black carbon (BC) may modify the atmospheric dynamics of planetary boundary layer (PBL), essentially determined by its vertical distribution. In this study we performed simultaneous measurements of detailed BC properties at both surface (50m) and mountain sites (1344m) over Beijing region. The latter represents the top of PBL and was influenced by surface anthropogenic emissions, particularly around midday when PBL was developed, allowing continuous investigations on the evolution of BC during vertical transport in the PBL. Experiments in cold and warm seasons were performed to reflect seasonal difference in emission and meteorology: winter had additional emission of residential heating and dry air; summer had moist air with more precipitation. The net ratio of BC/CO relative to background (ΔBC/ΔCO) is used to indicate the emission signature and scavenging of BC. At surface, both seasons peaked at similar ΔBC/ΔCO, however showed contrast shifts between both sites. In winter, mountain showed slightly higher ΔBC/ΔCO than surface due to receiving sources from wider area, whereas in summer, a rBC mass scavenging efficiency of 35%-62% was derived from the significantly lowered ΔBC/ΔCO on mountain. This scavenging process could incorporate BC into the summer moist air or low-level clouds on a daily basis, exerting potential indirect effects. The resultant BC after scavenging exhibited smaller core size and increased coatings, leading to a higher absorption efficiency by 45%. These factors should improve the representation of boundary layer processing of BC in evaluating its direct and indirect radiative impacts over the anthropogenically influenced region.

论文编号：01–012

东北典型城市地区大气颗粒物浓度垂直分布特征及边界层结构的影响研究

李晓岚[1,*]，马雁军[1,*]，王扬锋[1]，魏伟[2]，张云海[1]，刘宁微[1]，洪也[1]

[1]中国气象局沈阳大气环境研究所，辽宁省沈阳市和平区长白南路388号，110166

[2]中国气象科学院灾害天气重点实验室，北京，100081

*Email: leexl.ouc@163.com

摘要正文：

东北地区秋冬季节大气污染频繁发生，然而该地区边界层结构对气溶胶垂直分布的影响还尚未弄清。本研究利用2018年11月边界层加密探空资料，研究了东北典型城市沈阳地区大气颗粒物(PM_1, $PM_{2.5}$, and PM_{10})质量浓度的垂直分布特征，并揭示了大气边界层结构的影响作用。结果表明：沈阳地区秋季大气气溶胶浓度基本随高度的增加而减小；夜间气溶胶多集中在400 m以下高度，白天受对流湍流的影响其分布范围更高（~800 m）（图1）。整体而言，随着大气稳定度的增加，近地面颗粒物浓度增加且垂直梯度增大（图2）。针对四次污染过程（11月1-4日、7-10日、14-15日、25-27日）发现，由于夜间大气稳定度较强，垂直混合作用较弱，导致气溶胶主要集中在浅薄的稳定层内（< 300 m）和残余层底部（250–500 m）。次日日出后，气溶胶在边界层内逐渐混合均匀（边界层高度从200 m增加至1 km以上），进而影响近地面的空气质量（图3）。此外，夜间低空急流和冷锋系统引起的大风和较强的风剪切也会影响污染的生成和演变（Li et al., 2019b）。这些过程决定了气溶胶的输送/扩散，同时影响大气稳定度和边界层高度。本文研究结果对加深理解东北城市地区气溶胶的垂直分布特征具有帮助，同时有助于加深认识边界层结构在气溶胶污染中发挥的重要作用。

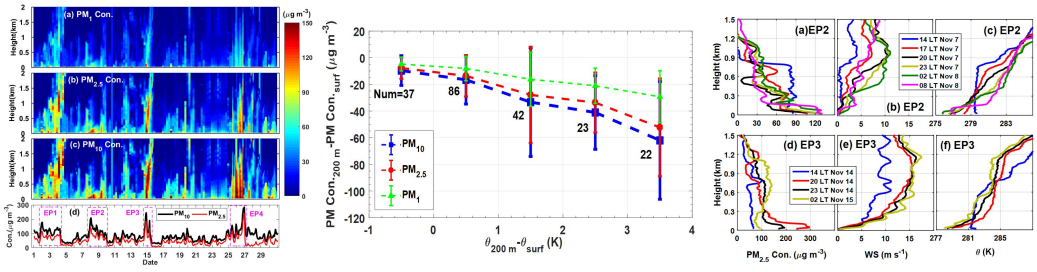

Fig. 1. Height-time cross-sections of mass concentrations of (a) PM_1, (b) $PM_{2.5}$, and (c) PM_{10}, and (d) variation of surface $PM_{2.5}$ and PM_{10} concentrations in Shenyang during November 2018. Rectangles represent air pollution episodes.

Fig. 2. Relationship between vertical gradient of PM concentrations and potential temperature during November of 2018 in Shenyang. The bar represents the standard deviation of PM concentration differences of all samples in each bin.

Fig. 3. Vertical profiles of (a, d) $PM_{2.5}$ concentration, (b, e) wind speed, and (c, f) potential temperature in Shenyang during EP2 on November 7–8 and during EP3 on November 14–15, 2018

关键词：垂直分布；大气颗粒物；大气边界层结构；大气污染；东北地区

参考文献

[1] Li, X., Ma, Y., Wang, Y., Wei, W., Zhang, Y., Liu, N. and Hong, Y.. Vertical distribution of particulate matter and its relationship with planetary boundary layer structure in Shenyang, Northeast China. 2019aAerosol and Air Quality Research, 19(11), 2464–2476.

[2] Li X L, Hu X M, Ma Y J et al., 2019. Impact of planetary boundary layer structure on the formation and evolution of air-pollution episodes in Shenyang, Northeast China. Atmospheric Environment, 214: 116850. doi: 10.1016/j.atmosenv.2019.116850.

[3] Deng, X., Li, F., Li, Y., Li, J., Huang, H. and Liu, X., 2015. Vertical distribution characteristics of PM in the surface layer of Guangzhou. Particuology, 20, 3–9.

论文编号：01–012

Vertical distribution of particulate matter and its relationship with planetary boundary layer structure in Shenyang, Northeast China

Xiaolan Li[1*], Yanjun Ma[1*], Yangfeng Wang[1], Wei Wei[2], Yunhai Zhang[1], Ningwei Liu[1], Ye Hong[1]

[1]Institute of Atmospheric Environment, China Meteorological Administration, Shenyang, Liaoning 110166, P. R. China

[2]State Key Laboratory of Severe Weather, Chinese Academy of Meteorological Sciences, Beijing 100081, P. R. China

论文编号：01–013

基于山帽云观测研究黑碳气溶胶的云中过程及清除效率

张国华[1,*]，林钦浩[2]，阳宇翔[1]，傅玉珍[1]，毕新慧[1]，王新明[1]

[1]中国科学院广州地球化学研究所，广州市天河区科华街 511 号，510640

[2]广东工业大学，广州市番禺区大学城外环西路 100 号，510006

*Email: zhanggh@gig.ac.cn

摘要正文：

黑碳(黑碳)气溶胶不仅具有很强的吸光能力和成云潜力，对人类健康也有危害。湿沉降被认为是黑碳的主要清除方式，影响黑碳的寿命及其环境、气候效应。然而，在目前的研究中，黑碳的湿清除过程中存在争议。但针对含黑碳颗粒成云活化及其影响因素的外场观测研究较少，特别是对云内清除的研究。黑碳的质量清除效率在世界范围内呈现较大的差异，其影响因素包括物理和化学性质(如大小和化学成分)以及气象条件(云水含量、温度等)。

本研究选择南岭天井山国家背景站，针对于山帽云过程中气溶胶的理化特征开展在线观测。观测平台能够在线分析云雾过程中活性云雾滴和间隙颗粒的粒径、化学组成、数浓度和黑碳质量浓度的测量。研究分析了三个云事件共 2 万以上的云滴残余物颗粒：发现老化的黑碳颗粒在云滴残余物中数量占比最大，约 50%。该结果充分证实即使在没有直接人为活动影响的高山背景地区，黑碳颗粒仍是活性云滴的重要凝结核。对黑碳的清除效率的研究发现黑碳老化后与其他颗粒具有相似的云清除率，在 15-54%之间。然而，有机物的包裹显著降低了黑碳的云清除率，这种混合特征占所有黑碳颗粒的 20%左右。此外，还针对云雾形成、发展、消散等过程中黑碳的清除率进行了初步的探讨。结果指出，不同云雾阶段含水量的差异是黑碳清除率差异的重要原因。研究结果有助于认识黑碳和云滴之间的相互作用以及人为排放气溶胶对云形成的影响。

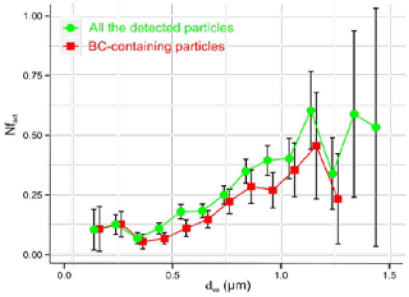

Fig. 1 size-resolved activated fraction of BC-containing and all the detected particles

关键词：山帽云；黑碳；云中过程；清除效率；单颗粒

参考文献

[1] Schroder, J. C., Hanna, S. J., Modini, R. L., Corrigan, A. L., Kreidenwies, S. M., Macdonald, A. M., Noone, K. J., Russell, L. M., Leaitch, W. R., and Bertram, A. K.: Size-resolved observations of refractory black carbon particles in cloud droplets at a marine boundary layer site, Atmos. Chem. Phys., 15, 1367–1383, 2015.

[2] Cozic, J., Verheggen, B., Mertes, S., Connolly, P., Bower, K., Petzold, A., Baltensperger, U., and Weingartner, E.: Scavenging of black carbon in mixed phase clouds at the high alpine site Jungfraujoch, Atmos. Chem. Phys., 7, 1797– 1807, 2007.

论文编号：01–014

交通排放与固态燃料燃烧对城市空气质量的影响

林春水 [1,*]

[1] 中国科学院地球环境研究所，陕西省西安市雁塔区雁翔路 97 号，710061

*Email: linchunshui@ieecas.cn

摘要正文：

全球快速的城市化和人口增长对城市空气质量产生负面影响，并增加了城市居民的暴露风险。细致了解主要排放源（例如交通和固体燃料燃烧）对城市空气质量的影响，可以更好地为公众和决策者提供信息。在这项研究中，我们在西欧城市（都柏林）和中国城市（石家庄）的不同环境（街道与居民区）中部署了最新的气溶胶质谱仪（ACSM）用于在线气溶胶组分观测和来源解析。通过在不同环境下对亚微米气溶胶成分和有机因子的详细比较，我们发现在都柏林地区车辆排放物与街道峡谷效应的作用下，其导致路边的黑碳（BC）和一次有机气溶胶（POA）浓度升高。然而，其对居住区的空气质量影响较小。在供暖季节，固体燃料燃烧产生的排放在都柏林和石家庄均起着重要作用。对比不同城市的有机来源，我们发现固态燃料的一次排放在都柏林地区可以影响所研究的街道和居民区，而其二次污染在京津冀地区有重要影响。

在都柏林地区，为了更好地了解PM1的化学成分和浓度的变化，我们选择了两个时段，其中9月10日至17日为非供暖的一周，10月27日至11月4日为供暖的一周[1]。在非供暖期间，BC表现出最大的路边增量，增量比率为15（Fig. 1）。在加热期间，BC增量比略低（10），这主要是由于固体燃料燃烧的额外排放同时影响了两个站点。BC的路边增加主要归因于车辆排放，这被NOx的气体污染物证实，其增加比为7-11。我们的测量的交通排放具有代表性，不会被单一高排放的车辆影响，因此都柏林路边排放增加量很大，会增加路边居民和行人的暴露风险。在石家庄地区的结果表明，二次污染源在平时（NDs，58％或105.7 μg m^{-3}）和农历新年期间（CNY，79％或72.6 μg m^{-3}）中占NR-PM1的一半以上。在总的二次气溶胶的有机成分中，氧化有机气溶胶（OOA）的38-48％（8.0-14.4μgm-3）归因于富含硝酸盐的OOA（即OOA-NO3）因子，表明部分的OOA是新形成的和/或具有与硝酸盐相似的挥发性。我们的研究结果对控制一次排放具有重要意义，而在区域范围内需要采取联合措施以减少石家庄的二次气溶胶。具体结果和结论请参考 Lin et al., ACP, 2020 和Lin et al., ACS Earth Space Chem., 2020.

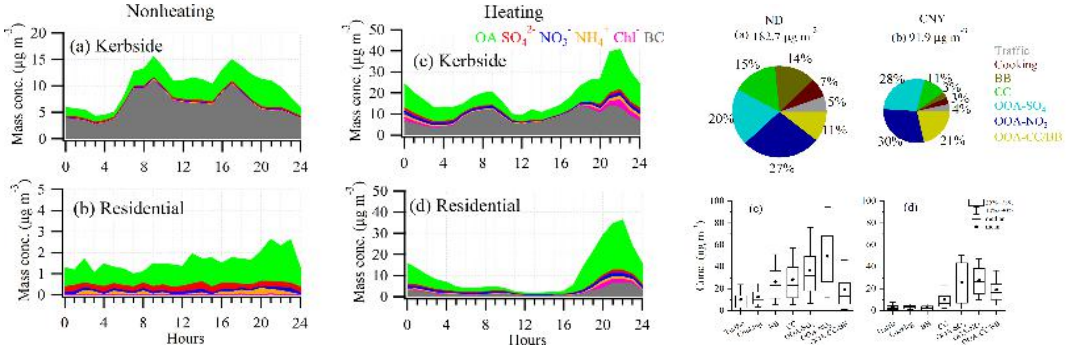

Dublin, Ireland　　Shijiazhuang, China

Fig. 1 Diurnal pattern of the submicron aerosols components in Dublin, Ireland (left panel)[1]; and relative contribution of different organic factors in Shijiazhuang, China (right panel)[2].

关键词：交通排放；生物质燃烧；化石燃料；源解析；NR-PM1

参考文献

[1] C. Lin; D. Ceburnis; W. Xu; E. Heffernan; S. Hellebust; J. Gallagher; R. J. Huang; C. O'Dowd; J. Ovadnevaite, The impact of traffic

on air quality in Ireland: insights from the simultaneous kerbside and suburban monitoring of submicron aerosols. Atmos. Chem. Phys. 2020, 20, (17), 10513-10529.
[2] C. Lin; R.-J. Huang; W. Xu; J. Duan; Y. Zheng; Q. Chen; W. Hu; Y. Li; H. Ni; Y. Wu; R. Zhang; J. Cao; C. O'Dowd, Comprehensive Source Apportionment of Submicron Aerosol in Shijiazhuang, China: Secondary Aerosol Formation and Holiday Effects. ACS Earth and Space Chemistry 2020, 4, (6), 947-957.

论文编号：01–014

Impact of traffic and solid fuel burning on urban air quality

Chunshui Lin[1,*]

[1]Institute of Earth Environment, Chinese Academy of Sciences, Xi'an, China, 710061

*Email: linchunshui@ieecas.cn

Rapid urbanization and population growth across the world has a negative impact on urban air quality and increases the exposure risks for urban dwellers. Understanding the impacts of the street-level air pollution (e.g., traffic) and solid fuel (e.g., biomass and coal) burning on urban air quality can better inform the public as well as policy makers. In this study, we deployed the state-of-the-art aerosol mass spectra monitor (ACSM) in different environments (street-side vs. residential area) within a moderately sized western European city (Dublin) and Chinese city (ShijiaZhuang). Through the detailed comparison of the submicron aerosol composition and organic factors in different environments, we found the vehicular emissions coupled with street-canyon effects led to the elevated concentration of black carbon (BC) and primary organic aerosol (POA) at the street-side in Dublin but with a minor impact on the air quality in the residential area. During the heating season, the emissions from solid fuel burning played an important role in both Dublin and Shijiazhuang. However, primary emissions are more important in Dublin while secondary emissions are more important in Shijiazhuang.

Key Words: Vehicular emission; Solid fuel burning; Urban air quality

论文编号：01–015

沈阳地区大气气溶胶消光特性的观测研究

刘宁微[1]，马雁军[1]，王扬锋[1]

[1]中国气象局沈阳大气环境研究所

摘要正文：

利用沈阳地区大气总消光系数、气体分子吸收系数、气溶胶吸收和散射系数以及大气可吸入颗粒物数浓度的小时数据，对沈阳地区的大气消光特别是气溶胶消光性质进行了高时间分辨率的研究。结果表明: 总消光系数和气溶胶散射系数在一天内呈单周期峰谷型分布，05—06时达到峰值，15 时达到谷值。大气总消光系数在雪天最大、霾天次之、晴天最小。气溶胶消光系数与粒子数浓度的相关性随着粒径的减小而增大。

关键词：气溶胶; 消光系数; 散射系数; 粒子数浓度

论文编号：01–016

Description of aggregated aerosol dynamics using an inverse Gaussian distributed method of moments

Jindong Shen[1], Mingzhou Yu[1]

[1] China Jiliang University, Hangzhou, China

Abstracts:

For nearly 60 years, lognormal distribution has been the most widely used function in the field of atmospheric science for characterizing atmospheric aerosol size distribution. In this talk, we verify whether the three-parameter inverse Gaussian distribution (IGD) is a more suitable function than the lognormal distribution for characterizing aerosol size distribution. An attractive feature of IGD is that with it a new method of moments (MOM) can be established for resolving atmospheric aerosol dynamics—inverse Gaussian distributed MOM (IGDMOM). The advantage of IGDMOM is that all of its moments can be analytically calculated using a closure moment function inherited from IGD. The precision and efficiency of IGDMOM are verified by comparing it with other recognizable methods in test cases of four representative atmospheric aerosol dynamics. Several key statistical quantities determining aerosol size distributions, including k-th moments ($k = 0, \frac{1}{3}, \frac{2}{3}, \text{and } 2$), geometric standard deviation, skewness, and kurtosis, are evaluated. IGDMOM has higher precision than the lognormal MOM with nearly identical efficiency. In addition, the inverse Gaussian distributed method of moments (IGDMOM) (J. Atmospheric Sci. 77 (9): 3011, 2020) is developed to analytically solve the kinetic collection equation (KCE) for the first time. Using IGDMOM, we obtained both new analytical and asymptotic solutions to the KCE. This is shown for both the free molecular and continuum regime collision frequency functions. The new analytical solutions to the KCE is found to be very suitable for the demonstration of *self-preserving size distribution theory* (SPSD).

References

[1] Shen, J., M. Yu, T. L. Chan, C. Tu, and Y. Liu, 2020a: Efficient method of moments for simulating atmospheric aerosol growth: model description, verification, and application. J. Geophys. Res. Atmos., 125, 1–22, https://doi.org/10.1029/2019jd032172.

[2] Shen, J., M. Yu, and J. Lin, 2020b: Description of Atmospheric Aerosol Dynamics Using an Inverse Gaussian Distributed Method of Moments. J. Atmos. Sci., https://doi.org/10.1175/JAS-D-20-0077.1.

[3] Yu, M., J. Lin, J. Cao, and M. Seipenbusch, 2015: An analytical solution for the population balance equation using a moment method. Particuology, 18, 194–200, https://doi.org/10.1016/j.partic.2014.06.006.

论文编号：01–017

冷冻循环法控制细颗粒及气溶胶室内空气污染

潘纲 [1,2,*]

[1]Integrated Water-Energy-Food （iWEF）Facility, School of Animal, Rural and Environmental Sciences，Nottingham Trent University，Brackenhurst Campus, Southwell NG25 0QF, UK

[2] 南京翔莱生态环境科技研究院（Ltd），南京市经济技术开发区恒泰路汇智科技园 A2 栋 5 层

*Email: gang.pan@ntu.ac.uk

摘要正文：

气溶胶(aerosol)是新冠病毒的可能播途径之一。如何对现有室内空气循环系统进行快速升级改造使之具备室内空气净化和杀毒杀菌的能力，成为保障公众健康、阻止病毒传播的紧迫任务。最近，我们提出一种控制室内污染物包括细颗粒和气溶胶的方法（Science of The Total Environment，2019, 651,1451）。其原理是让污染空气连续通过一个可控制湿度和温度小冷冻腔，携带病毒的细微颗粒在冷冻腔内凝结成大颗粒从空气中分离，去除细颗粒的清洁空气从冷冻腔出口经过回温调湿后进入室内空间，以此循环。理论上，任何均相或非均相污染物都可以在足够低温的冷冻腔中凝结去除，从而使以电能换健康成为可能。与现有的过滤技术相比，该技术可连续去除纳米级可穿透滤网的细颗粒，而且可以去除其他污染物比如氮氧化物、硫化物、和可挥发性有机物。该方法无需采用或更换任何滤料、滤网、吸附剂和催化剂，且不产生有害次生污染物，仅靠电能即可持续净化室内空气。对于气溶胶液滴或较高湿度下的悬浮固体颗粒及其附着的病毒病菌，则可能在接近冰点的冷冻仓中浓缩去除，基于冷冻空气凝结换热，可达到高效节能地使冷冻净化后的空气加湿加温，进而将无菌空气调节到适合人体舒适要求的室温输送状态。

论文编号：01–018

An EOS-Based Multiphase Lattice Boltzmann Model for Pulmonary Airway Reopening

Bing He, Chunyan Qin, Wenbo Chen, Binghai Wen*

Guangxi Key Lab of Multi-Source Information Mining & Security, Guangxi Normal University, Guilin, China, 541004

Department of Computer Science and Information Engineering, Guangxi Normal University, Guilin, China, 541004

*Email: oceanwen@gxnu.edu.cn

Abstract：

Equation of state (EOS) plays a key role in the thermodynamic process of liquid-gas transition. Theoretically, it connects the thermodynamic free energy to a specific substance; practically, it controls the liquid-gas equilibrium to satisfy the Maxwell equal-area construction. Here, we propose an EOS-based multiphase lattice Boltzmann model, in which the nonideal force is directly evaluated by EOSs. Since its derivation is within thermodynamics, the model is thermodynamic consistent and Galilean invariant, and the numerical simulations verify the theoretical analyses. Furthermore, the multiphase model is used to model the pulmonary airway reopening and study aerosol droplet production during exhalation. The result show that when the thickness of the liquid plug keeps constant, aerosol droplet size exhaled in pulmonary airway increase with the increase of pulmonary airway pressure. When pulmonary airway pressure keeps constant, aerosol droplet size exhaled from the pulmonary airway increase with the thickness of the liquid plug increase. The present multiphase model can be extended to study the generation and transmission of bioaerosols which can carry the bioparticles of influenza or coronavirus.

Key words: equation of state; bioaerosol; pulmonary airway reopening; lattice Boltzmann method; multiphase flow

论文编号：01–019

Cytotoxicity and potential pathway to vascular smooth muscle cells induced by PM2.5 emitted from raw coal chunks and clean coal combustion

Jian Sun[1]，Zhenxing Shen[1,*]，Junji Cao[2]

[1]Department of Environmental Science and Engineering, Xi'an Jiaotong University, Xi'an 710049, China

[2]Key Lab of Aerosol Chemistry & Physics, Institute of Earth Environment, Chinese Academy of Sciences, Xi'an, 710049, China

*Email: zxshen@xjtu.edu.cn

Abstract：

Coal combustion emits large amount of $PM_{2.5}$ (particulate matters with aerodynamic diameters less than 2.5 μm) and causes adverse damages to cardiovascular system. In this study, emissions from anthracite and bitumite were examined. Red mud (RM) acts as an additive and was mixed in coal briquetting with content of 0% to 10% as a single variable to demonstrate the reductions of the $PM_{2.5}$ emissions. Burnt in a regulated combustion chamber, the 10% RM-containing bitumite and anthracite briquettes showed 52.3% and 18.6% reductions of the $PM_{2.5}$ compared with their chunk coals, respectively. Lower cytotoxicity (in terms of oxidative stresses and inflammation factors) was observed on the $PM_{2.5}$ emitted from the RM containing briquettes than non-RM briquettes, especially for the bitumite groups. Besides, the results of Western blotting illustrated that the inhibitions of NF-κB and MAPK were the potential pathways for the reductions of cytokine levels by the RM addition. The regression analyses further demonstrated that the reductions were attributed to the lower emissions of transition metals (i.e., Mn) and PAHs (i.e., acenaphthene). This pilot study provides solid evidences on the cytotoxicity to cardiovascular system induced by coal combustion $PM_{2.5}$, and potential solution for reducing emission of the toxic pollutants from human health perspectives.

Key words: clean coal briquette, red mud, emission reduction, cardiovascular disease, signaling pathway

论文编号：01–020

大气中臭氧关键前体物的光/常温催化控制技术

张宇飞[1,*]，黄宇[2]，曹军骥[2]

[1]西安建筑科技大学，陕西省西安市碑林区雁塔路中段 13 号，710055

[2]中国科学院地球环境研究所气溶胶化学与物理重点实验室，陕西省西安市雁塔区雁翔路 97 号，710061

*Email: zhangyufei@xauat.edu.cn

摘要正文：

“十三五”以来，我国臭氧（O_3）污染浓度呈现逐年加重的趋势。O_3的非线性形成机制导致了其关键前体物挥发性有机化合物（VOCs）和氮氧化合物（NO_x）的控制难度极大。本论文通过构筑同质异相/异质结、贵金属负载、空位/碳量子点诱导的强关联界面，调控与强化热电子和载流子迁移特性，多电子活化表/界面甲醛（HCHO，典型VOCs）和NO_x吸附位点，诱导C-H键解离促成高反应活性基团，降低反应活化能垒，有效地调控反应氧物种以及产物等，实现了光/常温催化高效去除环境低浓度HCHO和NO_x，并建立了强关联表/界面非均相的光/常温催化反应机制。此外，旨在探索光/常温催化材料合成与环境大气污染治理融合发展的新途径，本论文开展了建筑物外立面光催化玻璃幕墙的应用基础研究工作，为局域大气污染控制提供了一个新的策略和科学的支撑。

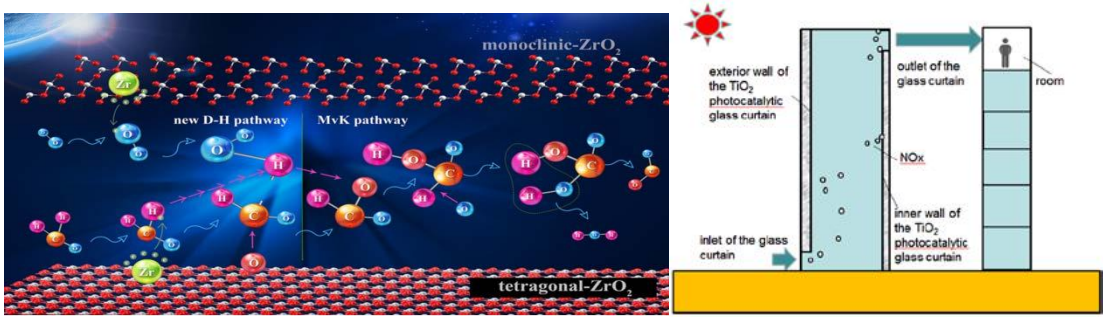

Fig. 1 Schematic illustration of proposed mechanism for the enhanced catalytic reaction of HCHO over the nano-zirconia phase-junction catalyst interface and the full-scale glass curtain wall combined with TiO_2.

关键词：臭氧前体物；光/常温催化；强关联界面；C-H键解离；光催化玻璃幕墙

参考文献

[1] Y. F. Zhang, Y. Huang, S. C. Lee, J. -J. Cao, The mechanism of room temperature catalytic C–H dissociation and oxygenation of formaldehyde over nano-zirconia phase-junction. Chem. Eng. J. 2020, 380: 122498.

[2] Z. Y. Wang, Y. Huang, X. J. Shi, Y. F. Zhang, J. -J. Cao, W. Ho, S. C. Lee, The roles of N-vacancies over porous g-C3N4 microtubes during photocatalytic NOx removal. ACS Appl. Mater. & Inter. 2019, 11: 10651-10662.

[3] Y. F. Lu, Y. Huang, Y. F. Zhang, T. Huang, H. Li, J. -J. Cao, W. Ho, Effects of H2O2 generation over visible light–responsive Bi/Bi2O2-xCO3 nanosheets on their photocatalytic NOx removal performance. Chem. Eng. J. 2019, 363: 374-382.

[4] H. Y. Shen, F. L. Du, Y. H. Liu, Y. Huang, Y. F. Zhang, Z. Y. Wang, Q. Wu, W. B. He, CFD investigation of the statistical characteristics of NOx photo-catalytic degradation in a glass curtain wall in hazy winter weather. Sustain. Cities Soc. 2019, 50: 101668.

[5] Y. Lu, Y. Huang, Y. F. Zhang, J. –J. Cao, H. Li, C. Bian, S. C. Lee, Oxygen vacancy engineering of Bi2O3/Bi2O2CO3, heterojunctions: implications of the interfacial charge transfer, NO adsorption and removal. Appl. Catal. B: Environ. 2018, 231: 357-367.

[6] Y. Huang, Y. Gao, Q. Zhang, Y. F. Zhang, J. -J. Cao, W. Ho, S. C. Lee, Biocompatible FeOOH-carbon quantum dots nanocomposites for gaseous NOx removal under visible light: improved charge separation and high selectivity. J. Hazard. Mater. 2018, 354: 54-62.

论文编号：01–021

层状钙钛矿$Bi_4Ti_3O_{12}$铁电纳米片高效光催化去除NO_x

张倩[1]，黄宇[1,*]

[1] 中国科学院地球环境研究所，气溶胶化学与物理重点实验室，中国西安雁翔路 97 号，710061

*Email: zhangqian@ieecas.cn

摘要正文：

钙钛矿无机纳米材料具有低成本、高稳定性以及优异的光催化活性，在太阳能产氢、CO_2还原和污染物降解方面研究较多。前期我们通过水热法制备了钙钛矿$SrTiO_3$纳米立方体材料，并采用氧空位构建、等离子体敏化等策略拓宽光谱吸收范围，在NO_x光催化氧化反应中展现出一定的催化活性，但是依旧面临载流子分离困难、产物选择性低等问题。这里，我们采用微波法合成了层状钙钛矿$Bi_4Ti_3O_{12}$铁电纳米片。相比较水热法，微波反应能够大大缩短材料制备时间（<2 h），能量利用率高，产物尺寸分布均匀。合成的$Bi_4Ti_3O_{12}$纳米片具有铁电极化性质，其层状结构之间存在的内建电场有利于光生电荷（e^-和h^+）分离，能够促进表面反应的发生。光催化NO_x实验结果表明，$Bi_4Ti_3O_{12}$纳米片的单位面积反应活性（比活性）显著高于锐钛矿TiO_2；光沉积金属Pd颗粒能够进一步提高NO去除效率（接近60%），且NO_2生成几乎受到抑制。这可能归因于增强的光生电荷分离以及Pd颗粒与铁电载体之间的协同催化作用。

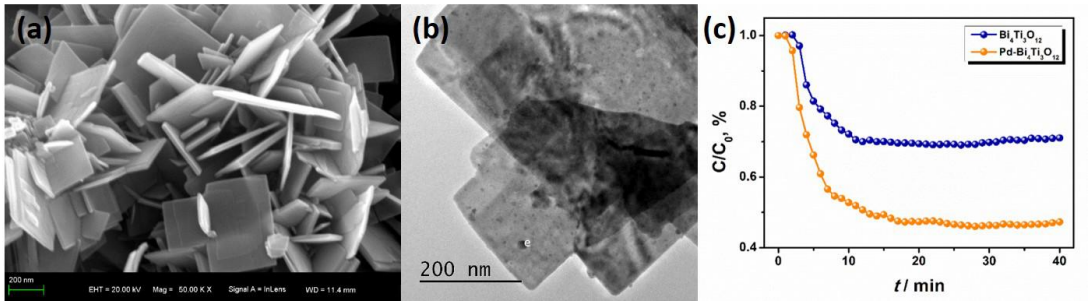

Fig. 1 (a) SEM image of $Bi_4Ti_3O_{12}$; (b) TEM image of $Bi_4Ti_3O_{12}$; and (c) photocatalytic performance of various samples with testing conditions as follow: initial NO concentration of 400 ppb; flow rate 1 L/min; sample amount 0.1 g；R.H. 50%; light source: 500 W Xe lamp ($\lambda > 420$ nm)

关键词：层状钙钛矿；铁电极化；NO光催化

参考文献

[1] Y. Liu, S. Ye, H.C. Xie, J. Zhu, Q. Shi, N. Ta, R.T. Chen, Y.Y. Gao, H. Y. An, W. Nie, H.W. Jing, F.T. Fan, and Can Li. Internal-Field-Enhanced Charge Separation in a Single Domain Ferroelectric PbTiO3 Photocatalyst. Adv. Mater. 2020, 32: 1906513

[2] N. Dahal, S. Garcı´a, J.P. Zhou, and S. M. Humphrey. Beneficial Effects of Microwave-Assisted Heating versus Conventional Heating in Noble Metal Nanoparticle Synthesis. ACS Nano, 2012, 6(11): 9433

[3] S.C. Tu, H.W. Huang, T.R. Zhang, Y.H. Zhang. Controllable synthesis of multi-responsive ferroelectric layered perovskite-like Bi4Ti3O12: Photocatalysis and piezoelectric-catalysis and mechanism insight. Appl. Catal. B: Environ., 2017, 219: 550-562

[4] Q. Zhang, Y. Huang, S.Q. Peng, T.T. Huang, J.J. Cao, W.K. Ho, S.C. Lee, Synthesis of SrFexTi1-xO3-δ nanocubes with tunable oxygen vacancies for selective and efficient photocatalytic NO oxidation, Appl. Catal. B: Environ., 2018, 239: 1-9

[5] Q. Zhang, Y. Huang, L.F. Xu, J.J. Cao, W.K. Ho, and S. C. Lee, Visible-Light-Active Plasmonic Ag-SrTiO3 Nanocomposites for the Degradation of NO in Air with High Selectivity. ACS Appl. Mater. & Interf., 2016, 8(6): 4165-4174

论文编号：01–022

Evidence for the Formation of Imidazole from Carbonyls and Reduced Nitrogen Species at the Individual Particle Level in the Ambient Atmosphere

Xiufeng Lian[a], Guohua Zhang[a, b], Yuxiang Yang[a] , Qinhao Lin[a] , Xinming Wang[a, b], Xinhui Bi[a, b, *]

[a] State Key Laboratory of Organic Geochemistry and Guangdong Provincial Key Laboratory of Environmental Protection and Resources Utilization, Guangzhou Institute of Geochemistry, Chinese Academy of Sciences, Guangzhou 510640, PR China

[b] Guangdong-Hong Kong-Macao Joint Laboratory for Environmental Pollution and Control, Guangzhou Institute of Geochemistry, Chinese Academy of Sciences, Guangzhou 510640, PR China

*Email: bixh@gig.ac.cn

Abstract：

We investigated the detailed mixing-state of carbonyls, ammonium, amines, and imidazole (as a surrogate of BrC) in cloud residual, interstitial, and cloud-free particles by single-particle mass spectrometry. The results provide the first ambient evidence on the formation of imidazole through reactions between carbonyls and ammonium/amines at the individual particle level. The key evidence for this is that 60% of the imidazole particles are internally mixed with carbonyls and ammonium/amines. The number fraction of imidazole was significantly enhanced in particles with internally mixed carbonyls and ammonium (7.8%)/amines (26.7%), compared with that (1.4%) in all the measured cloud-free particles. Furthermore, a higher fraction of imidazole was observed in all cloud residual and interstitial particles than in the cloud-free particles (2.9% and 1.4% by number). This is due to the enhancement by amines and/or the synergistic effect of ammonium and amines in the formation of imidazole in cloud residual and interstitial particles.

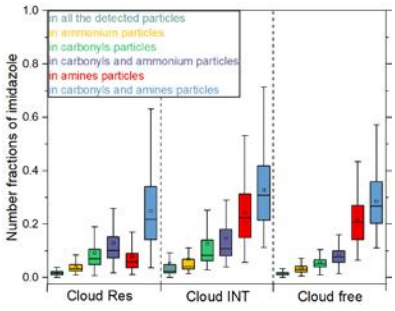

Fig. 1 Number fractions of imidazole in each particle-type for the cloud RES, cloud INT, and cloud-free particles

论文编号：01–023

关中盆地大气降水中棕碳的化学组成及其来源研究

李小飞[1]，陈庆彩[1]

[1]陕西科技大学，环境科学与环境工程学院

摘要正文：

棕碳（Brown carbon，BrC）在地球辐射能量平衡中扮演者重要的角色。尤其在大气降水中，溶解性有机质对区域和全球尺度上的生物地球化学循环起着重要的调节作用，但是关于其化学组成及其来源的认知仍然相对比较贫乏。基于三维荧光光谱仪和平行因子分析法，我们对关中地区4个采样点获得的降水样品中溶解性有机质进行了分析。结果表明，通过平行方法获得3种棕碳组分，分别为腐殖质类（C1，C2）和蛋白质类（C3）。其中，C1和C2对总荧光强度的贡献吕分别为42%和36%，C3的贡献率为21%。同时，我们通过水溶性离子分析并结合后向气团轨迹对降水中溶解性有机质的来源进行了研究。通过对关中盆地大气降水中溶解性有机质的研究，丰富和促进有机质相关的研究，为区域和全球碳循环模型提供可靠数据。

关键词：棕碳；EEMs；FARAFAC；关中盆地

论文编号：01–024

我国西北地区沙尘-灰霾事件中挥发性有机物的来源与转化

薛永刚[1]，王丽琴[1]，曹军骥[1]，黄宇[1,*]

[1] 气溶胶化学与物理实验室，中国科学院地球环境研究所，陕西省西安市 雁塔区 雁翔路 97 号，710061

*Email: huangyu@ieecas.cn

摘要正文：

随着大气污染控制的进程，二次有机气溶胶（SOA）在大气颗粒物污染中的起到越来越重要的作用[1]。挥发性有机物（VOCs）是大气SOA的重要前体物，因此其来源及转化过程受到广泛关注。近年来，沙尘中具有活性的金属氧化物，如二氧化钛/铁，被认为对大气中VOCs的光化学反应具有促进作用[2]。本研究于2016年冬季沙尘-灰霾时期在西安市城区开展系统大气非甲烷烃VOCs、醛酮类VOCs、颗粒物化学组分及无机气体污染物监测，以期研究在此特殊时期VOCs的来源、转化及其对SOA形成过程的影响。研究发现，本地机动车尾气（43%）及冬季生物质燃烧（25%）是冬季大气中VOCs的主要来源。沙尘过境时，大气中VOCs浓度迅速降低(由沙尘前期43.3±17.5ppbv降至沙尘过境后17.3±7.7ppbv)，同期，大气活性较强VOCs与活性较弱VOCs(T/B,X/E)比值迅速降低，且VOCs氧化产物，如二元醛的浓度持续升高，表明存在大气VOCs的快速氧化过程。在颗粒物组分中，随着VOCs浓度及组成的变化，二次形成的组分，如OC、硫酸盐、硝酸盐组分占比显著升高，表明沙尘过境期存在较强的二次转化过程。此外，在沙尘过境过程中，颗粒物中钛、铁元素丰度升高2-3倍，随着颗粒物化学组成的变化，大气中两种同源的同分异构体比值发生迅速变化（反式/顺式-2-丁烯比值迅速降低），证明在沙尘过境时VOCs发生迅速氧化过程，进一步形成SOA的前体物。

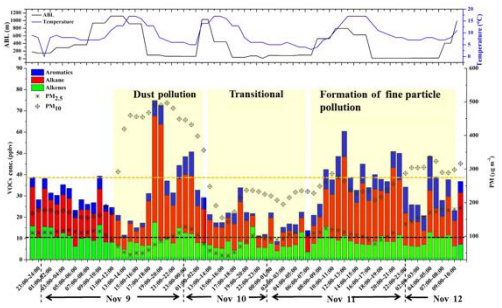

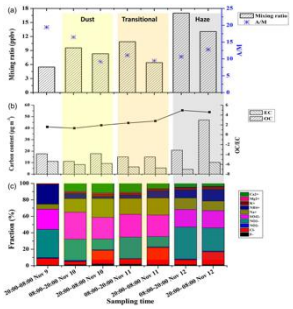

Fig. 1(left) Temporal variations in volatile organic compound (VOC) concentrations and particle levels during the sampling period (9–13 November 2016).

Fig. 2(right) Variations in (a) the mixing ratios of 17 carbonyl compounds and acetone to methylglyoxal (A/M) ratios in the gas phase,(b) particulate carbon fractions, and (c) particulate water-soluble ions during the study period.

关键词：挥发性有机物；二次有机气溶胶；沙尘

参考文献

[1] R. Huang, Y. Zhang, C. Bozzetti, K. Ho, J. Cao, A.S.H. Prevot, et al. High secondary aerosol contribution to particulate pollution during haze events in China, Nature, 2014, 514: 218–222.

[2] H. Chen, C. E. Nanayakkara, and V. H. Grassian Titanium Dioxide Photocatalysis in Atmospheric Chemistry, Chemical Review, 2012, 112: 5919–5948.e

论文编号：01–025

Mechanistic and Kinetics Investigations of Oligomer Formation from Criegee Intermediates Reactions with Hydroxyalkyl Hydroperoxides（烯烃大气光化学反应形成二次气溶胶的理论研究）

Long Chen,[1,2] Yu Huang,[*,1,2] Yonggang Xue,[1,2] Junji Cao,[*,1,2] Wenliang Wang[3]

[1] Key Lab of Aerosol Chemistry & Physics, Institute of Earth Environment, Chinese Academy of Sciences, Xi'an, Shaanxi, 710061, China

[2] State Key Laboratory of Loess and Quaternary Geology, Institute of Earth Environment, Chinese Academy of Sciences, Xi'an 710061, China

[4] School of Chemistry and Chemical Engineering, Key Laboratory for Macromolecular Science of Shaanxi Province, Shaanxi Normal University, Xi'an, Shaanxi, 710119, China

Email: huangyu@ieecas.cn; cao@loess.llqg.ac.cn

Abstracts:

Although secondary organic aerosols (SOA) are major components of PM2.5 and organic aerosol (OA) particles and therefore profoundly influence air quality, climate forcing and human health, the mechanism of SOA formation via Criegee chemistry is poorly understood. Herein, we perform high-level theoretical calculations to study the gas phase reaction mechanism and kinetics of four Criegee intermediates (CIs) reactions with four hydroxyalkyl hydroperoxides (HHPs) for the first time. The calculated results show that the consecutive reactions of CIs with HHPs are both thermochemically and kinetically favoured, and the oligomers containing CIs as chain units. The addition of -OOH group in HHPs to the central carbon atom of CIs is identified as the most energetically favorable channel, with a barrier height strongly dependent on both, CI substituent number (one or two) and position (syn- or anti-). In particular, the introduction of a methyl group into the anti-position significantly increase the rate coefficient, dramatic decrease is observed when the methyl group is introduced into the syn-position. These findings are expected to broaden the reactivity profile and deepen our understanding of atmospheric SOA formation processes.

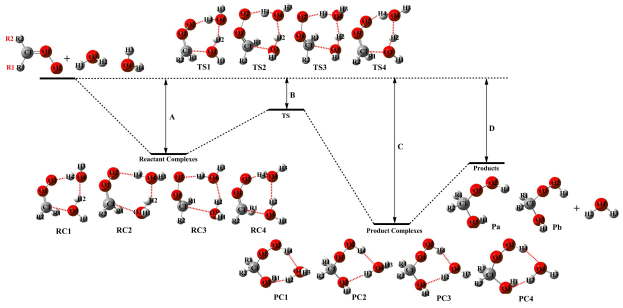

Fig. 1 Schematic PES for the bimolecular reaction of SCIs with water dimer

References

[1] Long Chen, Yu Huang, Yonggang Xue, Junji Cao, Wenliang Wang, Mechanistic and Kinetics Investigations of Oligomer Formation from Criegee Intermediates Reactions with Hydroxyalkyl Hydroperoxides, Atmospheric Chemistry & Physics, 2019, 19, 4075-4091.

论文编号：01–026

西安夏季二次有机气溶胶生成：雨雾期液相化学的贡献

段静[1]，黄汝锦[1,*]

[1]中国科学院地球环境研究所，陕西省西安市雁塔区雁翔路97号，710061

*Email: rujin.huang@ieecas.cn

摘要正文：

二次有机气溶胶（SOA）是有机气溶胶（OA）的重要组成部分，然而，由于对其形成及老化机制认识不足，SOA浓度和氧化状态的模型模拟仍然存在很大的不确定性。本研究基于2019/6/22-2019/7/21在西安市区开展的非难熔性$PM_{2.5}$（NR-$PM_{2.5}$）化学组分高分辨率在线测量和有机气溶胶来源解析，对西安夏季非雨雾期和雨雾期SOA的生成及老化机制进行了对比分析。结果表明，SOA（包括低氧化性SOA（LO-OOA），高氧化性SOA（MO-OOA）以及液相生成SOA（aq-OOA））在OA中的平均贡献可达到69%，而在NR-$PM_{2.5}$中的平均贡献为43%，表明西安夏季增强的大气氧化性以及SOA对气溶胶浓度的重要贡献。光化学氧化是LO-OOA和MO-OOA的主要生成途径，同时在非雨雾期和雨雾期都是SOA生成的主要贡献者；相比之下，aq-OOA主要在雨雾期通过液相化学过程生成，其在OA中的占比从非雨雾期的2%显著升高至雨雾期的19%。进一步分析表明持续的高湿度（RH）及高液态水含量（ALWC）是西安夏季aq-OOA形成的决定性因素，而在此基础上高Ox浓度可进一步促进其形成；同时，后向轨迹分析显示来自东南方向的湿润气团更有利于形成长期的雨雾天气，促进aq-OOA的生成。

关键词：二次有机气溶胶；液相生成氧化性有机气溶胶；雨雾期；光化学氧化

论文编号：01–027

Field comparison of electrochemical gas sensor data correction algorithms for ambient air measurements

Cheng Wu[1*], Yue Liang[1], Shutong Jiang[2], Yong Jie Li[3], Dui Wu[1,4], Mei Li[1], Peng Cheng[1], Wenda Yang[1], Chunlei Cheng[1], Lei Li[1], Tao Deng[4], Jia Yin Sun[1], Guowen He[1], Ben Liu[3], Teng Yao[5], Zhen Zhou[1]

[1]Institute of Mass Spectrometry and Atmospheric Environment, Jinan University, Guangzhou 510632, China

[2]Shenzhen Soarability Technologies Co., Ltd., Shenzhen 518057, China

[3]Department of Civil and Environmental Engineering, Faculty of Science and Technology, University of Macau, Taipa, Macau, China

[4]Institute of Tropical and Marine Meteorology, CMA, Guangzhou 510080, China

[5]Division of Environment & Sustainability, Hong Kong University of Science and Technology, Hong Kong, China

Abstract：

Electrochemical gas sensors (ECGS) have gained substantial popularity in ambient measurements. Several data correction algorithms had been proposed to tackle the drifting response of ECGS due to environmental factors, but there is a lack of performance evaluation of these data correction schemes. To fill this knowledge gap, we conduct a comprehensive evaluation of these data correction algorithms using a large dataset from field comparisons. The dataset covered three commonly used gas pollutants, including CO, NO_2 and O_3 measured by both ECGS and reference instruments, with a time resolution of 1 minute and a duration of 6 months. Taking advantage of this large dataset, the performance of 8 different data correction schemes (2 new algorithms and 6 algorithms from the literature) was benchmarked by a set of evaluation metrics using raw signals from ECGS (nA level currents from the working and auxiliary electrodes). Eight scenarios were considered to examine the robustness of correction algorithms in response to different training and evaluation data period configurations. In addition, the bias dependence on temperature, RH, target gas levels and cross-sensitivity by different correction algorithms was investigated. Recommendations on data correction scheme selection are provided based on the comparison results.

References

[1] Liang, Y., **Wu, C.***, Jiang, S., Li, Y. J., Wu, D., Li, M., Cheng, P., Yang, W., Cheng, C., Li, L., Deng, T., Sun, J. Y., He, G., Liu, B., Yao, T., Wu, M., and Zhou, Z.: Field comparison of electrochemical gas sensor data correction algorithms for ambient air measurements, ***Sens. Actuators B Chem.***, 327, 128897, doi: https://doi.org/10.1016/j.snb.2020.128897, 2021.

论文编号：01–028

基于Igor的大气数据处理及可视化工具包

吴晟 [1]

[1] 暨南大学质谱仪器与大气环境研究所,广东 广州 510632

*Email: wucheng@foxmail.com

摘要正文：

为了实现快速高效的大气数据处理及可视化，开发了一系列的基于Igor的工具包，包括Scatter Plot, Histbox, MRS, RT-OCEC data processor, Aethalometer data processor, DRI2001a data processor, OCEC data processor, SMPS toolkit等等。能够极大地缩短观测数据的处理时间，在短时间内处理大量的数据。这些工具包能从多个维度进行条件循环批量画图，使得用户可以便捷地进行科学绘图，直接输出达到出版级别的精美高质量矢量图。

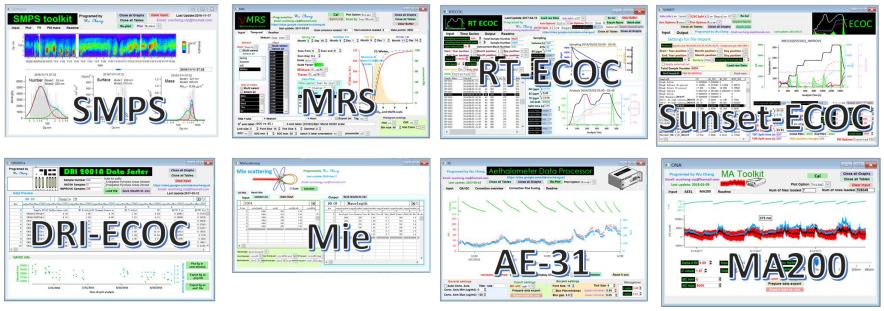

Fig. Igor based data processing and visualization toolkits.

关键词：大气数据处理；数据订正；数据可视化

参考文献

[1] Wu, C*., Wu, D., and Yu, J. Z.*: Quantifying black carbon light absorption enhancement with a novel statistical approach, Atmos. Chem. Phys., 18, 289-309, doi:10.5194/acp-18-289-2018, 2018.

[2] Wu, C. and Yu, J. Z.*: Evaluation of linear regression techniques for atmospheric applications: the importance of appropriate weighting, Atmos. Meas. Tech., 11, 1233-1250, doi:10.5194/amt-11-1233-2018, 2018.

论文编号：01–029

Effects of solid fuel combustion emissions on biomarkers of housewives in rural areas of Fenwei Plain, China

Rong Feng[1], Hongmei Xu[1, 2,*], Kailai He[1], Zexuan Wang[1], Zhenxing Shen[1, 2], Kin Fai Ho[3]

[1]Department of Environmental Science and Engineering, Xi'an Jiaotong University, 28 Xianning Road, Xi'an, 710049

[2]Institute of Earth Environment, Chinese Academy of Sciences, 97 Yanxiang Road, Xi'an, 710061

[3]JC School of Public Health and Primary Care, The Chinese University of Hong Kong, Hong Kong, China

*Email: xuhongmei@xjtu.edu.cn

Abstract:

Domestic solid fuel combustion posed nonnegligible negative health impacts on rural residents in Fenwei Plain, China. 73 housewives over 60 years old were selected in this area to analyze their health indicators among the three different energy groups (Coal, Biomass and Non-solid fuel Groups). In each group, IL-6 and 8-OHdG in urine of housewives, as well as blood pressure (BP) and heart rate (HR) in winter were significantly higher than those in summer. Significant differences of 8-OHdG, HR, and SBP between winter and summer were both observed in Coal and Biomass Groups. Excluding the influence of confounding factors, coal burning emission showed greater impacts on inflammatory cytokines (IL-6) than biomass burning in winter, but we did not observe this phenomenon in summer. Therefore, excessive use of solid fuels in rural households during winter adversely affected the inflammatory factors and DNA oxidative stress of housewives in rural areas of Fenwei Plain.

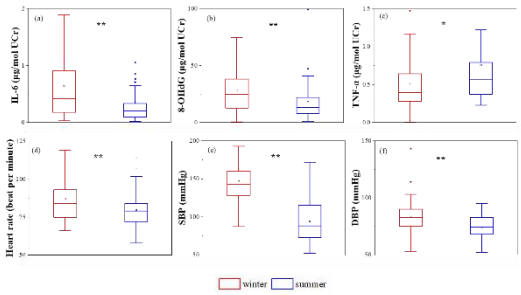

Fig. 1 Heart rate, blood pressure (BP) and biomarkers in urine of subjects in winter and summer

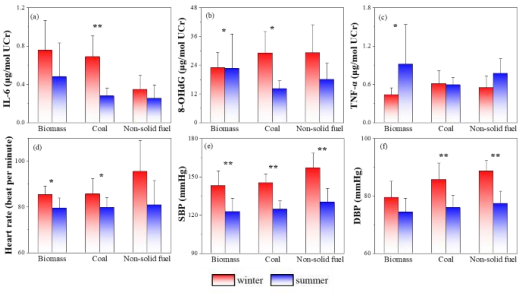

Fig. 2 Heart rate, blood pressure (BP) and biomarkers in urine of subjects in different fuel groups

Keywords: Solid fuel combustion, biomarker, health effect, rural household, Fenwei Plain

论文编号：01–030

道路扬尘控制措施及其效率评估研究进展

张月帆[1]，陈建华[1,*]，李冬[1]，高健[1]

[1]中国环境科学研究院，北京 100012

*Email: sept_zyf@163.com

摘要正文：

道路扬尘是当前城市大气颗粒物的主要来源之一，且会对人体健康产生严重危害。定量检测并采取有效措施控制道路扬尘是城市大气环境管理中的重要一环。因此，针对当前国内实际的道路扬尘控制措施的效率进行评估、完善和发展，对于高效精准地削减道路扬尘排放量具有重要的意义。通过文献调研等方法，研究了当前国内外主要的道路扬尘控制措施及控制效果评价方法，重点介绍了TRAKER法和AP-42法两种主要的道路扬尘检测方法在道理扬尘控制效率评估中的应用，并对我国道路扬尘控制措施及控制效率的现状及存在问题进行了分析和展望。经过综合对比分析，发现：

（1）目前国内外主要道路扬尘措施有：洒水抑尘、道路清扫（人工清扫、机械清扫、真空吸尘、再生式空气清扫）、用水冲洗、化学抑尘剂等。当前我国各城市实际采取的主要道路扬尘控制措施为上述措施的单独或选择组合使用。而由于各城市发展水平不均衡，道路扬尘的控制范围和控制措施的作业频率存在差异。

（2）道路扬尘控制措施的效率评估有两个重要指标：指标一是除沙效率；指标二是对环境空气质量的影响。目前已有的研究内容大多对应于指标二，缺乏对指标一的评估。在未来的研究中可以同时对两个指标进行评估，即一是计算积尘负荷，二是计算排放潜势，并可扩展到更多不同的扬尘控制措施及其组合。

（3）道路扬尘控制措施效率评估的研究主要集中在欧美国家，而我国缺乏相关研究。且国外的相关研究结果因时间、地域和研究方法的差异而不同，因此有必要在我国开展相关研究，可将TRAKER与AP-42联合应用到该问题中深入探究。

关键词：道路扬尘；控制措施；效率评估；TRAKER；AP-42

参考文献

[1] CALVILLO S J, WILLIAMS E S, BROOKS B W. Street dust: implications for stormwater and air quality, and environmental through street sweeping [J]. Rev Environ Contam Toxicol, 2015, 233(71-128.

[2] AMATO F, ESCRIG A, SANFELIX V, et al. Effects of water and CMA in mitigating industrial road dust resuspension [J]. Atmospheric Environment, 2016, 131(334-40.

[3] AMATO F, QUEROL X, JOHANSSON C, et al. A review on the effectiveness of street sweeping, washing and dust suppressants as urban PM control methods [J]. Sci Total Environ, 2010, 408(16): 3070-84.

[4] GULIA S, GOYAL P, GOYAL S K, et al. Re-suspension of road dust: contribution, assessment and control through dust suppressants—a review [J]. International Journal of Environmental Science and Technology, 2018, 16(3): 1717-28.

[5] CHANG Y, CHOU C, SU K, et al. Effectiveness of street sweeping and washing for controlling ambient TSP [J]. Atmospheric Environment, 2005, 39(10): 1891-902.

[6] ZHU D, KUHNS H D, GILLIES J A, et al. Analysis of the effectiveness of control measures to mitigate road dust emissions in a regional network [J]. Transportation Research Part D: Transport and Environment, 2012, 17(4): 332-40.

[7] KUHNS H, ETYEMEZIAN V, LANDWEHR D, et al. Testing Re-entrained Aerosol Kinetic Emissions from Roads : a new approach to infer silt loading on roadways [J]. Atmospheric Environment, 2001, 35(16):

[8] KUHNS H. Vehicle-based road dust emission measurement—Part II: Effect of precipitation, wintertime road sanding, and street sweepers on inferred PM10 emission potentials from paved and unpaved roads [J]. Atmospheric Environment 2003, 37(32): 4573–82.

论文编号：01–031

区域化学模式对中国O_3和$PM_{2.5}$模拟效果比较

张皓然[1]，李楠[1,*]

[1]南京信息工程大学环境科学与工程学院，南京，210044

* Email: linan@nuist.edu.cn

摘要正文：

本研究采取WRF-GC, WRF-Chem和WRF/CMAQ这三种模式对2016年7月中国东部空气质量模拟结果进行评估，比较不同的区域大气化学模式对于$PM_{2.5}$和O_3的模拟能力。在 $PM_{2.5}$的模拟上，WRF-GC除了在北京冬季表现较好，在其他模拟案例中$PM_{2.5}$的模拟值都明显高于观测值。这是由于排放清单的差异导致的，GEOS-Chem内的HEMCO只提供2010年MIX排放清单，对于自此之后的排放会默认采用2010年的排放活动水平，因此用来模拟2016年的$PM_{2.5}$可能会有较大差异。而WRF-Chem（SAPRC99-MOSAIC, MOZART-MOSAIC 和RADM2-MADE/SORGAM）及CMAQ（SAPRC99-AERO6）模拟的$PM_{2.5}$更好一些。由于WRF-Chem和CMAQ由于采用了2016年bottom-up的MEIC清单，并没有出现类似于WRF-GC对$PM_{2.5}$的高估现象。总体的浓度量级与观测一致，r在0.4~0.6。相比于$PM_{2.5}$, 三类模式的O_3的模拟效果更好一些，r在0.59~0.8。但WRF-GC模拟的O_3浓度在三个城市都有明显的低估，NMB在北京，上海，广州分别为-37%，-57%以及-19%。这主要是由于WRF-GC没有捕捉到日内O_3峰值。而WRF-Chem的三种机制能够较好的捕捉到O_3日内的峰值。但在北京，由于WRF-Chem对夜间O_3低值的高估，导致三种机制最终结果分别有33-41%的高估。CMAQ在北京与上海的模拟效果最好，但在广州却表现出1倍的高估。未来研究中，将对WRF-GC的排放模块进行更新，并进一步评估气象-化学耦合机制对模拟能力的提升。

关键词：O_3；$PM_{2.5}$；数值模式

论文编号：01–032

对一次跨境传输沙尘污染的消减作业分析

范思睿[1,2,3]，王维佳[2,4]，

[1]四川省人工影响天气办公室，成都，610072；

[2]中国气象局云雾物理环境重点实验室，北京，100081；

[3]高原与盆地暴雨旱涝灾害四川省重点实验室，成都，610072；

[4]成都市气象局，成都，611133

*Email: fansr110@163.com

摘要正文：

本文对2019年5月12日的一次跨境传输的沙尘污染实施人工增雨，以达到减轻空气污染，首先利用FY-4A卫星资料对人工增雨作业前的云降水条件进行分析，综合分析增雨可播性，判别增雨潜力区和作业高度，为开展人工增雨作业提供可靠的依据，然后利用空气质量指数、颗粒物污染物浓度、多普勒天气雷达、地面气象台站等多种数据资料分析人工增雨作业前后作业云体宏观情况和空气质量、雨量的变化，对其作业效果进行分析。结果表明：①5月12日四川盆地西部有云系发展，作业前6小时作业区附近主要为积层混合云，存在大量过冷水，红色对流泡云顶温度约为-30℃，粒子有效半径为15～40μm，作业前0-3小时作业区位于深厚对流降水云边缘，云顶温度约为-40℃，粒子有效半径为7～40μm，作业区南部有大片积层混合云，提供大量过冷水；②作业区内，高低空配合的环流场形成了较有利的降水形势，作业云体过冷水丰沛，增雨潜力较好，符合人工播撒催化剂条件，适宜开展人工增雨作业；③经过人工增雨作业后，作业区雨量峰值降雨时间延长，总体雨量增加，作业区的AQI从82降到29，PM_{10}从94μg/m³下降到28μg/m³，$PM_{2.5}$从49μg/m³降到17μg/m³，空气质量等级持续优良，而3个对比区没有实施人工增雨作业，空气质量指数持续超标数小时。作业区的降水经过人工催化后，雨量峰值持续时间延长；同时发现经过人工催化，作业云体持续发展，云内液体水含量增加，云顶升高。说明经过人工增雨作业后有效减轻空气污染，同时使得作业云体持续发展，峰值降雨时间延长，总体雨量增加。

关键词： FY-4A；空气质量指数；颗粒物污染物浓度

论文编号：01–033

华中县级城市道路灰尘重金属污染及人体健康风险评价

张喜皓[1,2,3,4]，张家泉[2,3]，张慧迪[2,3]，汪昂绿[2,3]，王鹏飞[2,3]，蔡传生[5]，刘美婧[5]，占长林[2,3]，张淑琴[1,4,*]

[1] 武汉科技大学资源与环境工程学院，武汉 430081

[2] 湖北理工学院环境科学与工程学院，黄石 435003

[3] 矿区环境污染控制与修复湖北省重点实验室，黄石 435003

[4] 湖北省工业安全工程技术研究中心，武汉 430081

[5] 黄石市生态环境局阳新县分局，阳新 435200

*Email: zhangjiaquan@hbpu.edu.cn

摘要正文：

本研究采集阳新县开发区、老城区和城东新区的不同类型道路灰尘样品48个，测试灰尘中重金属Cd、Co、Cr、Cu、Mn、Ni、V、Pb、Zn的质量，分别采用地累积指数法和美国环保署（USEPA）人体健康风险评价法对道路灰尘重金属污染程度和人体健康风险水平进行评价。结果表明：阳新县道路灰尘中重金属有较明显富集，平均含量分别为6.51、302.47、190.70、122.23、1595.57、138.07、187.98、50.69和208.36mg/kg，均高于湖北省土壤环境背景值，除Cd、Pb和Zn外老城区中重金属含量均高于开发区和城东新区；阳新县城区道路灰尘中Cd为中-重度污染，Co为中度污染，Cu为轻-中度污染，Cr、Pb和Zn为轻度污染，Ni和V为清洁；手-口接触摄入是路面灰尘风险暴露主要途径，各类重金属非致癌风险从高到低为Cr、V、Mn、Co、Zn、Cd、Cu、Ni、Pb，手-口接触摄入、呼吸吸入和皮肤接触3种途径对儿童和成人产生的非致癌总风险分别为1.59和0.48，灰尘暴露导致的儿童非致癌健康风险高于成人，在相同暴露途径下儿童更易受到灰尘中重金属的危害；具有致癌暴露风险重金属从高到低依次为Cr、Co、Cd、Ni，均在人体可承受风险范围内。

关键词：城区道路灰尘；重金属；暴露途径；地积累指数；健康风险；阳新县

参考文献

[1] Al-Khashman O A.The investigation of metal concentrations in street dust samples in Aqaba city, Jordan[J]. Environmental Geochemistry & Health,2007, 29(3):197-207.

[2] 黄春霞,韦妮玉.河池市矿区地表灰尘中重金属污染及生态风险评价[J].能源环境保护, 2019, 033(003):45-50.

[3] 钟萍,张家泉,占长林,等.华中冶金工业走廊表层土壤、道路尘重金属污染特征及健康风险[J].环境化学, 2019, 038(001):87-96.

[4] 王正文.闽三角城市群道路土壤及灰尘重金属污染现状与风险评价[D].厦门大学,2018.

[5] Abdullah M, Fasola M, Muhammad A, et al. Avian feathers as a non-destructive bio-monitoring tool of trace metals signatures: A case study from severely contaminated areas[J]. Chemosphere, 2015, 119:553-561.

[6] Han N, Latif M, Othman M, et al. Composition of selected heavy metals in road dust from Kuala Lumpur city centre[J]. Environmental Earth Sciences, 2014.

[7] Akoto O,Bismark Eshun F, Darko G,et al.Concentrations and Health Risk Assessments of Heavy Metals in Fish from the Fosu Lagoon[J].International Journal of Environmental Research,2014, 8(2):403-410.

[8] Kamunda C, Mathuthu M, Madhuku M. Health risk assessment of heavy metals in soils from Witwatersrand Gold Mining Basin, South Africa[J]. International Journal of Environmental Research and Public Health,2016,13:663. https://doi.org/10.3390/ijerph13070663.

论文编号：01–034

基于VIIRS-NPP卫星灯光数据的人为源排放清单优化

殷子涵[1]，张嘉祺[1]，聂姝翰[1]，汤克勤[1,*]，李楠[1,*]

[1]南京信息工程大学环境科学与工程学院，南京，210044

* Email: tangkq@nuist.edu.cn; linan@nuist.edu.cn

摘要正文：

构建准确精细、完整及时的大气污染物排放清单是有效进行大气污染防治工作的前提和基础。MEIC清单是中国目前最先进的人为源排放清单之一，被众多环保工作者和研究者广泛使用。然而，MEIC清单的空间分辨率为0.25°× 0.25°，无法精细地反应城市尺度的大气污染物排放特征。为了进一步提高MEIC清单的空间分辨率，本研究采用美国国家海洋和大气管理局VIIRS-NPP卫星1*1 km空间分辨率的夜间灯光数据对MEIC清单进行优化，以进一步提高排放清单对人为活动水平的表征能力。本研究通过GIS技术对2016年的卫星图像进行处理，反演获得包含经纬度的灯光数据。结果表明，我国平均灯光密度为0.49，灯光强度总体呈现沿海(0.59-0.71)强于内陆(0.4-0.47)的特征。经卫星灯光数据校正后的排放清单能够更加明显地反映城市内不同功能区地排放量分布特征。以上海市为例，MEIC清单中SO2的排放量从市中心到郊区的变化梯度为0.85 mol km-3 hr-1，优化后的排放清单中SO2排放变化梯度显著提高了22.6%。进一步，本研究将结合区域大气化学模式WRF-Chem定量评估排放清单空间分辨率的改进对城市大气污染物模拟能力的提升。

关键词：卫星灯光数据；人为源排放清单；空间分辨率

论文编号：01–035

基于单颗粒气溶胶质谱技术的西安冬季$PM_{2.5}$污染事件研究：粒径分布和化学组分

严梦园[1,2]，王启元[1]

[1]中国科学院地球环境研究所，陕西省西安市雁塔区雁翔路97号，710061

[2]西安交通大学，陕西省西安市碑林区咸宁西路28号，710049

*Email: yanmengyuan@stu.xjtu.edu.cn

摘要正文：

利用高时间分辨率的在线观测仪器对大气中$PM_{2.5}$进行观测，分析其化学组分浓度信息和来源贡献特征，有助于政府对大气污染防治开展有效的政策治理提供科学依据。本研究基于单颗粒气溶胶质谱仪（SPAMS）在西安市的2018年12月6日−12月12日时段开展高时间分辨率的实时在线观测，结合$PM_{2.5}$（空气动力学当量直径小于等于2.5μm的颗粒物）质量浓度和常规气体数据分析颗粒物化学组分。结果显示：观测期间颗粒物数浓度和$PM_{2.5}$质量浓度变化趋势一致，表明颗粒物数浓度可以反映大气污染状况；使用神经网络算法和人工分类方法将颗粒物分为以下7类，分别是元素碳颗粒、有机碳与元素碳混合颗粒、有机碳颗粒、富钾颗粒、左旋葡聚糖颗粒、扬尘颗粒、重金属颗粒，占比最大的是含碳颗粒，总占比达到66.9%；观测到88.6%的颗粒物的粒径分布在0.2−0.5 μm之间，各化学组分的粒径分布特征与总颗粒物的分布特征类似，有机碳与元素碳混合颗粒、元素碳颗粒、有机碳颗粒在整个测径范围内占比都较大；在污染期间，元素碳颗粒、富钾颗粒和粉尘颗粒的占比升高较为明显（尤其是元素碳颗粒和富钾颗粒），表明此次$PM_{2.5}$污染事件主要是由于元素碳颗粒和富钾颗粒物排放增多引起的。**关键词：**结构光场；群体颗粒；光学捕获；定向移动

关键词：单颗粒气溶胶质谱；$PM_{2.5}$；粒径分布；化学组分

论文编号：01–036

Spatial distribution and sources of winter black carbon and brown carbon in six Chinese megacities

Qian Zhang[a,b], Zhenxing Shen[b*,c], Shaofei Kong[d], Qiyuan Wang[c], Jun Tao[e], Renjian Zhang[f], Chong Wei[g], Song Cui[h], Steven Sai Hang Ho[i]

[a]Key Laboratory of Northwest Resource, Environment and Ecology, MOE, Xi'an University of Architecture and Technology, Xi'an 710055, China

[b]Department of Environmental Science and Engineering, Xi'an Jiaotong University, Xi'an 710049, China

[c]Key Lab of Aerosol Chemistry & Physics, SKLLQG, Institute of Earth Environment, Chinese Academy of Sciences, Xi'an, China

[d]Department of Atmospheric Science, School of Environmental Sciences, China University of Geosciences, Wuhan, 430074, China

[e]South China Institute of Environmental Sciences, Ministry of Environmental Protection, Guangzhou, China

[f]Key Laboratory of Middle Atmosphere and Global Environment Observation, Institute of Atmospheric Physics, Chinese Academy of Sciences, Beijing 100029, China

[g]Shanghai Carbon Data Research Center, Shanghai Advanced Research Institute, Chinese Academy of Sciences, Shanghai 201210, China

[h]International Joint Research Center for Persistent Toxic Substances (IJRC-PTS), School of Water Conservancy and Civil Engineering, Northeast Agricultural University, Harbin, China

[i]Divison of Atmospheric Sciences, Desert Research Institute, Reno, NV89512, United States

*E-mail: zxshen@mail.xjtu.edu.cn

Abstract：

The light-absorbing carbonaceous aerosols, including black carbon (BC) and brown carbon (BrC), influenced heavily on aerosol environmental and radiative effects. Here, a winter campaign to characterize BC and BrC in $PM_{2.5}$ was conducted simultaneously in six Chinese megacities (i.e., Harbin, Beijing, Xi'an, Shanghai, Wuhan, and Guangzhou) using continual aethalometers. The averaged light-absorbing coefficients of BC (b_{abs}-BC) and BrC (b_{abs}-BrC) were 28.6 and 21.8 Mm^{-1} in the northern cities, they were 1.4 and 2.7 times higher than those in the southern cities. Also, the BrC dominated the total b_{abs} (40.6%-46.3%) in the northern cities, whereas only contribution of 20.3%-30.6% were seen in southern cities. The diurnal trend showed the peaks of secondary-BrC (b_{abs}-BrC_S) and b_{abs}-BrC_S/ΔCO in the northern cities occurred at high relative humidity in nighttime, implying the secondary BrC formation was possibly related to aqueous reactions in winter. In contrast, in the southern cities of Shanghai and Guangzhou, the peaks of b_{abs}-BrC_S and b_{abs}-BrC_S/ΔCO appeared with a distinct time lag under high oxidant levels after the morning traffic rush hours, demonstrating the formation of secondary BrC through photochemical reactions.

论文编号：01–037

咸阳市碳组分的季节变化特征

田瑞霞 [1,*]，曹军骥 [1]，朱崇抒 [1,2]，马丽 [2]

[1] 中国科学院地球环境研究所气溶胶化学与物理重点实验室，西安，710061

*Email: tianruixia@ieecas.cn

摘要正文：

本研究于2019年对咸阳市三个常规监测站点（中医学院、气象站、实验中学）不同季节进行了$PM_{2.5}$颗粒物滤膜样品的采集并分析了样品中有机碳(organic carbon，OC) 和元素碳(elemental carbon，EC) 的含量。结果表明: 各个季节$PM_{2.5}$中OC的平均浓度分别为6.98 μg·m^{-3} (春季)、6.29 μg·m^{-3} (夏季)、9.73 μg·m^{-3} (秋季)、17.67μg·m^{-3} (冬季)；EC的平均浓度为1.52 μg·m^{-3} (春季)、0.87 μg·m^{-3} (夏季)、2.86 μg·m^{-3}(秋季)、3.65 μg·m^{-3} (冬季)。结果表明OC和EC的浓度存在的季节变化均是冬季＞秋季＞春季＞夏季，与$PM_{2.5}$浓度的季节性变化一致。OC和EC在各个季节的浓度变化存在较好的一致性，但OC的浓度变化波动更加剧烈，尤其是秋冬季重污染期间，说明OC的污染除了市区污染源产生之外，还存在外源输送的影响，这种现象在冬季更加明显，夏季和秋季OC的增长除了市区污染源产生之外，由于存在较高的温度和光照强度，OC组分可以由光化学反应等化学二次转化生成而继续累积。对不同季节$PM_{2.5}$中OC和EC的浓度值进行线性拟合，可以看出各个季节OC、EC的相关性均较好，$PM_{2.5}$中OC和EC相关系数分别为0.91（冬季）、0.76(春季)、0.73(夏季)、0.89(秋季)。以上数据表明咸阳市OC、EC来源较为单一，秋季和冬季OC和EC相关性较好，说明这两个季节咸阳市OC和EC可能具有相同的排放源，以局地排放为主。而春季和夏季的相关性较差则可能与复杂的来源扰动有关。这对于咸阳市未来污染物的排放管理控制具有指导意义。

关键词：有机碳；元素碳；二次有机气溶胶

参考文献

[1] 曹军骥; 李顺诚; 李杨; Judith C. Chow; Kochy Fung, 2003 年秋冬季西安大气中有机碳和元素碳的理化特征及其来源解析[J]. 自然科学展，2005,15（12）:1460-1466.

[2] 曹军骥, PM2.5 与环境[M].科学出版社，2014.

[3] Cao Jun Ji, Zhu Chong Shu, Chow Judith C. , Watson John G. , Han, Yong-Ming,Wang Ge-hui , Shen, Zhen-xing , An Zhi-Sheng, Black carbon relationships with emissions and meteorology in Xi'an, China[J], Atmospheric Research, 2009, 94(2): 194-202.

论文编号：01–038

Characteristics of indoor and personal exposure to particulate organic compounds emitted from domestic solid fuel combustion in rural areas of northwest China

Kailai He[1], Hongmei Xu[1,2,*], Rong Feng[1], Zhenxing Shen[1,2], Yue Zhang[1], Jian Sun[1]

[1]Department of Environmental Science and Engineering, Xi'an Jiaotong University, 28 Xianning Road, Xi'an, 710049

[2]Institute of Earth Environment, Chinese Academy of Sciences, 97 Yanxiang Road, Xi'an, 710061

*Email: xuhongmei@xjtu.edu.cn

Abstract:

This study investigated the concentrations and health risks of particulate matter (PM) and its organic compounds, i.e., PAHs, OPAHs, and PAEs, in indoor and housewives' personal exposure (PE) samples emitted from different domestic solid fuel combustion in winter in Guanzhong rural area. Indoor PM primarily comprised $PM_{2.5}$ (76% of TSP), and its organics were abundance in $PM_{2.5}$ (96%) too and in households that only used coal as fuel (Group C). The mean concentration of PE to $PM_{2.5}$ was 307±120 $\mu g \cdot m^{-3}$, 2.4-times higher than the indoors. Organic compounds were 44% higher in PE samples than indoors. The PE/indoor ratio of high molecular weight PAHs in Group C (2.5) was higher than that of the other organic compounds (1.3). This further led to higher inhalational cancer risks for housewives in Group C (2.4- and 1.2-times higher risks for PAHs and PAEs, respectively) than the group using coal and biomass (Group M).

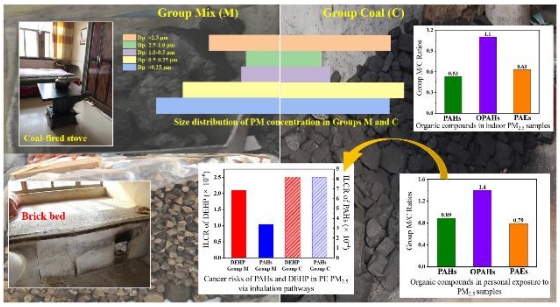

Fig. 1 The concentration characteristics and health risks of PM and its organic compounds in Groups M and C

Key words: Indoor air pollution, personal exposure to PM, domestic solid fuel, size distribution, health risk

论文编号：01–039

冬季青藏高原极端增温对亚洲气溶胶分布特征的影响机制

赵丹 [1]，陈思宇 [1,*]

[1] 兰州大学 大气科学学院，兰州，甘肃，730000

*Email: zhaod18@lzu.edu.cn

摘要正文：

青藏高原的加热作用对其周围环境甚至全球气候都有着重要的影响。目前的研究主要集中在高原热源气候特征和年代际变率及其对大气环流、季风、水分循环、大气污染和ENSO的影响。高原增温对我国气溶胶的时空分布特征是否有影响？影响机制是什么？本文基于观测结果，探讨了1980-2020年青藏高原温度的特征及其变化趋势，并进一步基于合成分析揭示了高原增温对我国气溶胶时空分布特征的影响机制。结果表明：高原温度的强弱对我国不同季节气溶胶的时空分布特征影响显著。具体来说，在夏季高原温度高值年，南亚高压增强，西风减弱，高原南侧西风风速增强，东亚大槽东移对我国东部地区气溶胶的扩散提供了有利的气象条件。在环流形势的影响下，气溶胶的高值区主要集中在我国东北部地区。在高原热源较弱时，环流形势相反，我国华北地区的污染物相对不易扩散。在冬季高原冷源高值年时，高原上空有一个明显的低压系统，此时西风较弱，气溶胶聚集在华北地区不易扩散。而在低值年时，西风相对较强，气溶胶会向东北地区进行传输。温度高低值年时这种环流模式的差异可能与我国上空经向低水平温度异常有关，该异常通过瞬态涡旋反馈调节高空大气环流。

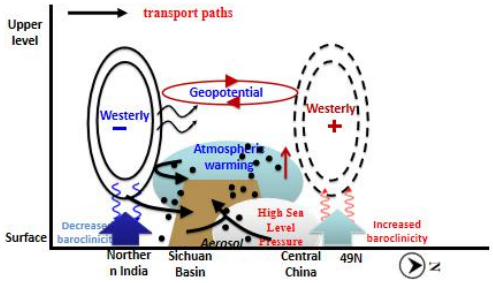

Fig. 1 Schematic diagram of the influencing mechanism of aerosol concentration

关键词：青藏高原；气溶胶；温度

参考文献

[1] Bond T C, Doherty S J, Fahey D W, et al. Bounding the role of black carbon in the climate system: A scientific assessment. Journal of Geophysical Research: Atmospheres, 2013, 118(11): 5380-5552.

[2] Kang S, Xu Y, You Q, et al. Review of climate and cryospheric change in the Tibetan Plateau. Environmental Research Letters, 2010, 5(1): 015101.

[3] Chung C E, Ramanathan V, and Decremer D. Observationally constrained estimates of carbonaceous aerosol radiative forcing. Proceedings of the National Academy of Sciences, 2012, 109(29): 11624-11629.

[4] Duan A , and Wu G X. Role of the Tibetan Plateau thermal forcing in the summer climate patterns over subtropical Asia. Climate dynamics, 2005, 24(7-8): 793-807.

[5] Duan A, and Xiao Z. Does the climate warming hiatus exist over the Tibetan Plateau? Scientific reports, 2015, 5: 13711.

[6] Flanner M G, Zender C S, Hess P G, et al. Springtime warming and reduced snow cover from carbonaceous particles. Atmospheric Chemistry and Physics, 2009, 9(7): 2481-2497.

论文编号：01–040

Tiramisu snow and the weakening of surface albedo

Siyu Chen[1], Hongru Bi[2], Jianping Guo[1,*], Yong Wang, Chengxi Liu, Dan Zhao

[1]Department of Atmospheric Science, University of Lan Zhou, No.222 , Tian Shui Road(south) ,Cheng Guan District,Lan Zhou City, Gan Su Province,730000

Abstract：

Since 1850, Earth's cryosphere has shown a global shrinking trend. The retreat of snow and ice had strongly impact on the hydrological cycle and the energy balance of the Earth system. And the melting of snow and ice attributed to the variation in snow albedo caused by LAIs deposited on the snow surface. These LAIs absorbed solar radiation, accelerated snow aging process, reduced albedo of the snow surface, and enhanced the melting of snow. Dust is as a key factor in controlling albedo and subsequent glacier melting within the global warming perspective. On December 1st, 2018, a rare weather event occurred in Urumqi, China, where snow accumulating on the land surface was covered with a layer of yellow dust. Based on ground observation data and reanalysis data such as MERRA-2 and ERA5, it was found that the dust snow was mainly caused by the large-scale strong cold caused by the Siberian trough and the southeast transport of dust-storms particles under the influence of the westerly jet. The generation dust particles reduced reflected radiation 20 W m^{-2} approximately. Compared with the changes of solar radiation under similar historical conditions, it was found that the cloud cover resulted in the surface albedo increase by about 0.23, when snow lead to counterpart increase about 0.28. But dust particles in the snow cover significantly reduced the surface albedo. Compared to historical conditions with the same snow depth and cloud cover, snow albedo caused by dust in snow decreased by approximately 28% and up to 34%.

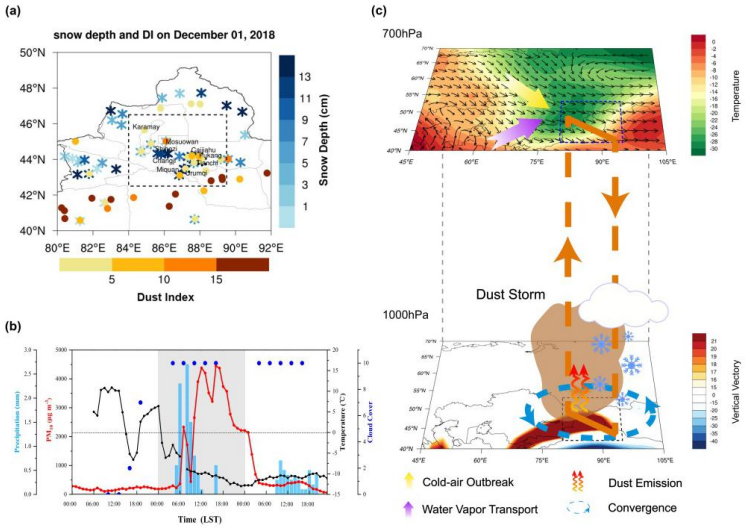

Figure. 1 (a) The spatial distribution of "Tiramisu" snow in the Northern Xinjiang region on December 1st, 2018 (blue stars represented snow depth; orange dots represented dust index). (b) The evolutions of PM10 concentrations (red line, units: μg m-3), precipitation (blue bars, units: cm), temperature at 2 m (black line, units: ℃), cloud cover (blue dots) in Urumqi from November 30th to December 2nd, 2018. (c) Schematic diagram of "Tiramisu" snow mechanism. The bottom panel showed the spatial distributions of vertical velocity at 1000 hPa, and the top panel showed the meteorological field at 700 hPa on December 1st (vectors indicated wind field, color contours indicated temperature field).

Key words： surface albedo, dust snow, solar radiation

论文编号：01–041

固定源烟气中可凝结颗粒物的排放特性研究

袁畅[1]，成海容[1]，梁胜文[2]，蒋鹭翔[1]，吴佳伟[1]，胡远致[2]，王祖武[1,*]

[1]武汉大学资源与环境科学学院　武汉 430000

[2]武汉市环境监测站 武汉 430000

*Email:hjgcapc@163.com

摘要正文：

固定源烟气中排放的颗粒物有两种类型,一类是目前我国排放标准中已监控的可过滤颗粒物（Filterable Particulate Matter，FPM）,另一类是我国尚无标准控制的可凝结颗粒物（Condensable Particulate Matter， CPM）。本研究对2个330MW机组的超低排放燃煤电厂（#1，#2）、2个1000MW机组的超低排放燃煤（#3，4#）、1个600MW机组的超低排放燃煤电厂（#5），以及一个垃圾焚烧厂（#6）和生物质燃烧厂（#7）排放的CPM进行了采样分析。这7个固定源烟气中排放的CPM的浓度分别为20.3，26.0，21.5，9.8，14.5，6.8和25.5 mg/Nm^3，是FPM浓度的1～15倍。研究结果表明，固定污染源中不仅燃煤锅炉会排放一定量的CPM，垃圾焚烧锅炉和生物质燃烧锅炉也会排放一定量的CPM。尤其是生物质燃烧锅炉，虽然没有安装脱硫系统但是排放了较高浓度的CPM。采用离子色谱对CPM的无机组分进行分析，结果表明SO_4^{2-}、Cl^-、NH_4^+和NO_3^-是CPM中主要的水溶性离子，占总离子的90%以上,以上离子主要由其气态前体SO_X、HCl、NO_x和NH_3转化而来。SO_4^{2-}在CPM的水溶性离子中的浓度相对较高，这是由于稀释降温后烟气中的SO_3非均相冷凝在已有的颗粒物表面上,导致颗粒物中的SO_4^{2-}增加,致使最终排口处CPM中的SO_4^{2-}占比较大。

Tab. 1 Basic information of the test power plants.

采样点	锅炉类型	污染控制装置	机组容量	负荷
#1	燃煤锅炉	SCR+ESP+WFGD	330MW	90%
#2		SCR+ESP+WFGD+WESP	330MW	90%
#3		SCR+ESP+WFGD+WESP	1000MW	100%
#4		SCR+ESP+WFGD+WESP	1000MW	100%
#5		SCR+FF+WFGD	600MW	90%
#6	垃圾焚烧锅炉	FFs+NID+absorption tower		
#7	生物质燃烧锅炉	SCR/SNCR+Ultrasonic Dedusting		

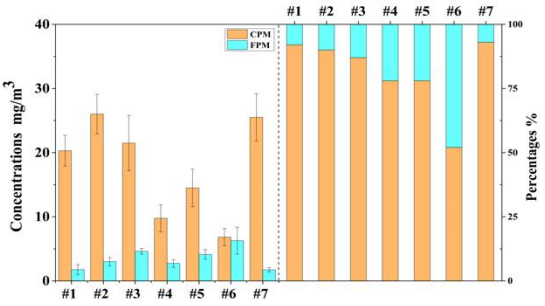

Fig. 1 Mass concentrations and Percentages of CPM and FPM.

关键词：可凝结颗粒物；固定源；SO_4^{2-}；生物质燃烧锅炉

论文编号：01–42

中韩两国典型城市冬季$PM_{2.5}$化学组分特征对比

刘亚妮[1,2]，任丽红[2]，王慧超[3]，李刚[2]，张佳浩[2]，任丽红[2,*]，

[1]兰州理工大学，兰州市，730050

[2]中国环境科学研究院，北京，100012

[3]齐齐哈尔大学，黑龙江，161000

*Email: renlh@craes.org.cn

摘要正文：

为对比研究中韩两国典型城市冬季$PM_{2.5}$的污染特征及主要来源，于2018年12月5日~2019年1月30日在天津、上海、青岛、济州、首尔和仁川6个城市采集 $PM_{2.5}$样品，对 $PM_{2.5}$质量浓度及其化学组分（碳组分和水溶性离子）进行测定分析。结果显示,采样期间中国3个城市（天津、上海和青岛）的$PM_{2.5}$平均质量浓度分别为117.0±66.9μg/m³，31.2±25.6μg/m³，74.9±54.6μg/m³，日均值的最高值分别为280.8，113.1和273.5μg/m³，分别是国家《环境空气质量标准》（GB 3095-2012）日均二级标准限值（75μg/m³）的3.7，1.5和3.6倍，采样期间日均值的超标率分别为44.1%，6.67%和34.0%，相对而言，天津和青岛冬季$PM_{2.5}$污染严重，上海较好。韩国3个城市（济州、首尔和仁川）的$PM_{2.5}$平均质量浓度分别为16.39±10.43μg/m³，38.26±25.40μg/m³ 和44.93±29.93μg/m³，日均值的最高值分别为51.9，137.2和148.4μg/m³，分别是韩国国家日均二级标准限值（35μg/m³）的1.5，3.9和4.2倍，采样期间日均值的超标率分别为5.7%，35.3%和44.1%，相对而言，首尔和仁川冬季$PM_{2.5}$污染严重，济州较好。从6个城市对比来看，在采样期间，天津、青岛和仁川的$PM_{2.5}$均值和日超标率略高于首尔，上海和济州，故他们的$PM_{2.5}$污染情况更应该引起重视。

由化学分析得到，本次采样的6个城市$PM_{2.5}$的主要组分是二次无机盐（SO_4^{2-}, NO_3^-和NH_4^+）和有机物OC。中国3个典型城市二次无机盐的平均浓度分别为35.1±42.9μg/m³，12.9±14.6μg/m³和35.4±34.2μg/m³，其在$PM_{2.5}$中的占比分别为23.2%，41.8%和42.1%；OC的平均浓度分别为18.7±8.0，8.4±5.2和16.5±8.9，其在$PM_{2.5}$中的占比分别为17.8%，31.7%和25.0%。韩国3个典型城市（济州、首尔和仁川）二次无机盐的平均浓度分别为9.6±9.1μg/m³，16.4±18.9μg/m³和22.9±23.9μg/m³，其在$PM_{2.5}$中的占比分别为52.0%，38.6%和47.1%；OC的平均浓度分别为3.1±1.2，7.3±3.0和9.2±3.5，其在$PM_{2.5}$中的占比分别为22.2%，21.7%和25.4%。

采样期间，天津、上海、青岛、首尔和仁川5个城市的二次无机盐组分浓度特征均呈现为$NO_3^- > SO_4^{2-} > NH_4^+$，而济州的呈现为$SO_4^{2-} > NO_3^- > NH_4^+$，因为$SO_4^{2-}$的气态前体物为$SO_2$，大气中$SO_2$主要来自工业化石燃料的燃烧与居民燃煤，另一个自然来源是海洋，NO_3^-的气态前体物为NO_x，主要为NO和NO_2，城市大气来源主要包括机动车尾气排放和工业生产排放。天津、上海、青岛、首尔和仁川当前排放源以机动车为主，而济州是个岛屿城市，故济州地区高浓度的硫酸盐部分来源于海洋。其排放差异性使得组分特征也有所不同。

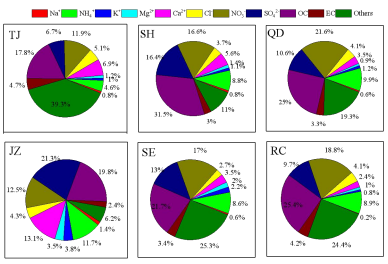

Fig.1 Contribution of ionic constituents to $PM_{2.5}$ mass measured in six typical sities between China and Korea

关键词：典型城市；$PM_{2.5}$；水溶性离子；碳组分

论文编号：01–043

汾渭平原四城市秋冬季$PM_{2.5}$的化学组成与来源解析

李致宇[1,2]，蔺悦[1,2,3]，张新[1,2,3]，曹军骥[1,2]，韩月梅[1,2,*]

[1]中国科学院地球环境研究所，西安 710061

[2]中国科学院气溶胶化学与物理重点实验室，西安 710061

[3]中国科学院大学，北京 100049

*Email: yuemei.han@ieecas.cn

摘要正文：

汾渭平原地区作为我国当前三大$PM_{2.5}$污染管控区域之一，在秋冬季仍面临着严重的大气污染问题，首要的污染物为大气细颗粒物（$PM_{2.5}$）。为深刻认识该地区城市大气$PM_{2.5}$的污染特征及来源，本研究于2018年11月至2019年1月在西安、咸阳、宝鸡和铜川四个主要城市同步采集秋冬季大气$PM_{2.5}$滤膜样品。基于测定的$PM_{2.5}$质量浓度与各化学组分含量（碳组分、水溶性离子组分、元素组分），阐明该地区的$PM_{2.5}$质量浓度及其主要化学组分的时空分布特征。利用正交矩阵因子分析法（PMF）对各城市$PM_{2.5}$的污染来源进行了定量解析。运用气团后向轨迹模型对各城市$PM_{2.5}$的传输路径以及潜在污染源区进行了深入分析。根据研究结果，对该地区大气$PM_{2.5}$的污染防控提出有针对性的措施和建议。研究期间各城市的$PM_{2.5}$平均质量浓度均超过了国家空气质量二级标准日均值（75 μg m^{-3}）。其中咸阳与西安的$PM_{2.5}$污染最为严重，平均质量浓度分别为112与111 μg m^{-3}；宝鸡与铜川的污染相对较轻，平均浓度分别为90与84 μg m^{-3}。碳组分分析表明西安、宝鸡和铜川的OC与EC的相关性较好表明三城市的OC与EC来源较为一致；而咸阳的OC与EC相关性较差，表明其OC与EC可能来自于不同的污染源。四城市有机碳与元素碳比值的平均值均在3.7—4.2之间，说明四城市的二次有机碳在碳组分中的占比接近。水溶性离子组分分析结果显示，NO_3^-、SO_4^{2-}和NH_4^+为四城市中含量最高的水溶性离子组分，三者浓度加和均超过了总离子浓度的80%，表明各城市都存在较多的二次污染物。运用富集因子法对元素的来源进行初步分析，发现受自然源的影响的元素为Al、Si、Ca、Ti和V，受自然源和人为源的共同影响的元素有Cr、Mn和Ni，主要受人为源的影响的元素包括Cu、As、Pb和Zn。PMF对四城市$PM_{2.5}$解析出六种染源，包括二次形成、生物质燃烧、燃煤、扬尘、机动车和工艺过程排放。其中二次形成、生物质燃烧与燃煤源在各城市中均为主要的来源，对各城市的贡献分别为：西安（29%、24%和21%），咸阳（34%、22%和13%），宝鸡（37%、15%和11%），铜川（31%和21%、13%）。铜川市的机动车源贡献为24%，显著高于其他三个城市（西安10%，咸阳11%，宝鸡13%），可能是由于铜川相较于其他城市人口较少且其经济工业活动较少，同时该城市处于交通要道，过境的重型运输车辆产生较多排放，导致机动车源贡献显著高于其他城市。气团后向轨迹分析表明，四个城市$PM_{2.5}$的潜在污染源区在河南、山西省等人口密集、工业集中且大气细颗粒物污染严重的区域。为有效控制汾渭地区的$PM_{2.5}$污染，应注重削减气态前体物的排放，减少二次污染物的生成；同时落实生物质燃烧和燃煤的管控措施，减少一次污染源的排放；并加强整个汾渭平原地区的大气细颗粒物的联防联控综合治理，避免区域传输造成的污染扩散问题。

关键词：$PM_{2.5}$；化学组成；来源解析；潜在源区；污染管控

论文编号：01–044

新冠疫情前后棕碳气溶胶光学特征及污染来源变化分析—以西安市为例

张 勇[1,2]，王启元[1,2,*]，田 杰[1]，曹军骥[1,2,*]

[1] 中国科学院地球环境研究所 黄土与第四纪地质国家重点实验室，中国科学院气溶胶化学与物理重点实验室，西安，710061

[2] 中国科学院大学，北京 100049

*Email: wangqy@ieecas.cn; jjcao@ieecas.cn

摘要正文：

2020年1月底，由于湖北武汉突然爆发新型冠状病毒疫情，基于防控需求，全国范围内均实行了强制隔离管控措施，使得人为活动水平及工业活动水平大幅度降低，这为探讨研究人为活动对气溶胶影响创造了天然条件。本研究基于美国Magee公司生产的AE-33黑碳测量仪（Aethalometer）对新冠疫情前后（2020年1月1日至2月9日）西安市大气中多波段（370nm、470nm、520nm、590nm、660nm、880nm和950nm）光学吸收进行测量，并对棕碳（Brown Carbon, BrC）气溶胶光学特征展开分析；同时利用美国Aerodyne公司生产的气溶胶化学成分在线监测仪（ACSM）对西安市大气颗粒物化学组分进行同步观测。初步研究表明疫情爆发前期（2020年1月1日至1月24日）370nm、470nm、520nm、590nm和660nm波段下的棕碳吸收系数分别为64.8±41.8 Mm^{-1}, 26.0±16.6 Mm^{-1}, 14.5±9.3 Mm^{-1}, 10.2±6.5 Mm^{-1}和5.2±3.5 Mm^{-1}；占各波段下的总吸收比例分别为36±8%, 23±5%, 16±4%, 13±3%和8±2%。疫情防控期（2020年1月25日至2月9日）370nm、470nm、520nm、590nm和660nm波段下的棕碳吸收系数分别为42.6±32.8 Mm^{-1}, 17.1±11.5Mm^{-1}, 9.9±6.2 Mm^{-1}, 6.9±4.2 Mm^{-1}和3.8±2.3 Mm^{-1}，相对疫情前各波段下的吸收均下降30%左右；占各波段下的总吸收比例分别为39±10%, 26±6%, 19±4%, 16±3%和11±2%，相对疫情前各波段的棕碳吸收占比均略有提升。除此之外，基于ACSM观测的颗粒物有机物组分信息，对西安市疫情前后的有机物来源进行了解析。在有机物来源解析的基础上，结合颗粒物棕碳吸收系数，利用多元线性回归（MLR）方法对棕碳吸收的来源进行了深入分析，探讨了新馆疫情前后棕碳吸收的来源变化特，同时也对不同有机气溶胶的棕碳吸收质量系数（MAC）进行了探讨分析。

关键词：新冠疫情；棕碳；光学特征；来源解析

参考文献

[1] Q. Y. Wang, J. H. Ye, Y. C. Wang, et al. Wintertime Optical Properties of Primary and Secondary Brown Carbon at a Regional Site in the North China Plain, Environmental Science & Technology 2019 53 (21), 12389-12397.

[2] V. Moschos, N. K. Kumar, K. R. Daellenbach, et al. Source Apportionment of Brown Carbon Absorption by Coupling Ultraviolet–Visible Spectroscopy with Aerosol Mass Spectrometry, Environmental Science & Technology Letters 2018 5 (6), 302-308

[3] N.Y. Kasthuriarachchi, L. H. Rivellini, M. G. Adam, et al. Light Absorbing Properties of Primary and Secondary Brown Carbon in a Tropical Urban Environment, Environmental Science & Technology 2020 54 (17), 10808-10819

论文编号：01–045

光化学氧化二次有机气溶胶在新冠肺炎疫情期间的形成增强

钟昊斌[1]，黄汝锦[1,*]

[1]中国科学院地球环境研究所，陕西省西安市雁塔区雁翔路 97 号，710061

*Email: rujin.huang@ieecas.cn

摘要正文：

2019年末发生的新冠肺炎(COVID-19)大流行严重影响了人们的经济和社会活动模式，导致全球范围内人为排放的大幅减少。然而，尽管一次排放在封锁期间大幅减少，在中国东部和北部等一些特大城市仍出现了严重的重霾污染事件。为了进一步了解原因，我们使用飞行时间质谱气溶胶化学组分监测仪在中国西北的背景点对整个期间进行了连续观测分析，其中包括国家颁布全国封闭(2020年1月23/24日)的前三周和后两周。结果显示，在全国封闭期间，光化学氧化相关的二次有机气溶胶(OOA)从封闭前的3.2±1.6 微克每立方米(占总有机气溶胶的24%)增长至封闭后的4.5±1.3微克每立方米(占总有机气溶胶的54%)，也是疫情后唯一绝对浓度上升的污染物。OOA的增加可能是由于在封闭期间氮氧化物排放的大幅减少导致臭氧和大气氧化能力的大幅增加导致。此外,我们发现OOA的占比在封闭期间一直占主导,然而,在高气溶胶液态水含量(ALWC)条件下大量增加的液相氧化生成的二次有机气溶胶(aqSOA)则可能是封锁期间污染事件发生的主要原因。因此，在严格管控条件下所产生的二次有机气溶胶的增强可能是在未来减排控制政策下不可忽视的问题。

关键词：新冠病毒；光化学氧化二次有机气溶胶；液相二次有机气溶胶；全国封闭；二次生成

论文编号：01–046

利用单颗粒气溶胶质谱仪探讨新冠疫情前和期间关中城市气溶胶颗粒物的化学组分特征

李丽[1]，王启元[1,*]，曹军骥[1,*]

[1]中国科学院地球环境研究所，陕西 西安，710061

*Email: wangqy@ieecas.cn

摘要正文：

在 2019 年的新冠状病毒爆发期间，我国采取了严格限制人为活动的一系列措施，引起污染物排放浓度的差异，为研究人为排放对空气质量的影响提供契机。针对此次疫情封锁前和封锁期间，本文利用单颗粒气溶胶质谱仪（SPAMS）在关中城市地区开展气溶胶颗粒物连续观测活动。与封锁前相比，封锁期间 $PM_{2.5}$ 的质量浓度下降了 24.6%，SO_2、CO 和 NO_2 分别下降了 16.2%、25.7%和 59.6%。根据 ART-2a 分析方法，得到 10 种具有不同质谱特征的颗粒类型：Dust、EC-aged、EC-fresh、NaK-SN、Lev、Metal、OC、OCEC、Other和 PAH，它们在控制前期的占比是：2.3%、31.5%、0.5%、42.2%、12.1%、1.0%、5.3%、1.9%、0.9%、2.2%；在控制期间的占比是：1.1%、23.7%、0.5%、54.0%、12.6%、0.5%、1.8%、0.6%、1.1%、4.2%。对比封锁前和期间不同化学组分的颗粒物的占比可以发现 EC-aged、NaK-SN、OC 和 PAH 的变化较为显著，占比较大的 Lev 在两个阶段基本保持不变，说明生物质排放稳定。粒径分布图显示限制期间的颗粒物的浓度普遍较限制前大，这可能是因为在限制期间气体污染物发生二次反应转化为固态物质，且附着在气溶胶颗粒物的表面，从而引起颗粒物的粒径发生不同程度的增大。不同类型颗粒物与一次（Cl^- , Lev）和二次（HSO_4^- , NO_3^- , NH_4^+, Oxalate）物种的混合态结果表明，硫酸盐和硝酸盐在控制前和期间的混合态基本相同，二次有机组分在控制期间与 OCEC 的占比显著升高，草酸盐在控制器件的混合态普遍高于控制前。通过对比新冠肺炎封锁前和期间的化学组分、粒径和混合态特征，有助于我们了解人为源排放浓度降低后大气污染的成因。

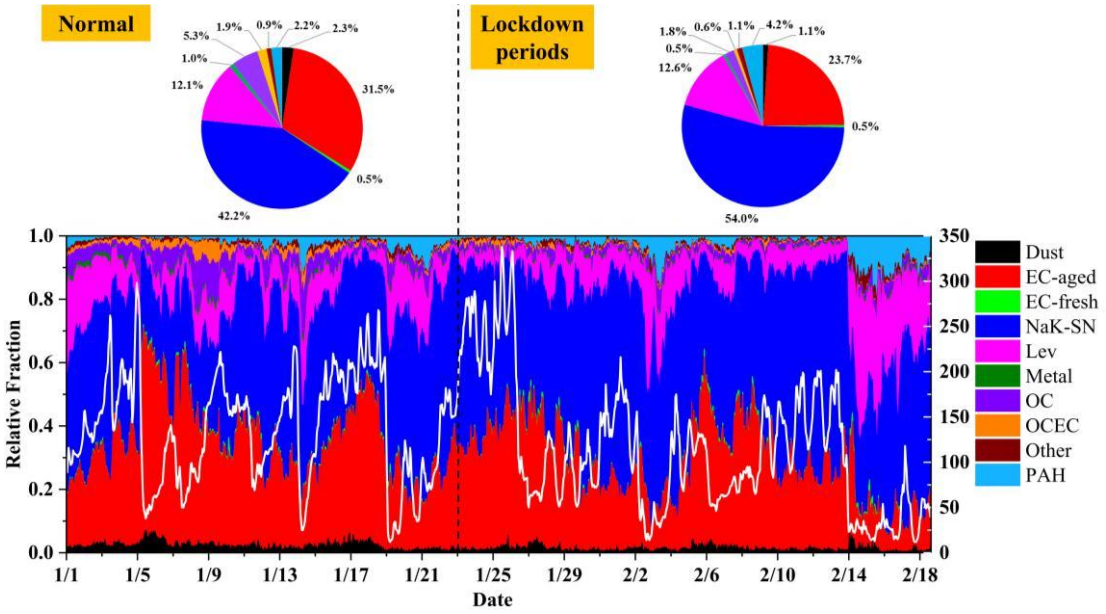

Fig. 1 Pie chart and time series of relative fraction of 10 groups

关键词：新冠疫情；单颗粒；化学组分；混合态

论文编号：01–047

Significant Enhancement of α-Pinene SOA with Organic Seed

江浩[1]，丁翔[1,*]

[1]中国科学院广州地球化学研究所，广州市科华街 511 号，510640

*Email: xiangd@gig.ac.cn

Abstract：

The impact of organic seed and aging on transformation of secondary organic aerosol (SOA) was studied by a series of chamber experiments using polyethylene glycol (PEG) as organic seed, which has controlled viscosity and stability in atmosphere. SOA formed from α-pinene ozonolysis was aged by HONO under UV lamp condition in chamber. Condensed-phase compounds were collected twice that the first were collected after all α-pinene consumed and the second were after aging period. Samples were analyzed by Fourier transformation ion cyclotron resonance mass spectrometer (FT-ICR MS) with ultra-high-resolution (m/Δm=1,000,000) to get comprehensive information on chemistry composition. Results demonstrate that the yield of α-pinene ozonolysis SOA increased from 9.9% to 30.2% with the addition of PEG, indicating the presence of organic seed promotes the formation and growth of SOA and implying the possibility of potential ambient atmosphere aerosol missed in model. Moreover, the yields of SOA with organic seed also fit to two-product model, which means we could simulate the formation of SOA with organic seed. Addition of PEG changed the distribution of organic compounds in condensed-phase. Monomers (≤C10) and dimers (C11-20) compounds increase substantially when SOA formed with PEG seed, however no significant increase was observed on higher polymers as trimer (C21-C30), indicating organic seed may change particle-gas partition that allow more low-volatile compounds condensed into particle phase. We compared compounds distribution before/after aging and found similar changes in molecular characteristic of both kinds of SOA. Monomers and dimers already existed before aging decrease obviously, on the contrary, higher polymers increase slightly. In particular, some of the most reduced substances in the monomer have a high oxygen content (nc≥5). There are a few newly formed substances with a high molecular weight (dimer or higher polymer) and a low oxygen content (nc≤3), which may represent oligomerization and fragmentation processes.

Key Words: Organic Seed, Aging, FT-ICR MS

论文编号：01–048

Polycyclic aromatic hydrocarbons emissions from traditional way of rural heating

Yue Zhang[1], Zhenxing Shen[1,*], Junji Cao[2]

[1]Department of Environmental Science and Engineering, Xi'an Jiaotong University, Xi'an, 710049, China

[2]Key Lab of Aerosol Chemistry & Physics, SKLLQG, Institute of Earth Environment, Chinese Academy of Sciences, Xi'an, 710049

*Email: zxshen@mail.xjtu.edu.cn (Zhenxing Shen)

Abstract：

To characterize emissions of polycyclic aromatic hydrocarbons (PAHs) from rural heating in field environments, fine particle ($PM_{2.5}$) samples were collected from the burning of six types of biomass in Heated Kang—a low-efficiency traditional heating stove in rural areas. The emission factors (EFs) of total PAHs ranges from 84.5-344 mg/kg with a variation up to a factor of 4. The EFs decreased with the increase in fuel density, where highest and lowest were achieved by wheat straw and apple wood trunk, respectively. Four subgroups, namely, Parent PAHs, oxygenated PAHs, alkylated PAHs, and nitrated PAHs, accounted for 81.1%, 12.6%, 6.2% and 0.1% of the total PAHs EFs, respectively. And $PM_{2.5}$-bound PAHs profiles remained stable among all the fuels tested, where PHE, 9FO and 2N-BIP stand out for their highest abundances in each subgroup and thus be categorized as characteristic species for domestic biomass burning source.

Key words: Biomass burning, Field experiments, emission factors, source profiles

论文编号：01–049

Composition and light absorption of aromatic compounds in a coastal city of south China

Ziyi Li[a], Qian Zhang[a,*]

[a] Key Laboratory of Northwest Resource, Environment and Ecology, MOE, Xi'an University of Architecture and Technology, Xi'an 710055, China

*E-mail: zhangqian2018@xauat.edu.cn

Abstract：

The aromatic compounds were important light-absorbing organic aerosols at near-ultraviolet-visible wavelengths, which affect global climate change and human health. Here, day- and nighttime $PM_{2.5}$ mass, nitrated aromatic compounds (NACs) and polycyclic aromatic hydrocarbons (PAHs) were measured on selected representative days from 11 April to 15 May 2017 in Sanya city, China. The results showed that the total light absorption coefficient (b_{abs}) of methanol-soluble organic carbon (Mb_{abs}) was 2.2 times higher than that of water-soluble organic carbon (Wb_{abs}) during sampling days, highlighting that water-insoluble organic matter were dominated in light absorbing organic compounds. Strong relationships among Mb_{abs}, NACs (nitrophenol, nitrocatechols and dimethyl-nitrophenol) and combustion-derived PAHs species ($r>0.65$, $P<0.001$) were observed in daytime indicated that light absorbing aromatic compounds mainly influenced by complex sources, including gasoline combustion, biomass burning and secondary formation. In contrast, the Mb_{abs} at night only showed high correlations with secondary NACs ($r>0.65$, $P<0.001$). Additionally, typical ship emission tracers accounted for 84.3% and 15.7% in alkanes and PAHs in daytime, whereas, those of them low to 81.3% and 12.8% in nighttime.

论文编号：01–050

联合AP-42法和TRAKER法的城市道路扬尘颗粒物排放的检测方法研究

李冬[1]，陈建华[1,*]，张月[1]，高健[1]，张凯[1]，竹双[1]

[1]中国环境科学研究院，北京 100012

*Email: lidong_craes@163.com

摘要正文：

道路扬尘是城市大气颗粒物的主要来源之一，研究道路扬尘颗粒物排放对城市大气颗粒污物治理具有重要意义。积尘负荷（sL）是计算道路扬尘排放量、反映道路扬尘排放的重要参数之一，美国环保署（EPA）在AP-42指导文件中已给出了测定sL的方法和步骤。然而，AP-42法需要在实际路面手工采样，耗费大量人力物力且不安全。与之相比，近年来基于车载的TRAKER法被广泛应用于测量道路扬尘排放潜势（θ），TRAKER法具有快速、安全、实时、动态的特点。本研究旨在联合应用AP-42法和TRAKER法提高检测便利性，并分析保定市道路扬尘排放特征。为实现此目标，本研究分别采用AP-42法和TRAKER法于2019年3月对保定市城区典型道路进行采样和走航检测，经过数据处理与对比分析，得出以下结论：

（1）分别基于两种不同方法获得的积尘负荷值与排放潜势之间具有较高相关性，其中线性拟合结果最好，拟合方程为sL=0.75·θ，相关系数约为0.88。说明利用TRAKER法及拟合方程可以获得sL，从而实现检测便利性。

（2）采用TRAKER法走航保定市城区道路，利用上述拟合方程计算不同道路的积尘负荷值发现：保定市道路污染状况整体表现为：城市外环路优于城市中心区域道路；不同类型道路按积尘负荷值大小排序表现为：快速路<主干道<次干道<支路。

（3）按照道路扬尘污染等级划分，保定市处于污染等级为“优”的道路约占8%；污染等级为“良”的道路约占28%；污染等级为“中”的道路约占36%；污染等级为“差”的道路约占28%。其中，支路在污染等级为“差”的道路中占比最高。

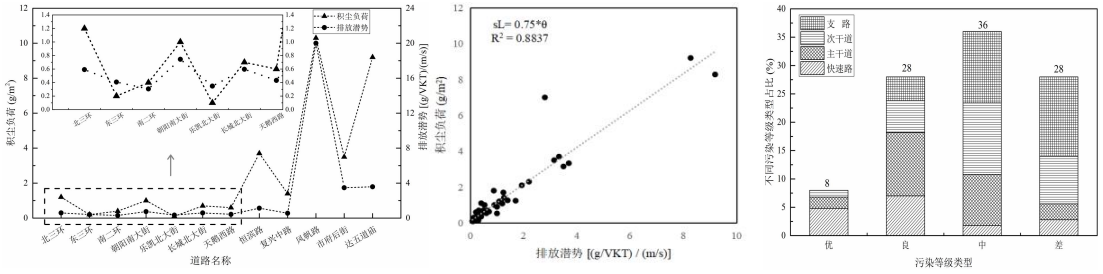

Fig. 1 The relationship of sL and θ

Fig. 2 Regression equations of sL and θ

Fig. 3 The proportions of pollution levels of different roads

关键词：AP-42法；TRAKER法；道路扬尘；颗粒物

参考文献

[1] V. Etyemezian, H. Kuhns, J. Gillies, et al. 2003. Vehicle-based road dust emission measurement (III):: effect of speed, traffic volume, location, and season on PM10 road dust emissions in the Treasure Valley, ID. Atmos. Environ. 2003, 37(32): 4583–459.

[2] H. Kuhns, V. Etyemezian, D. Landwehr, Testing re-entrained aerosol kinetic emissions from roads (TRAKER): A new approach to infer silt loading on roadways. Atmos. Environ. 2001,35(16), 2815–2825.

[3] 黄玉虎, 李钢, 杨涛, 等. 道路扬尘评估方法的建立和比较[J]. 环境科学研究, 2011, 24(1): 27-32.

[4] 张伟, 姬亚芹, 李树立, 等. 天津市春季典型道路积尘负荷分布特征[J]. 中国环境监测, 2018, 34(01): 54-59.

论文编号：01–051

青藏高原东缘冬季$PM_{2.5}$中碳组分特征和来源解析

张成虎[1]，吴丹[2]，郑小波[3]，赵天良[1,*]，夏俊荣[1]，王红磊[1]，吴明[4]

[1]南京信息工程大学大气物理学院，中国气象局气溶胶-云-降水重点开放实验室，气候与环境变化国际合作联合实验室，江苏 南京 210044

[2]南京信息工程大学环境科学与工程学院，江苏省大气环境与装备技术协同创新中心，江苏省大气环境监测与污染控制高技术研究重点实验室，江苏 南京 210044

[3]贵州省山地环境气候研究所，贵州 贵阳 550002

[4]河北省气象科学研究所，河北 石家庄 050021

*Email: tlzhao@nuist.edu.cn

摘要正文：

为了研究青藏高原$PM_{2.5}$中碳组分的化学特征,应用2017年冬季12月13~21日在青藏高原东缘地区理塘分昼夜采取的$PM_{2.5}$样品,分析测定了有机碳(OC)和元素碳(EC)的质量浓度.$PM_{2.5}$质量平均浓度为44.34μg·m^{-3},OC和EC的质量浓度分别为12.72和3.85μg·m^{-3},分别占$PM_{2.5}$质量浓度29.61%和8.96%.昼夜浓度对比显示,$PM_{2.5}$白天和夜间的质量浓度分别为53.88和33.44μg·m^{-3},OC和EC浓度白天高于夜间,白天人为排放相对较高.OC和EC较高的相关性表明OC和EC的来源相似,受燃烧源影响较大.冬季观测期间$PM_{2.5}$中二次有机碳SOC平均质量浓度为2.11μg·m^{-3},约占$PM_{2.5}$中OC的16.59 %,碳质气溶胶主要为一次来源.理塘$PM_{2.5}$中碳质气溶胶主要来源于机动车、燃煤以及生物质燃烧.

Tab. 1 Mass concentrations of OC and EC in the Tibetan Plateau region

采样点	采样时间	海拔高度(m)	颗粒物	OC(μg/m^3)	EC(μg/m^3)	OC/EC	分析方法
玉龙雪山	2014,15(冬)	4510	TSP	1.75±0.8	1.81±1.5	1.45±1.1	TOR
甘海子	2014,15(冬)	3054	TSP	4.09±1.7	2.42±0.74	1.93±1.58	TOR
纳木错	2012(冬)	4730	$PM_{2.1}$	3.69±0.33	0.21±0.08	17.6	TOR
鲁朗	2008(冬)	3300	TSP	3.65±1.07	0.58±0.16	6.45±1.68	TOR
青海湖	2011(冬)	3200	$PM_{2.5}$	3.88±1.60	1.05±0.52	4.15±1.81	TOR
本研究	2017(冬)	3948.9	$PM_{2.5}$	12.69±4.42	3.92±1.47	3.47±0.84	TOR

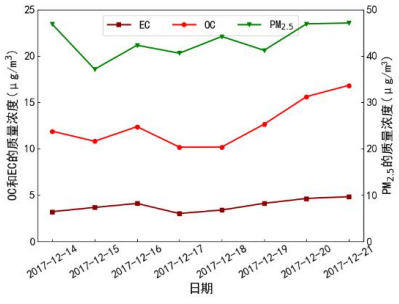

Fig.1 Temporal variation of mass concentrations of $PM_{2.5}$, OC and EC

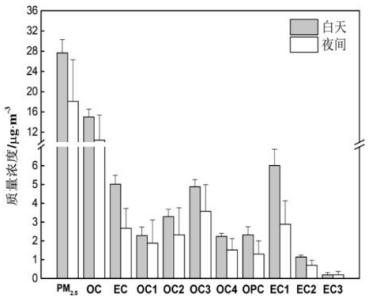

Fig.2 Diurnal variation of $PM_{2.5}$ and its carbon components in Litang

关键词：青藏高原东缘；有机碳(OC)；元素碳(EC)；昼夜差异；源解析

参考文献

[1] Kumar A, Attri A K. Biomass combustion a dominant source of carbonaceous aerosols in the ambient environment of Western

Himalayas [J]. Aerosol and Air Quality Research, 2015, 16(3): 519-529.

[2] 张伟, 姬亚芹, 李金, 等. 鞍山市夏冬季 PM2.5 中碳组分化学特征及来源解析[J]. 中国环境科学, 2017, 37(5): 1657-1662.

[3] Wang L P, Zhou X H, Ma Y J, et al. Carbonaceous aerosols over China-review of observations, emissions, and climate forcing [J]. Environmental Science and Pollution Research, 2016, 23(2): 1671-1680.

[4] Nunes T V, Pio C A. Carbonaceous aerosols in industrial and coastal atmospheres [J]. Atmospheric Environment. Part A. General Topics, 1993, 27(8): 1339-1346.

[5] Bond T C, Bhardwaj E, Dong R, et al. Historical emissions of black and organic carbon aerosol from energy-related combustion, 1850–2000 [J]. Global Biogeochemical Cycles, 2007, 21(2): 1-16.

[6] Turpin B J, Huntzicker J J. Identification of secondary organic aerosol episodes and quantitation of primary and secondary organic aerosol concentrations during SCAQS [J]. Atmospheric Environment, 1995, 29(23): 3527-3544.

[7] Ming J, Xiao C D, Du Z C, et al. An overview of black carbon deposition in High Asia glaciers and its impacts on radiation balance [J]. Advances in Water Resources, 2013, 55: 80-87.

[8] Wang M, Xu B Q, Cao J J, et al. Carbonaceous aerosols recorded in a southeastern Tibetan glacier: analysis of temporal variations and model estimates of sources and radiative forcing [J]. Atmospheric Chemistry and Physics, 2015, 15(3): 1191-1204.

[9] Hansen J, Nazarenko L. Soot climate forcing via snow and ice albedos [J]. Proceedings of the national academy of sciences, 2004, 101(2): 423-428.

[10] Ji D S, Li L, Pang B, et al. Characterization of black carbon in an urban-rural fringe area of Beijing [J]. Environmental Pollution, 2017, 223: 524-534.

论文编号：01–052

张家口周边城市和区域传输对$PM_{2.5}$浓度的贡献及其对区域大气污染联合治理的影响

李嘉鼎 [1,*]

[1] 南京信息工程大学气象灾害预报预警与评估协同创新中心

Email: 2835894212@qq.com

摘要正文：

2022年2月北京冬奥会部分赛事将在张家口崇礼举行，优良的空气质量是赛事成功举办和向世界展示中国形象的绝佳契机。张家口市颗粒物区域联合减排措施需要定量计算周边城市和区域$PM_{2.5}$贡献。WRF-CAMx-PSAT用于模拟2019年2月张家口周边城市和5种源类贡献。张家口市2月本地平均贡献为55%，发现3条传输通道分别是大同、乌兰察布和北京，贡献分别为15%、17%和18%。华北平原的其他城市$PM_{2.5}$可以沿北京至张家口的传输通道传输至张家口。张家口地区本地源类贡献最大为工业源，北京和大同对张家口贡献最大源也为工业源，乌兰察布贡献最大为居民源。计算出2019年2月份各城市各源对张家口贡献总量，为制定区域联合减排提供科学支撑。

关键词：大气污染；CAMx-PSAT模式；源解析；区域传输

参考文献

[1] An Z S, Huang R J, Zhang R Y et al. Severe haze in northern China： A synergy of anthropogenic emissions and atmospheric processes[J]. PNAS, 2019, 116(18)8657-8666.

[2] Chan C, and Yao X. Air pollution in mega cities in China[J]. Atmospheric Environment, 2008, 42(1): 1-42.

[3] Ding A, Wang T, Fu C. Transport characteristics and origins of carbon monoxide and ozone in Hong Kong, South China[J]. Journal of Geophysical Research: Atmospheres, 2013, 118(16):9475-9488.

[4] Epa U.S.E.P. 2013a. Cross-State Air Pollution Rule. https://www.epa.gov/csapr/cross-state-air-pollution-final-and-proposed-rules. 2014-04-25.

[5] Epa U.S.E.P. 2013b. Clean Air Interstate Rule. https://www.epa.gov/csapr. 2014-09-15.

[6] Foy B.D., Burton S.P., Ferrare R.A. et al. 2011. Aerosol plume transport and transformation in high spectral resolution lidar measurements and WRF-Flexpart simulations during the MILAGRO Field Campaign[J]. Atmospheric Chemistry and Physics, 2011, 11(7): 3543-3563

[7] Gao M, Carmichael G R, Wang Y et al. Modeling study of the 2010 regional haze event in the North China Plain[J]. Atmospheric Chemistry and Physics, 2016, 16(3): 1673-1691.

[8] Hsu A, Esty D C, Levy M A et al. Environment Performance Index[R]. New Haven, CT: Yale University, 2016.

[9] Huang Q, Cheng S, Li J et al. Assessment of PM 10 Emission Sources for Priority Regulation in Urban Air Quality Management Using a New Coupled MM5-CAMx-PSAT Modeling Approach[J]. Environmental Engineering Science, 2012, 29(5):343-349.

[10] JIA B, WANG Y, YAO Y et al. A new indicator on the impact of large-scale circulation on wintertime particulate matter pollution over China [J]. Atmospheric Chemistry & Physics, 2015, 15, 20: 11919-29.

[11] Jian W.U., Guo J., Zhao D. Characteristics of aerosol transport and distribution in East Asia[J]. Atmospheric Research, 2013, 132(10): 185-198.

[12] Kan H., Zhang X., Lin Y. The “APEC Blue” phenomenon: Regional emission control effects observed from space[J]. Atmospheric Research, 2015, 164-165: 65-75.

[13] Kim E, Hopke P K, Edgerton E S. Source identification of atlanta aerosol by positive matrix factorization[J]. Air Repair, 2003, 53(6):731-739.

论文编号：01–053

四川盆地城市群间大气污染物输送特征研究

杜欣欣[1,*]

[1]南京信息工程大学，南京，210044

*Email: duxinxin@nuist.edu.cn

摘要正文：

四川盆地特殊的环流形势和复杂的地形造成污染颗粒物难以扩散，外源污染物也难以进入盆地内部。此外，盆地区域颗粒物污染源类型繁多且复杂，区域内城市群大气颗粒物特征、输送特征也与单个城市大气完全不同。因此，深入研究大气颗粒物在区域内的迁移扩散规律，对区域大气颗粒物联防联控技术十分必要。本文对利用HYSPLIT模型对四川盆地大气颗粒物的扩散特征进行模拟，通过初始气象数据对HYSPLIT模型在四川盆地应用的敏感性分析，选择WRF高分辨率气象场作为HYSPLIT的驱动场进行2018年10月四川盆地内的大气颗粒物格点化扩散模拟。由此分析四川盆地内47个城市不同高度层颗粒物扩散特征，如图（a）展示了成都在100-300m高度的扩散特征，并结合气象条件及排放因素的影响，总结出不同高度层的传输通道。具体通道如下：（1）四川盆地近地面颗粒物输送途径存在三条主要路径：第一条，颗粒物沿川西平原向南输送；第二条，颗粒物沿遂宁→资阳→内江，在乐山汇聚；第三条，颗粒物从泸州引出东西向两条通道，向西进入乐山，向东进入江津，从而影响到重庆主城区，这使得颗粒物在四川东南部、重庆荣昌区、永川区形成涡流，川东南部的污染物难以扩散。（2）四川盆地低空存在三条主要路径：第一条，颗粒物从渝西部城市向遂宁出发分别在遂宁、资阳、南充汇聚；第二条，污染物由泸州出发，经宜宾、乐山汇聚于眉山以及向东经过江津、璧山汇集于重庆主城区。（3）四川盆地高空颗粒扩散途径有：雅安→眉山→成都西部→绵阳，之后继续向东扩散在巴中汇集；峨眉山→内江→大足→广安东部，之后继续向东北方向扩散至达州；宜宾→泸州→重庆主城区→石柱，最终扩散至四川盆地以外区域。另外，按照行政区域划分城市群，如图（b）所示，计算城市群间净传输通量，确定了城市间区域输送的相互影响关系，即：川南城市群在盆地内部具有明显净输入特征，川东北城市群对成都平原城市群有明显的传输作用。

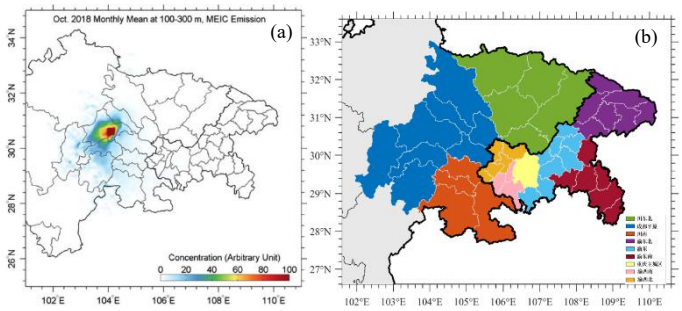

Fig. 1 (a) The distribution of the particulate matter concentration in one city, Chengdu, in the layers between 0-100m and (b) Divisions of urban agglomeration in Sichuan Basin

关键词：四川盆地；颗粒物；HYSPLIT扩散模拟；传输特征

论文编号：01–054

云南高原清洁大气环境背景下蒙自市$PM_{2.5}$和O_3相关性分析

路佩瑶[1]，赵天良[1*]，牛涛[2]，郑小波[3]，史建武[4]，张朝能[4]

[1]南京信息工程大学/中国气象局气溶胶-云-降水重点开放实验室/气候与环境变化国际合作联合实验室，江苏省南京市宁六路219号 210044

[2]中国气象科学研究院大气成分与环境气象研究所，北京市中关村南大街46号，100081

[3]贵州省山地环境气候研究所，贵州省贵阳市新华路翠微巷9号，550002

[4]昆明理工大学环境科学与工程学院，云南省昆明市景明南路727号，650500

*Email：tlzhao@nuist.edu.cn

摘要正文：

近年来蒙自市$PM_{2.5}$和O_3质量浓度均有所增加，分析两者的变化特征及其影响因素，对蒙自市大气环境治理具重要应用意义。应用蒙自市2015—2019年大气环境监测资料，分析云南高原清洁大气环境中$PM_{2.5}$和O_3之间的相互作用。结果表明：与云南高原夏季风盛行的雨季（5—10月）相比，东亚冬季风控制的云南高原干季（11月至次年4月）是蒙自市$PM_{2.5}$污染和O_3污染多发季节，但与中国中东部地区相比大气污染水平均较低。干季和雨季的$PM_{2.5}$和O_3变化均呈显著正相关，且干季相关性（r=0.62）大于雨季（r=0.43），两个相关性均通过了99%的置信检验，表明大气环境清洁的云南高原具有特殊的$PM_{2.5}$和O_3相互作用关系。基于气象和环境观测资料，进一步分析$PM_{2.5}$和O_3的相互作用潜在机理。云南高原低纬度的蒙自市总辐射曝辐量无明显干雨季节差异，这与云和降水对太阳辐射影响的干雨季节变化密切相关。雨季高温多云、降水集中，降水的湿沉降降低$PM_{2.5}$质量浓度，同时削弱到达地面的太阳直接辐射，减弱大气光化学反应的O_3产生；在云和降水缺少的干季，云对太阳辐射的减弱影响偏弱，大气光化学作用较为显著，O_3质量浓度较高，大气氧化作用较强，但无明显干雨季节差异。高原清洁大气中低浓度水平的$PM_{2.5}$季节性增加也难以有效地削弱到达地面的太阳直接辐射，对O_3的生成无明显的抑制作用。因此，清洁大气环境背景下云南高原低纬度城市大气复合污染主要表现为O_3主导的大气氧化性变化影响二次$PM_{2.5}$生成。

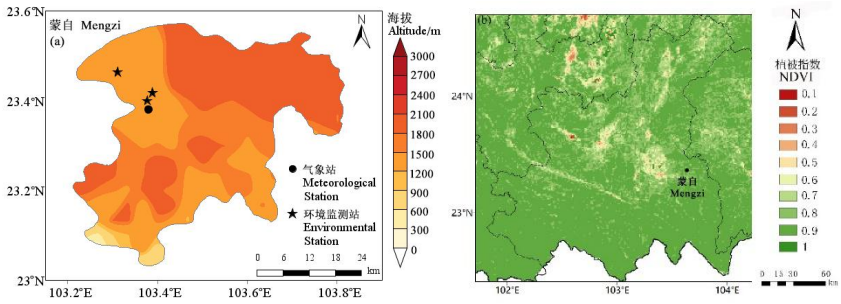

Fig. 1 The topography and location of air environmental monitoring site (a) and NDVI distribution of Mengzi (b)

Tab. 1 The seasonal differences of $PM_{2.5}$ in different levels in Mengzi in 2015–2019

Seasons	ρ/(μg·m^{-3})			Over limit rate
	≤35	35–75	>75	
Dry season	47.8%	46.4%	5.8%	3.6%
Rainy season	72.1%	26.4%	1.4%	

Tab. 2 The seasonal differences of $O_{3\_8\,h\_max}$ in different levels in Mengzi in2015–2019

Seasons	ρ/(μg·m^{-3})			Over limit rate
	≤100	100–160	>160	
Dry season	62.6%	36.3%	1.1%	1.1%
Rainy season	72.5%	26.4%	1.1%	

Tab. 3 The seasonal differences of atmospheric oxidation in different levels in Mengzi in 2015–2019 with the correlations passing significant level of 0.01

Seasons	OX/ (μg·m^{-3})	$\rho_{(O3)}$/ OX	OX and O_3 correlation
Dry season	84.37	0.86	0.99
Rainy season	72.29	0.85	0.99

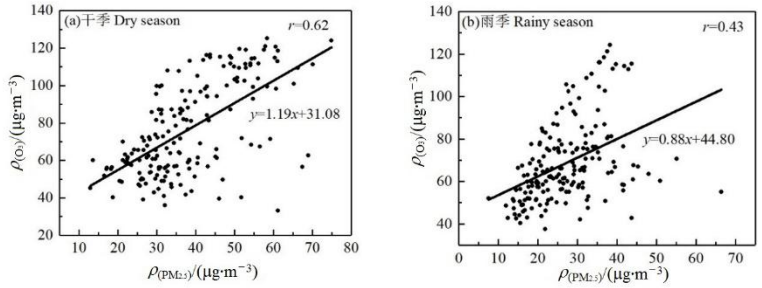

Fig. 2 Correlations of $PM_{2.5}$ and O_3 in 2015–2019 in Mengzi in (a) dry season and (b) rainy season

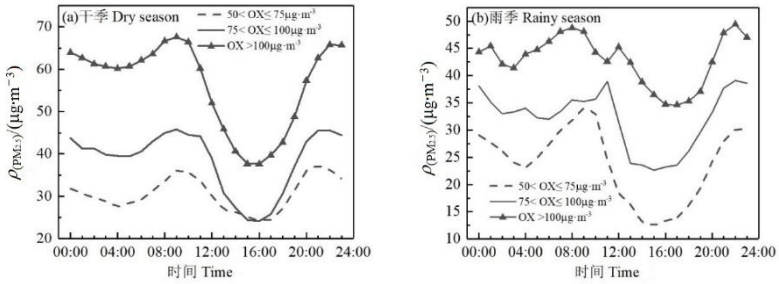

Fig. 3 Diurnal variation of $PM_{2.5}$ concentration at different OX levels (a) dry season (b) rainy season

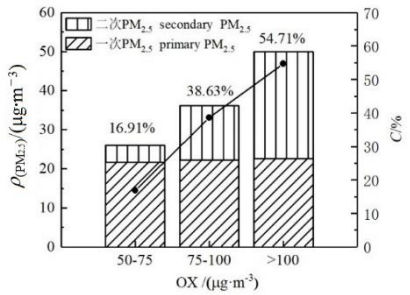

Fig. 4 The contribution of secondary $PM_{2.5}$ to $PM_{2.5}$ (C) under different levels of OX

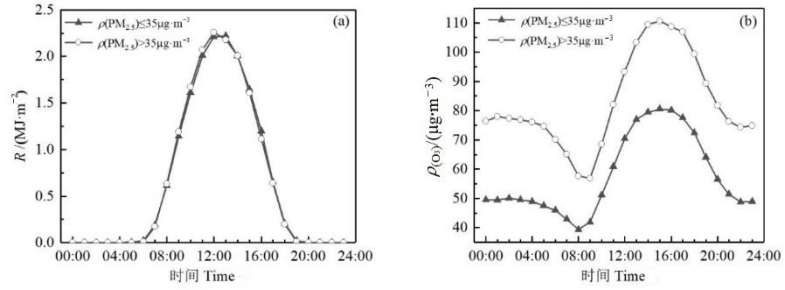

Fig. 5 Diurnal changes of (a) total radiation and (b) concentration of O_3at different $PM_{2.5}$ concentrations in Mengzi in 2015–2019

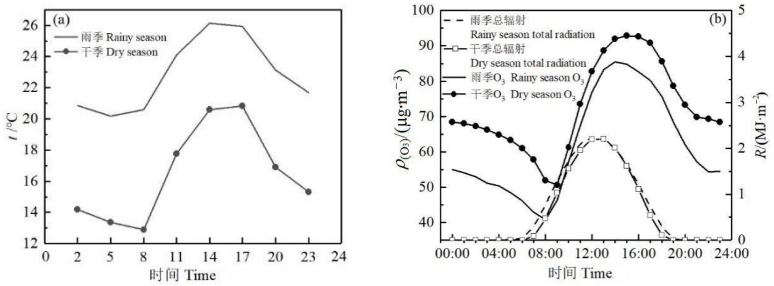

Fig. 6 Diurnal changes of (a) surface temperature, (b) O_3 and total radiation (R) in dry and rainy seasons in Mengzi in 2015–2019

关键词：$PM_{2.5}$；O_3；云南高原；清洁大气环境；大气氧化性

参考文献

[1] S. C. Chang, and C. T. Lee. Secondary aerosol formation through photochemical reactions estimated by using air quality monitoring data in Taipei City from 1994 to 2003 [J]. Atmospheric Environment, 2007, 41(19): 4002-4017.

[2] H. Chen, B. Zhuang, J. Liu, T. J. Wang, and M. Zhao. Characteristics of ozone and particles in the near-surface atmosphere in the urban area of the Yangtze River Delta, China [J]. Atmospheric Chemistry and Physics, 2019, 19(7): 4153-4175.

[3] V. T. F. Cheung, and T. Wang. Observational study of ozone pollution at a rural site in the Yangtze Delta of China [J]. Atmospheric Environment, 2001, 35(29): 4947-4958.

[4] L. J. Clapp, and M. E. Jenkin. Analysis of the relationship between ambient levels of O3, NO2 and NO as a function of NOx in the UK [J]. Atmospheric Environment, 2001, 35(36): 6391-6405.

[5] R. R. Dickerson, S. Kondragunta, G. Stenchikov, K. L. Civerolo, B. G. Doddridge, and B. N. Holben. The impact of aerosols on solar ultraviolet radiation and photochemical smog [J]. Science, 1997, 278(5339): 827-830.

[6] J. Ding and T. Zhu. Heterogeneous reactions on the surface of fine particles in the atmosphere [J]. Chinese Science Bulletin, 2003, 48(21): 2267-2276.

[7] M. W. Jia, T. L. Zhao, X. H. Cheng, S. L. Gong, X. Z. Zhang, L. L. Tang, D. Y. Liu, X. H. Wu, L. M. Wang, and Y. S. Chen. Inverse relations of PM2.5 and O3 in air compound pollution between cold and hot seasons over an urban area of east China [J]. Atmosphere, 2017, 8(12): 59.

[8] G. Li, N. Bei, X. Tie, and L. T. Molina. Aerosol effects on the photochemistry in Mexico City during MCMA-2006/MILAGRO campaign [J]. Atmospheric Chemistry and Physics, 2011, 11(3): 5169-82.

[9] X. Lu, J. Y. Hong, L. Zhang, O. R. Cooper, M. G. Schultz, X. B. Xu, T. Wang, M. Gao, Y. H. Zhao, and Y. H. Zhang. Severe surface ozone pollution in China: A global perspective [J]. Environmental Science and Technology Letters, 2018, 5(8): 487-494.

[10] D. D. Parrish, and T. Zhu. Clean air for megacities [J]. Science, 2009, 326(5953): 674-675.

论文编号：01–055

针对2022年张家口冬奥会$PM_{2.5}$源区变化的观测和模拟研究

陆汇丞[1]，赵天良[1,*]，马翠平[2]，孟凯[2]，顾尧[1]

[1]南京信息工程大学，江苏省南京市浦口区宁六路219号

[2]河北省环境气象中心，石家庄 050021

*Email：864904749@qq.com

摘要正文：

本文通过WRF-FLEXPART数值模拟，开展了冬奥会同期张家口$PM_{2.5}$周边源影响域的10年以上气候模拟研究，分析了其大气污染物周边源影响域的气候特征和边界划分，确定了对张家口市大气污染影响较大的源区，为科学制定2022年张家口冬奥会空气质量达标的污染治理对策提供保障。结果表明：2014-2020逐年2月张家口地区的$PM_{2.5}$污染天气共有8次；计算2010-2020年逐年2月张家口地区的$PM_{2.5}$贡献率后发现，本地贡献占54.83%，其次为乌兰察布、大同、呼和浩特，然而在污染天气发生时，本地贡献仅占35.13%，其次为大同、乌兰察布、呼和浩特。张家口地区发生$PM_{2.5}$污染天气时存在显著的区域传输，并存有鄂尔多斯-呼和浩特-乌兰察布-张家口这一污染物传输通道。

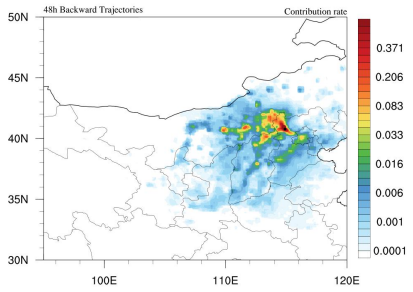

Fig. 1 Potential impact area of $PM_{2.5}$ in Zhangjiakou in February

Tab. 1 Pollution date and $PM_{2.5}$ concentration

日期		张家口	大同	太原	乌兰察布	呼和浩特	鄂尔多斯	北京	石家庄
年/月	日								
202002	11-13	27.31	12.02	0.73	7.87	5.11	7.44	10.48	2.02
202002	29	34.95	11.26	0.08	10.55	6.50	6.14	4.55	7.44
201902	5	38.52	8.69	0.00	14.93	18.22	12.31	3.80	0.01
201802	28	25.66	6.69	3.63	2.61	1.83	2.76	15.63	5.55
201702	15	33.33	14.49	0.00	14.07	13.57	11.92	0.00	0.00
201702	3	37.00	13.38	0.00	16.81	22.19	15.82	0.00	0.00
201602	12	63.10	14.34	0.02	9.30	4.87	3.03	0.32	0.00
201602	10	21.15	13.40	4.17	2.12	0.77	1.61	2.53	8.60
平均贡献率		35.13	11.78	1.08	9.78	9.13	7.63	4.66	2.95
11 年年均贡献率		54.83	5.97	0.97	15.7	5.66	3.25	2.68	1.66

关键词：WRF-FLEXPART；张家口；冬奥会；$PM_{2.5}$

参考文献

[1] 安俊岭，李健，张伟，等. 京津冀污染物跨界输送通量模拟[J].环境科学学报，2012，32(11) : 2684-2692.

[2] 薛文博，付飞，王金南，等.中国 PM2.5 跨区域传输特征数值模拟研究[J].中国环境科学，2014,34(6):1361-1368.

[3] 程真，陈长虹，黄成，等.长三角区域城市间一次污染跨界影响[J]．环境科学学报，2011，31(4)：686-694.

[4] 吴兑，吴晟，李菲，等. 粗粒子气溶胶远距离输送造成华南严重空气污染的分析[J].中国环境科学,2011,31(4):540-545.

[5] 孙彧, 牛涛, 马振峰. 中国雾霾分布特点以及华北霾环流特征分析[C]// S6 大气成分与天气气候变化. 2012.

[6] 胡晓宇，李云鹏，李金凤，等.珠江三角洲城市群 PM10 的相互影响研究[J].北京大学学报(自然科学版)，2011,47(3)：519-524.

[7] 刘晓慧,朱彬,王红磊,张恩红.长江三角洲地区 1980~2009 年灰霾分布特征及影响因子[J].中国环境科学, 2013, 33(11): 1929-1936.

[8] 李峰，朱彬，安俊岭，等. 2013 年 12 月初长江三角洲及周边地区重霾污染的数值模拟[J]. 中国环境科学，2015, 35(7): 1965-1974.

[9] 白永清，祁海霞，赵天良，杨浩，刘琳，崔春光.2018.湖北 2015 年冬季 PM2.5 重污染过程的气象输送条件及日变化特征分析[J] .气象学报，76（5）：803-815.

[10] 苏福庆,杨明珍,钟继红,等.华北地区天气型对区域大气污染的影响 [J].环境科学研究, 2004,17(3):16-20.

[11] 朱彤，尚静，赵德峰.大气复合污染及灰霾形成中非均相化学过程的作用[J]．中国科学：化学，2010，40（12）：1731-1740.

[12] C. Jiang, H. Wang, T. Zhao, et al. Modeling study of $PM_{2.5}$ pollutant transport across cities in China's Jing-Jin-Ji region during a severe haze episode in December 2013[J]. Atmospheric Chemistry and Physics, 2015,15:5803-5814.

[13] 邵平, 王莉莉, 安俊琳, et al. 河北张家口市大气污染观测研究[J]. 环境科学, 2012, 33(8):2538-2550.

[14] Pöschl U. Atmospheric aerosols: composition, transformation, climate and health effects [J]. Angewandte Chemie International Edition, 2005,44(46):7520-7540.

[15] González-Rocha, S.N., Cervantes-Pérez, J., Juárez-Pérez, F., González-Cerezo, Z.A., Velasco, L.R., Palomino-Méndez, I. and Recio, J.M.B. (2018) Circulation-Type Classification over Mexico by the Era-Interim Database and Cost733. Atmospheric and Climate Sciences , 8, 286- 305.

论文编号：01–056

黄石市黑碳气溶胶时间演变特征及来源分析

占长林[1,2,*]，张家泉[1,2]，郑敬茹[1,2]，刘红霞[1,2]，刘婷[1,2]，柳山[1,2]，刘先利[1,2]，肖文胜[2]

[1]湖北理工学院环境科学与工程学院，黄石，435003

[2]矿区环境污染控制与修复湖北省重点实验室，地址，435003

*Email: zhanchanglin@hbpu.edu.cn

摘要正文：

为研究黄石城区黑碳气溶胶的时间演变特征及黑碳来源，利用便携式七波段AE-42黑碳仪对2019年3月~2020年3月期间黑碳气溶胶进行实时观测，并对黑碳气溶胶的季节变化、日变化特征以及污染来源进行分析。结果表明，黄石的BC浓度具有明显的季节变化，冬季(2239±703.02 ng/m^3)＞春季(1918.48±216.67ng/m^3) ＞秋季(1615.09±649.04 ng/m^3)＞夏季(1466.39±332.15 ng/m^3)。四个季节日内变化有明显的双峰特征，峰值分别位于00:00~05:00和18:00~20:00。黄石城区BC浓度呈现白天高，夜间低的特征，说明白天黑碳气溶胶污染更为严重。根据气溶胶波长吸收指数AAE值的计算结果可知，AAE的年平均值为1.07，说明黄石城区黑碳气溶胶主要来源是来自化石燃料的燃烧。2020年1月21日黄石城区BC浓度出现异常高值，通过Hysplit后向轨迹模型判断本次污染事件主要受到东南亚生物质燃烧事件的影响，还可能受到邻近省份和湖北本地生物质燃烧的影响。

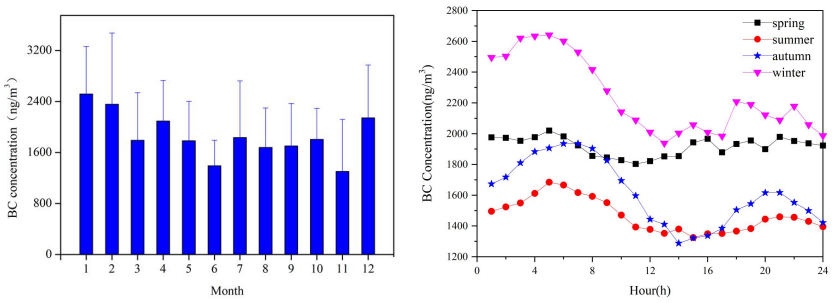

Fig. 1 (a) Annual variation in annual BC aerosol concentration; (b) Diurnal variation of BC concentration in different seasons

关键词：黑碳气溶胶；时间变化；来源解析；黄石市

论文编号：01–057

辽宁西南部典型城市$PM_{2.5}$及其化学组分季节变化

王慧超[1,]，刘亚妮[3]，李刚[2]，张佳浩[2]，任丽红[2*]

[1]齐齐哈尔大学，黑龙江省，161000

[2]中国环境科学研究院，北京市，100012

[3]兰州理工大学，甘肃省，73000

*Email:renlh@craes.org.cn

摘要正文：

为对比研究辽宁西南部典型城市葫芦岛市和朝阳市$PM_{2.5}$污染特征，本研究于2018年12月~2019年10月分别在葫芦岛市和朝阳市共采集$PM_{2.5}$样品75个，其中冬季(2018年12月3日~2019年1月1日，27个)，春季（2019年4月13日~2019年4月27日，14个），夏季（2019年7月2日~2019年7月19日，17个）及秋季（2019年10月13日-2019年10月31日，17个）。通过离子色谱仪和碳分析仪分别测试了9种水溶性离子和2种碳组分浓度，分析了不同季节$PM_{2.5}$的化学组分和污染特征。

结果表明：朝阳市 $PM_{2.5}$ 年均浓度分别为 49.47±22.49、45.65±20.91μg/m^3,分别超过国家环境空气质量标准（35μg/m^3）的 1.41 和 1.30 倍，葫芦岛市 $PM_{2.5}$ 浓度的季节变化表现为：秋季>冬季>夏季>春季（葫芦岛市），潮阳市 PM2.5 浓度的季节变化表现为：春季>秋季>冬季>夏季。

就水溶性无机离子的变化特征而言，9种水溶性无机离子分别占葫芦岛市和朝阳市$PM_{2.5}$的50%和42%，其中SNA(SO_4^{2-}、NO_3^-和NH_4^+)为主要的离子组分，占$PM_{2.5}$的39%和31%。两个城市3种主要水溶性无机离子的季节变化表现为：葫芦岛市（夏季>秋季>春季>冬季）和朝阳市（春季>夏季>秋季>冬季）。葫芦岛市和朝阳市SOR（硫氧化率）和NOR（氮氧化率）值均大于0.1，说明两个城市四个季节均存在明显的气溶胶二次转化过程。[NO_3^-]/[SO_4^{2-}]的结果表明葫芦岛市冬季和夏季主要以固定源为主，春季和秋季主要以移动源为主，朝阳市春季、夏季和冬季主要以固定源为主，秋季以移动源为主。

就碳组分而言，葫芦岛市和朝阳市OC和EC的浓度分别为7.0±4.5、2.7±1.8μg/m^3,7.4±4.4、2.6±1.9μg/m^3，碳组分（OC和EC）整体占$PM_{2.5}$浓度的19.7%和22.8%。本次研究的两个城市OC与EC的浓度均在春季和冬季较高，夏季和秋季变化不大；除葫芦岛市冬季、朝阳市夏季外OC与EC 的相关性较好，说明葫芦岛市和朝阳市的碳组分来源基本一致；OC/EC的比值在春季与秋季较高，在夏季和秋季无较大变化。

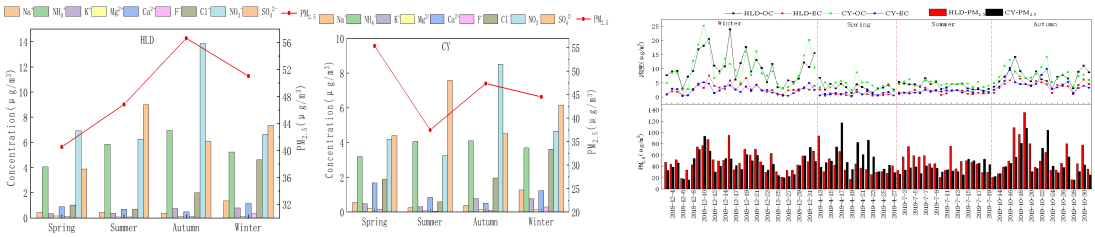

Fig. 1 $PM_{2.5}$ and ion concentration in different seasons in Huludao City and Chaoyang City

Fig.2 OC and EC time series of Huludao city and Chaoyang City

关键词：$PM_{2.5}$；水溶性无机离子；碳组分；OC/EC SOR

参考文献

[1] OHTA S,OKITA T.A chemical characterization of atmospheric aerosol in Sapporo[J].Atmospheric Environment Part A General Topics,1990,24(4):815-822.

[2] SHON Z,KIM K,SONG S,et al.Relationship Between Water-Soluble Ions in PM2. 5 and their Precursor Gases in Seoul Megacity [J].Atmospheric Environment,2012,59:540-550.

论文编号：01–058

基于3D-var的气溶胶多尺度资料同化和预报研究

胡译文[1,2]，臧增亮[2,*]，梁延飞[3]，张振东[1,2]，尤伟[2]

[1] 南京信息工程大学大气物理学院，江苏南京，210044

[2] 中国人民解放军国防科技大学气象海洋学院，江苏南京，211101

[3] 中国人民解放军 32145 部队，河南新乡，453000

*Email: zzlqxxy@163.com

摘要正文：

近年来，中国地区频繁出现以$PM_{2.5}$或以PM_{10}为首要污染物的大范围雾霾天气。研究表明，这类大范围气溶胶污染过程与稳定的大尺度环流背景、局地排放源、中小尺度天气系统以及光化学过程等因素密切相关（王跃思等，2014；张人和等，2014，张小曳，2014）。气溶胶的这种多尺度特征对大气化学模式的资料同化有重要影响。由于气溶胶污染分布除了受多尺度大气环流的影响，还与污染源的空间尺度及物理化学特征相关，对同化和预报的影响也更为明显。因此有必要对气溶胶的多尺度资料同化进行研究。

本文将利用WRF-Chem模式产品和NMC方法估计模式背景误差协方差，并基于气溶胶的多尺度谱特征，估计多尺度背景误差协方差，然后基于三维变分同化方法（3D-var）对2019年3月1日~2日的一次污染过程在两不同尺度上进行逐次同化，最后分别进行同化和预报试验。结果表明，多尺度同化更能提高同化气溶胶资料同化效果：相对于单纯的小尺度同化，多尺度和大尺度同化后得到的增量场范围更大，高值中心更高；与大尺度同化相比，多尺度同化的增量场能更反映出气溶胶的局地特征。对初始场的同化效果进行检验，结果表明多尺度同化后的初始场的RMSE和CORR分别为21.20μg m^{-3}和0.94，好于单纯的大/小尺度同化。对于气溶胶预报效果而言，同化后的预报试验都显著好于控制试验，影响时间超过24h，多尺度和大尺度同化试验要好于小尺度同化试验，但两者之间差异并不明显。对于如何更好的对多尺度同化进行组合还需要进一步的研究。

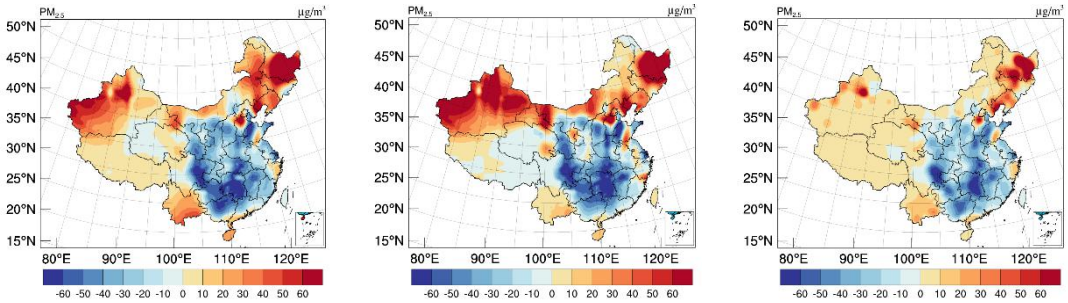

Fig. 1 the increment of $PM_{2.5}$ at initial time

(a)with Multi-scale background error covariance(BEC) (b) with large BEC (c) with small BEC

关键词：多尺度；气溶胶；资料同化；3D-var

参考文献

[1] 王跃思, 姚利, 王莉莉, 等. 2013 年元月我国中东部地区强霾污染成因分析[J]. 中国科学：地球科学, 2014, 44(1): 15-26.

[2] 张小曳. 中国不同区域大气气溶胶化学成分浓度、组成与来源特征[J]. 气象学报, 2014, 72(6): 1108-1117.

[3] 张人禾, 李 强, 张若楠. 2013 年 1 月中国东部持续性强雾霾天气产生的气象条件分析[J]. 中国科学:地球科学, 2014, 44(1): 27–36.

论文编号：01–059

Size Distribution and Health Risk Assessment of Water-soluble Metals in Atmospheric Particles over Xi'an, China

Xintian He[1], Hongmei Xu[1], Zhenxing Shen[1,2], Pingping Liu[1,2,*]

[1]Department of Environmental Science and Engineering, Xi'an Jiaotong University, Xi'an 710049, China

[2]SKLLQG, Institute of Earth Environment, Chinese Academy of Sciences, Xi'an 710061, China

*Email: Pingpingliu@mail.xjtu.edu.cn

Abstract:

Water-solubility of heavy metals is a major evaluation criterion for the bioavailability and thus toxicity. The size distribution and potential health risk of water-soluble metals in nine particle sizes < 0.43, 0.43-0.65, 0.65-1.1, 1.1-2.1, 2.1-3.3, 3.3-4.7, 4.7-5.8, 5.8-9, > 9 μm was investigated in Xi'an, China. The size distribution of water-soluble metals showed a typical bimodal distribution, with a dominant peak in the coarse mode (4.7-5.8 μm) and a minor peak in the fine mode (0.43-0.65 μm). In potential health risk assessment, ingestion was the leading exposure way, followed by dermal contact and inhalation. Water-soluble Cr and Pb showed obvious non-carcinogenic health risk both to children and adults, warrants special attention. Also, Cr had the highest incremental lifetime carcinogenic health risk (ILCR) of 8.68×10^{-6}, which was most contributed by the fine particles (< 0.65 μm), indicating more concerns need to be paid to fine particles.

Key words: heavy metals (HMs); bioavailability; seasonal variation; carcinogenic risk

论文编号：01–060

Water-soluble ion components of PM_{10} during the winter-spring season in a typical polluted city in Northeast China

Ye Hong[1], Yanjun Ma[1], Junying Sun[2,*], Chaoliu Li[3], Yunhai Zhang[1], Xiaolan Li [1], Deping Zhou [1], YangfengWang [1], Ningwei Liu[1]

[1]Institute of Atmospheric Environment, China Meteorological Administration, Shenyang 110166, China;

[2]State Key Laboratory of Severe Weather/Key Laboratory of Atmospheric Chemistry of China Meteorological Administration, Chinese Academy of Meteorological Sciences, Beijing 100081, China;

[3]Institute of Tibetan Plateau Research, Chinese Academy of Sciences, Beijing 100085, China

*Email: yehongofxf@126.com

Abstract:

From January 1 to April 22, 2014, an online analyzer for monitoring aerosols and gases (MARGA) was used to measure and analyze water-soluble ions in inhalable particulate matter with a diameter less than 10 μm (PM_{10}) during winter-spring in Shenyang city, China. The results yielded three main findings. (1) During the entire observation period and in 7 pollution episodes, SO_4^{2-}, NO_3^-, and NH_4^+ (SNA) accounted for 84.4%–93.1% of the total water-soluble ions (TWSIs). TWSIs accounted for 32% of PM_{10} mass during the entire observation period, and the contribution of TWSIs in PM_{10} ranged from 33.4%–43.1% in the 7 pollution episodes. The contribution of TWSIs components increased during the pollution episodes, but certain differences were observed in different pollution episodes. In terms of ionic equilibrium, the total concentration of negative ions was slightly greater than that of positive ions and the difference was 3.1% of total ion load on average, indicating that local aerosols are mainly neutral. The water-soluble ions show clear diurnal variation with the high concentration around 09:00 for SO_4^{2-}, NH_4^+ and Cl^- which is consistent with the high heating grade index.(2) Pollution episodes often occur in Northeast China, especially during the winter period. Due to the low temperature in winter, the local coal burning for heating is one of the main sources of pollution besides vehicle exhaust and industrial pollution, which is supported by the higher NO_3^-/SO_4^{2-} ratio in April than that in Jan.-March. Sometimes, under the prevailing wind directions, the long-distance transport of pollutants from the Beijing-Tianjin-Hebei region and Shandong province superimposed on local pollution leads to the most severe pollution, such as Ep3 and Ep5. (3) SO_4^{2-} concentration are closely related to ambient water vapor pressure (e*), with increase as e* increased depending on temperature. NO_3^- concentration showed a linear relationship of excess NH_4^+, which suggests homogeneous gas-phase reaction of ammonia and nitric acid is possibly an important pathways of nitrate formation in the haze pollution process in Shenyang City. In addition, our results also suggest the nighttime liquid-phase reaction may cause large increases of nitrate in the haze pollution process.

Key words: Haze; MARGA; PM_{10}; Shenyang; Water-soluble ions

论文编号：01–061

Description of Atmospheric Aerosol Dynamics Using an Inverse Gaussian Distributed Method of Moments

Jindong Shen[1], Mingzhou Yu[1]

[1]China Jiliang University, Hangzhou, China

Abstract:

For nearly 60 years, lognormal distribution has been the most widely used function in the field of atmospheric science for characterizing atmospheric aerosol size distribution. In this talk, we verify whether the three-parameter inverse Gaussian distribution (IGD) is a more suitable function than the lognormal distribution for characterizing aerosol size distribution. An attractive feature of IGD is that with it a new method of moments (MOM) can be established for resolving atmospheric aerosol dynamics—inverse Gaussian distributed MOM (IGDMOM). The advantage of IGDMOM is that all of its moments can be analytically calculated using a closure moment function inherited from IGD. The precision and efficiency of IGDMOM are verified by comparing it with other recognizable methods in test cases of four representative atmospheric aerosol dynamics. Several key statistical quantities determining aerosol size distributions, including k-th moments ($k = 0, \frac{1}{3}, \frac{2}{3}, \text{and } 2$), geometric standard deviation, skewness, and kurtosis, are evaluated. IGDMOM has higher precision than the lognormal MOM with nearly identical efficiency. In addition, the inverse Gaussian distributed method of moments (IGDMOM) (J. Atmospheric Sci. 77 (9): 3011, 2020) is developed to analytically solve the kinetic collection equation (KCE) for the first time. Using IGDMOM, we obtained both new analytical and asymptotic solutions to the KCE. This is shown for both the free molecular and continuum regime collision frequency functions. The new analytical solutions to the KCE is found to be very suitable for the demonstration of self-preserving size distribution theory (SPSD).

References

[1] Shen, J., M. Yu, T. L. Chan, C. Tu, and Y. Liu, 2020a: Efficient method of moments for simulating atmospheric aerosol growth: model description, verification, and application. J. Geophys. Res. Atmos., 125, 1–22, https://doi.org/10.1029/2019jd032172.

[2] Shen, J., M. Yu, and J. Lin, 2020b: Description of Atmospheric Aerosol Dynamics Using an Inverse Gaussian Distributed Method of Moments. J. Atmos. Sci., https://doi.org/10.1175/JAS-D-20-0077.1.

[2] Yu, M., J. Lin, J. Cao, and M. Seipenbusch, 2015: An analytical solution for the population balance equation using a moment method. Particuology, 18, 194–200, https://doi.org/10.1016/j.partic.2014.06.006.

论文编号：01–062

An evaluation of the ability to characterize aerosols by NASA's MERRA-2 Aerosol Reanalysis at WMO GAW regional background stations in eastern China

Xiaodan Ma[1], Peng Yan[2], Tianliang Zhao[1,*]

[1]Collaborative Innovation Center on Forecast and Evaluation of Meteorological Disasters, Key Laboratory for Aerosol-Cloud-Precipitation of China Meteorological Administration, Nanjing University of Information Science and Technology, Nanjing 210044, China

[2]CAWAS, Meteorological Observation Center of CMA, Beijing 100081, China

Abstract：

Using the data of PM10 (aerodynamic diameter less than 10μm) gravimetric concentrations and chemical compositions obtained from the routine sampling measurements at the World Meteorological Organization (WMO) the Global Atmosphere Watch (GAW) Programme regional background stations, Lin'An (LA) and JingSha (JS), in eastern China, we comprehensively evaluate the surface concentrations of PM10 and some of its chemical speciation such as sulfate [$SO4^{2-}$], organic carbon [OC] and black carbon [BC] derived from Aerosol Reanalysis of NASA's Modern-Era Retrospective Analysis for Research and Application, version 2 (MERRAero). Totally 302 and 156 PM10 samples collected respectively at LA and JS during the period from 2011 to 2013 are analyzed for the evaluations. Overall, the concentrations of PM10, SO42−, OC and BC from MERRAero agreed well with the measurements, despite a slight and consistent overestimation of BC concentration, and a moderate and consistent underestimation of PM10 concentrations throughout the study period. The MERRAero reanalysis of aerosol speciation performs better during the summertime than wintertime, especially in 2011. Considering the lack of nitrate [NO^{3-}] in MERRAero datasets, we estimate the MERRAero nitrate based on the observational ratio of [NO^{3-}] to [$SO4^{2-}$] to improve the PM10 mass reconstructions. It is found that the inclusion of nitrate particles can significantly improve model performance in reconstructed PM10 by increasing mean fraction of simulation and observation F from 0.64 up to 0.74 in LA site and 0.73 to 0.83 in JS site in our study period. Sensitivity experiments of MERRAero-nitrate calculation indicate that the yearly ratio of [NO^{3-}] to [$SO4^{2-}$] observation has the similar improvement with daily ratio of [NO^{3-}] to [$SO4^{2-}$]. Inclusion of nitrate based on the yearly ratio of [NO^{3-}] to [$SO4^{2-}$] would significantly improve the MERRAero's applicability in eastern China where nitrate contribution would be increasingly obvious in the future. The possible explanations for the observed discrepancies are discussed and the limitations of the study are listed.

论文编号：01–063

Assessing the contributions of meteorological changes and anthropogenic emissions to $PM_{2.5}$ decline from 2015 to 2019 over the Twain-Hu Basin, Central China

Xiaoyun Sun[1], Tianliang Zhao[1,*], Weiyang Hu[1]

[1] Key Laboratory for Aerosol-Cloud-Precipitation of China Meteorological Administration, Nanjing University of Information Science and Technology, Nanjing, China 210044

*Email: tlzhao@nuist.edu.cn

Abstract:

The annual mean $PM_{2.5}$ concentrations over the Twain-Hu basin (THB) decreased by 26% from 2015 to 2019. A modified Kolmogorov–Zurbenko (KZ) filter method was performed on the daily $PM_{2.5}$ concentrations to separate the contributions of different factors, and remove the influence of meteorological fluctuations on $PM_{2.5}$. Seasonal and short-term variations in meteorological and emission factors exerted the major influence on the rapid change in $PM_{2.5}$. The significant positive correlations between the long-term $PM_{2.5}$ and SO_2 trends indicated the important role of SO_2 emissions on $PM_{2.5}$ reductions. The changing anthropogenic emissions and meteorological conditions were both beneficial to the $PM_{2.5}$ decrease in the THB, with the northern cities more affected by meteorology than southern cities. Regarding the entire region, 28% of the $PM_{2.5}$ decrease was a result of the favorable meteorological conditions, and 72% of the decrease attributed to emission reductions, showing the large contribution of meteorology on the air quality in the THB.

Key words: Twain-Hu Basin; $PM_{2.5}$; KZ filter; Anthropogenic emissions;

论文编号：01–064

ENKF不同同化窗口对WRF-chem气溶胶预报的影响

张振东 [1,2]，臧增亮 [2]，陈丹 [3]，胡译文 [1,2]

[1] 南京信息工程大学大气物理学院，南京，210000

[2] 国防科技大学气象海洋学院，南京，210000

[3] 北京城市气象研究所，北京，100000

Email: NUIST_ZZD@163.com

摘要正文：

气溶胶作为重要的大气污染物，由于工业、汽车排放以及大气中各类污染物转化积累，易形成高浓度污染。因此精确预报气溶胶浓度分布对于社会生活和人体健康具有十分重要的意义。资料同化(Data assimilation)可以将观测资料融入模式，是目前提升大气化学模式预报精度的有效方法。其中，集合卡尔曼滤波（ENKF）是目前常见的资料同化方法，它不考虑伴随模式，且可以通过模式预报来不断更新背景误差协方差（Whitaker and Hamill, 2002; Pagowski et al., 2012 ）。同化窗口指同化更新模式的时间尺度，在气象要素的同化中，同化频率和同化窗口的选择会影响模式预报效果（刘君等，2013；冯佳宁等，2017；闵锦忠等，2015）。但目前大气污染物的同化窗口对于模式预报的影响尚不明确。另外，考虑ENKF往往需要30-50个集合成员，计算量较大，同化窗口过长将降低模式的预报效率。因此研究ENKF同化窗口对于气溶胶预报的影响具有重要意义。

本试验使用WRF-chem模式，选择MOSIC气溶胶方案模拟了2019年2月25日全国范围的$PM_{2.5}$和PM_{10}浓度。通过ENKF同化地面$PM_{2.5}$和PM_{10}观测资料对WRF-chem模式进行了初始场同化试验。其中同化频率为1h/次，同化窗口分别为1h,6h,12h，命名为DA01，DA06，DA12。比较不同同化窗口的发现（图2），同化后气溶胶浓度与观测更为接近,相比与同化前，相关系数（CORR）平均偏差（BIAS），均方根误差（RMSE）均有改善。比较不同同化窗口的同化效果发现，$PM_{2.5}$和PM_{10}的CORR和RMSE均在DA06中改进最明显，同化后$PM_{2.5}$的CORR为0.94，RMSE为22.90，$PM_{2.5}$的CORR为0.96，RMSE为30.51。BIAS则是DA01的同化窗口的结果最佳，同化后$PM_{2.5}$的BAIS为-5.8,PM_{10}的BIAS为-10.48。除此以外，为了分析不同同化窗口对预报效果的影响，利用同化后的分析场进行24h预报，结果如图3所示。对于$PM_{2.5}$而言，CORR，BIAS和RMSE的结果在24小时内均优于控制试验，不同同化窗口在预报的前12h的差异较明显。与分析场类似，对于CORR和RMSE的检验，DA06略优于DA12。但DA06和DA12的检验结果都比DA01更好，这主要是由于多次同化的效果能够吸收更多的观测信息，使得气溶胶浓度分布更接近实况。但就BIAS的效果而言，DA01则优于DA06和DA12。这很大程度上是由于在观测稀疏地区同化效果有限，多次同化放大了该地区同化不足的缺陷所导致的。总体而言，多次同化的预报效果优于单次同化，同化窗口在6h时获得了更好的检验效果。但是本试验目前模拟时间较短，同化窗口的分类太少，后续将继续进行长期模拟深入研究。

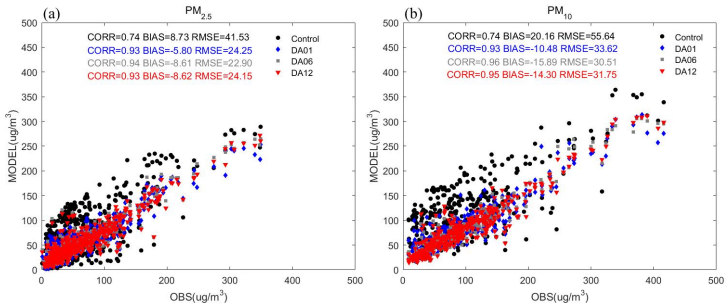

Fig. 1 The Scatter plot of the initial fields of $PM_{2.5}$ (a) and PM_{10} (b) from the control and DA experiments at the observation stations

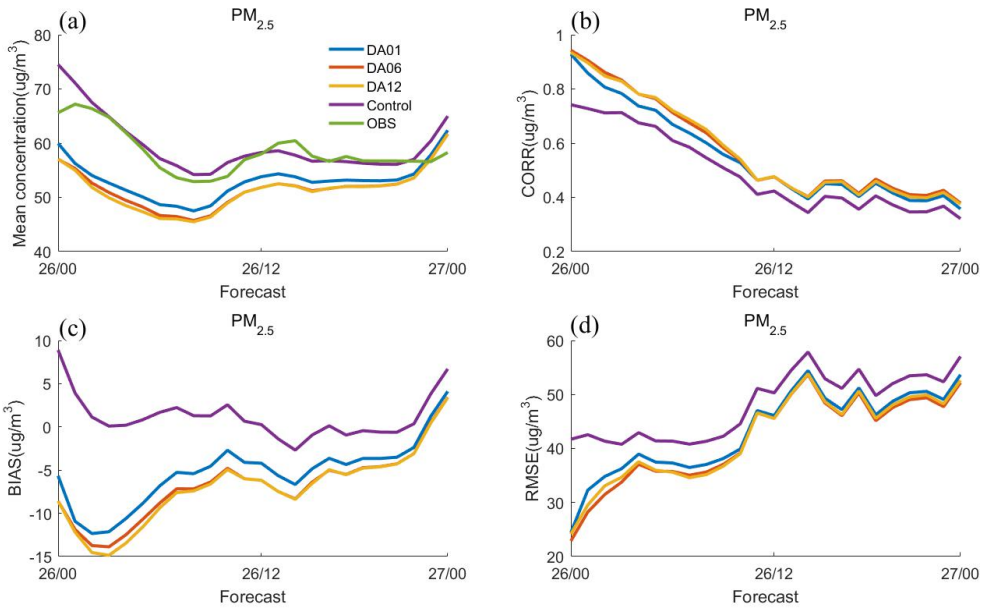

Fig. 2 The mean concentration, CORR, BIAS, and RMSE of $PM_{2.5}$ (a,b,c,d) forecast from the DA experiment and control experiment

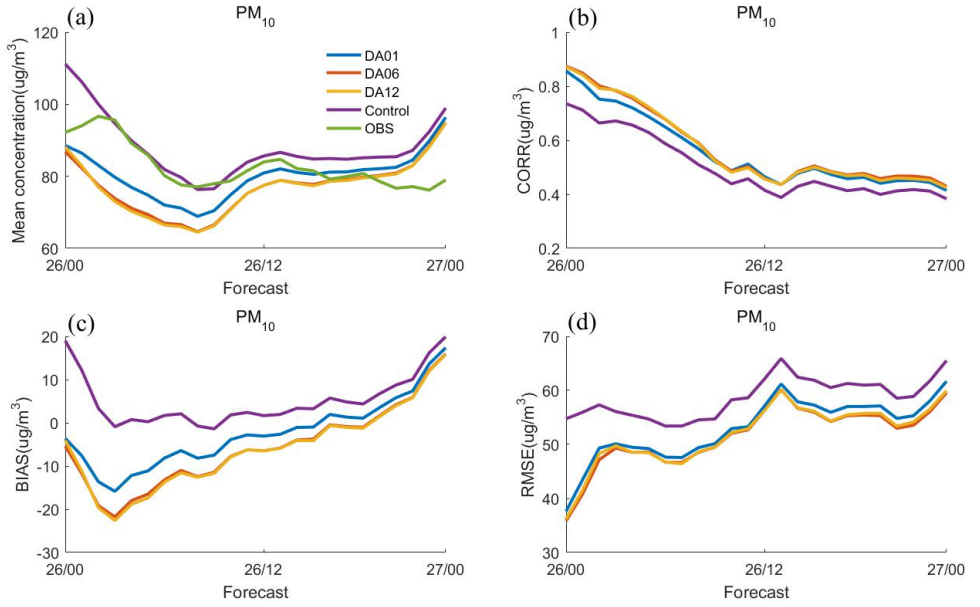

Fig. 3 Same as Fig.2 but for PM_{10}

关键词： WRF-chem；ENKF；气溶胶；同化窗口

参考文献

[1] Whitaker, J. S. and Hamill, T. M.: Ensemble data assimilation without perturbed observations, Mon. Weather Rev., 2002, 130, 1913–1924

[2] Pagowski, M. and Grell, G. A.: Experiments with the assimilation of fine aerosols using an ensemble Kalman filter, J. Geophys. Res.-Atmos.,2012, 117, D21302

[3] 刘君，黄江平，董佩明，等. 卫星资料循环同化应用对区域数值预报效果影响分析[J]. 气象, 2013, 39(2): 156-165.

[4] 冯佳宁，端义宏，徐晶，等. 雷达资料同化对 2015 年台风彩虹数值模拟改进[J]. 应用气象学报, 2017, 28(4):399-413.

[5] 闵锦忠，王修莹，沈菲菲，等. 多普勒雷达资料同化对江苏一次飑线过程的数值模拟[J]. 气象科学, 2015,35(3): 248-257.

论文编号：01–065

基于GFED数据京津冀地区火点监测与分析

杨佳璇[1]，许瑞广[1,2,*]，郝翔宇[1]，高鹏[1]，姜磊[1]，王丽涛[1,2]

[1]河北工程大学能源与环境工程学院，河北省邯郸经济技术开发区太极路19号，056038

[2]河北省大气污染成因与影响重点实验室，河北省邯郸经济技术开发区太极路19号，056038

*Email: xuruiguang@hebeu.edu.cn

摘要正文：

自然火灾的爆发会产生大量的气态污染物和颗粒物，给大气环境带来较大的影响，导致大气污染，雾霾天气出现，也会加速温室效应。本文基于全球火灾排放数据库(GFED)数据获取京津冀地区2003-2018年连续十五年火点监测数据来分析和评估京津冀地区火点的数量及其分布情况。结合区域内不同地区和年际间的火点数量差异，分析京津冀地区火点分布水平、年际时空变化规律等特征，并同步分析根据火点数量演算的颗粒物、干物质排、碳、一氧化碳、二氧化碳等排放量的年际时空变化特征其对区域大气环境的影响。研究表明：（1）从空间关系看，京津冀地区火点分布以南部为主，北部为辅。南部地区主要分布在保定市、衡水市、邢台市、石家庄市和邯郸市，其中以衡水市和保定市最为严重；北部地区则以张家口市为主要火点频发地区。（2）从地貌类型来看，京津冀地区的东北部分林地多，湿气大，火点相对较少；而西北部分草地多，视野开阔，火情相对来说容易发现，但若发生在有风的天气中，其火借风势，风助火势反而会更加难以扑灭；南部地区农业用地较为广泛，这就导致了当地秸秆焚烧现象尤为严重，又因为地区偏远、农民环保意识落后等因素的影响，导致南部地区火点密集。（3）从时间来看，每年的6月份因为已经步入夏季、天气炎热的等因素与10月份因粮食成熟、秸秆大量焚烧等因素导致这两个月基本上为当年火点数量最多的2个月；而每年的1月份和12月份由于天气寒冷、气温下降、人们外出活动少等因素导致这两个月基本上是当年火点数量最少的2个月；（4）从季节来看，每年的夏季由于气温升高等因素火点数量最多，冬季则由于人们户外活动减少、天气寒冷等因素火点数量最少；（5）随着火点数量的增多，污染物的排放量基本上也随之增多，但因火点的焚烧物的种类及数量不同，造成的污染程度也不尽相同，有时甚至出现当年火点增多但污染物的排放量相对较少的情况。及时掌握火情发生的时间和地点，以及夏秋收时节的秸秆焚烧的地点和范围，对改善京津冀空气质量和生态环境有至关重要的作用。

关键词：京津冀地区；GFED数据；火点监测；碳排放；卫星遥感

参考文献

[1] Akagi, S. K., Yokelson, R. J., Wiedinmyer, C., Alvarado, M. J., Reid, J. S., Karl, T., Crounse, J. D. and Wennberg, P. O.: Emission factors for open and domestic biomass burning for use in atmospheric models, Atmospheric Chemistry and Physics, 11(9), 4039–4072, doi:10.5194/acp-11-4039-2011, 2011.

[2] van der Werf, G. R., Randerson, J. T., Giglio, L., van Leeuwen, T. T., Chen, Y., Rogers, B. M., Mu, M., van Marle, M. J. E., Morton, D. C., Collatz, G. J., Yokelson, R. J., and Kasibhatla, P. S.: Global fire emissions estimates during 1997–2016, Earth Syst. Sci. Data, 9, 697-720, https://doi.org/10.5194/essd-9-697-2017, 2017

[3] Giglio, L., Randerson, J. T. and van der werf, G. R.: Analysis of daily, monthly, and annual burned area using the fourth-generation global fire emissions database (GFED4), Journal of Geophysical Research-Biogeosciences, 118(1), 317–328, doi:10.1002/jgrg.20042, 2013.

论文编号：01–066

COVID-19病区空气及通风系统SARS-CoV-2污染及原因探讨

徐斌[1]，沈益鸣[1]，黄英[2]，周连[1]，吴晓松[1]，丁震[1,*]

[1]江苏省疾病预防控制中心，南京，210009

[2]南京市第二医院，南京，210003

*Email: jscdc@126.com

摘要正文：

为了解某收治新冠肺炎患者的传染病医院COVID-19病区空气和通风系统表面SARS-CoV-2污染情况及原因，本研究采用应用四种空气气溶胶采样器，在该院COVID-19病区内外采集空气气溶胶样本46份，其中1份样本中SARS-CoV-2呈弱阳性。用无菌拭子采集病区空调及通风系统表面灰尘样本12份，1份样本SARS-CoV-2呈弱阳性。研究结果表明SARS-CoV-2存在于医院病区空气和部分通风系统物体表面，病毒有通过气溶胶短距离传播的风险，医护人员应加强个人防护，严格执行感染预防与控制措施，降低医院内部环境交叉感染的风险。

关键词：COVID-19；SARS-CoV-2；气溶胶；通风系统；厕所

参考文献

[1] Tran K, Cimon K, Severn M, et al. Aerosol generating procedures and risk of transmission of acute respiratory infections to health care workers: a systematic review [J]. PLoS One, 2012,7(4):e35797.

[2] Van Doremalen N, Bushmaker T, Morris DH, et al. Aerosol and surface stability of SARS-CoV-2 as compared with SARS-CoV-1 [J]. N Engl J Med 2020; 382: 1564–67

[3] 中国疾病预防控制中心新型冠状病毒肺炎应急响应机制流行病学组 新型冠状病毒肺炎流行病学特征分析 中华流行病学杂志，2020,41(2):145-151]

[4] Wang D W, Hu B, Hu C, et al. Clinical Characteristics of 138 Hospitalized Patients With 2019 Novel Coronavirus-Infected Pneumonia in Wuhan, China [J]. JAMA,2020, 323(11):1061-1069

[5] Hamner L, Dubbel P, Capron I, et al. High SARS-CoV-2 Attack Rate Following Exposure at a Choir Practice - Skagit County, Washington, March 2020 [J]. MMWR Morb Mortal Wkly Rep. 2020;69:606-10

[6] Lu J, Gu J, Li K, et al. COVID-19 Outbreak Associated with Air Conditioning in Restaurant, Guangzhou, China, 2020 [J]. Emerg Infect Dis. 2020 Jul;26(7):1628-1631

[7] Jang S, Han SH, Rhee J-Y. Cluster of Coronavirus Disease Associated with Fitness Dance Classes, South Korea [J]. Emerg Infect Dis. 2020 Aug;26(8):1917-1920

[8] Yu I T, Li Y G, Wong T W, et al. Evidence of airborne transmission of the severe acute respiratory syndrome virus[J]. N Engl J Med, 2004,350(17):1731-1739

[9] M Ki. 2015 MERS outbreak in Korea: hospital-to-hospital transmission[J]. Epidemiol Health, 2015,37:e2015033

[10] Azhar E I, Hashem A M, El-Kafrawy S A, et al. Detection of the Middle East respiratory syndrome coronavirus genome in an air sample originating from a camel barn owned by an infected patient[J]. mBio, 2014,5(4):e1414-e1450

论文编号：01–067

荆州市大气污染物周边源影响域的气候模拟研究*

顾尧[1]，白永清[2]，赵天良[1,*]，于超[3]，沈利娟[1]，胡未央[1]，周悦[2]，孔少飞[4]

[1]南京信息工程大学，气象灾害预报预警与评估协同创新中心，中国气象局气溶胶-云-降水重点实验室，PREMIC，南京，210044；

[2]中国气象局武汉暴雨研究所 暴雨监测预警湖北省重点实验室，武汉，430205；

[3]中国电力工程顾问集团西南电力设计院有限公司，成都，610051；

[4]中国地质大学(武汉)环境学院，武汉，430074

*Email:elena0617@163.com

摘要正文：

以大气污染物协同控制与精准治理的需求为导向，开展湖北省荆州市大气污染物溯源分析。基于FLEXPART-WRF模式揭示了2008-2017年荆州市$PM_{2.5}$周边源“影响域”的季节气候特征，估算了大气污染物区域传输和局地排放的相对贡献，确定出不同季节的大气污染物主要传输通道。结果表明，荆州地区$PM_{2.5}$主要“影响域”为湖北、湖南、河南和安徽省。不同季节湖北省外源传输对荆州$PM_{2.5}$“影响域”的贡献率分别为春季50.4%、夏季33.9%、秋季42.6%、冬季43.0%和年均45.1%。春季三条区域传输通道分别为北通道(河南南部-荆州)、东通道(沿长江航道-荆州)以及南通道(沿雪峰山-荆州)；夏季主要为南通道（沿雪峰山-荆州）；秋冬季分别为北通道（南阳盆地-荆州）、东北通道（沿大别山低山丘陵-荆州）以及东通道（沿长江航道-荆州）。针对荆州主要三类重污染天气型的典型个例“影响域”分析表明，高压静稳型$PM_{2.5}$污染主要来源本地排放，省内贡献率达87.8%；低压倒槽型$PM_{2.5}$污染主要来源偏南输送和本地累积，省内贡献达55.0%；冷锋输送型$PM_{2.5}$污染主要来源北路区域传输，省外贡献达77.2%。对于冬季重污染期间，建议重点围绕荆州本地与省内荆门、襄阳、孝感、天门、潜江、武汉、随州、宜昌以及省外常德、南阳、信阳等地开展协作，加强区域间大气污染联防联控。该项研究为区域大气污染精细化管控与靶向治理提供了科学依据。

关键词：气泡；粒径分布；光学法；声学法；探针法

参考文献

[1] Yan S, Zhu B, Kang H. Long-term fog variation and its impact factors over polluted regions of East China[J]. Journal of Geophysical Research: Atmospheres, 2019, 124: 1741-1754.

[2] Chan C K, Yao X. Air pollution in mega cities in China[J]. Atmospheric Environment, 2008, 42(1): 1-42.

[3] 张红艳, 魏春燕, 郑秀丽,等.浅谈大气污染的危害, 来源及防治措施[J]. 河南科技, 2013, 2013(1): 191-191.

[4] 蒋超, 龚建周, 孙家仁, 等. 2013-2016 年珠三角地区 PM2.5 分布时空演变[J]. 生态环境学报, 2018, 27(9): 1698-1705.

[5] 肖悦, 田永中, 许文轩, 等. 近 10 年中国空气质量时空分布特征[J]. 生态环境学报, 2017, 26(2): 243-252.

[6] 谭成好, 赵天良, 崔春光, 等. 近 50 年华中地区霾污染的特征[J]. 中国环境科学, 2015, 35(8): 2272-2280.

[7] 马德栗, 李兰, 鞠英芹. 湖北省霾日数气候特征及夏季典型霾过程气象因子分析[J]. 环境科学与技术, 2015, 38(11): 148-153

[8] SHEN L, WANG H, ZHAO T, et al. Characterizing regional aerosol pollution in central China based on 19 years of MODIS data: Spatiotemporal variation and aerosol type discrimination [J]. Environmental Pollution. 2020, 263.

[9] Chang X, Wang S X, Zhao B, et al. Contributions of inter-city and regional transport to PM2.5 concentrations in the Beijing-TianjinHebei region and its implications on regional joint air pollution control[J].The Science of the Total Environment, 2019,660: 1191-1200.

[10] Geoffrey D S, Kerry E K,Erik T C,et al.Wintertime PM2.5 concentrations during persistent, multi-day cold-air pools in amountain valley[J]. Atmospheric Environment,2011,46(1):17-24.

论文编号：01–068

Short-term weather patterns modulate air quality in Eastern China during 2015-2016 winter

Shuyu Zhao[1,2], Tian Feng[2,3], Xuexi Tie[1,2,*], Wenting Dai[1,2], Jiamao Zhou[1,2], Xin Long[1,2], Guohui Li[1,2], Junji Cao[1]

[1]Key Laboratory of Aerosol Chemistry and Physics, Institute of Earth Environment, Chinese Academy of Sciences, Xi'an 710061, China

[2]State Key Laboratory of Loess and Quaternary Geology, Institute of Earth Environment, Chinese Academy of Sciences, Xi'an 710061, China

[3]Xi'an AMS Center, Xi'an 710061, China

*Email: tiexx@ieecas.cn, zhaosy@ieecas.cn

Abstract:

Roles of anthropogenic emissions and weather conditions in air pollution over Eastern China have been widely discussed but still controversial. Here we focus on the impact of the intra-seasonal variability of mid-tropospheric weather circulations on air quality during 2015-2016 winter. We use ECMWF reanalysis data to calculate Westerly wind Index (WI) and meridionality in the mid-troposphere, and also calculate the intensity of Siberian High (SiH) at surface. Results suggest that lower WI, higher meridionality, and strengthened SiH in Jan 2016 cause more southward cold fresh air advection and result in the lower $PM_{2.5}$ concentrations over Eastern China. Model results show that the intra-seasonal weather variability not only counteracts increments in $PM_{2.5}$ concentrations induced by the increased emission, also reduces $PM_{2.5}$ concentrations by an extra 25 - 100 μg m^{-3} in Jan 2016. These findings suggest that understanding the intra-seasonal weather variability is the key to successfully forecasting short-term air quality.

Key words: Westerly wind index, Siberian High, air quality, WRF-Chem, Eastern China

论文编号：01–069

武汉医院及周边空气气溶胶中新冠病毒的分布特征与影响因素

曹军骥[1*]，关武祥等[2]

[1]中国科学院地球环境研究所，陕西省西安市雁塔区雁翔路97号，710061

[2]中国科学院武汉病毒研究所，湖北省武汉市武昌区小洪山中区44号，430071

*Email: cao@loess.llqg.ac.cn

摘要正文：

2020年1月新冠疫情发生以来，新冠病毒是否通过气溶胶传播引起国内外高度关注。我们在武汉的金银潭医院、协和医院及周边、方舱医院等开始大气气溶胶采样，已完成120余套气溶胶样品的采集与分析，发现气溶胶中存在新冠病毒，封闭室内空气中气溶胶样品中新冠病毒阳性检出率达到20%。此外，将核酸检测呈阳性的12个气溶胶样品和22个病人口罩浸泡样品进行了细胞培养，其中1个重症病人的口罩样品接种Vero-E6细胞盲传3代后病毒核酸检测呈阳性，而气溶胶样品在相同培养条件下均呈阴性。从病人口罩、环境空气以及健康研究人员的呼吸滤器检测到SARS-CoV-2的存在组成了一条病毒的呼出、传播和接收的链条，证明口罩可以有效阻断病毒的传播。我们在实验室模拟不同环境浓度下O_3对新冠病毒的抑制和杀灭作用，在250 μg m^{-3}的O_3低浓度下作用30分钟，样品Ct值下降2.2，表明O_3对新冠病毒有抑制作用。

关键词：新冠病毒；气溶胶；O_3

论文编号：01–070

Single particle diversity and mixing state of carbonaceous aerosols in Guangzhou, China

Chunlei Cheng[1,2], Chak K. Chan[3,*], Mei Li[1,2,*]

[1]Institute of Mass Spectrometry and Atmospheric Environment, Guangdong Provincial Engineering Research Center for on-line source apportionment system of air pollution, Jinan University, Guangzhou 510632, China

[2]Guangdong-Hongkong-Macau Joint Laboratory of Collaborative Innovation for Environmental Quality, Guangzhou 510632, China

[3]School of Energy and Environment, City University of Hong Kong, Hong Kong, China

Abstract:

Many field studies have investigated the formation mechanisms of organic aerosol (OA) based on bulk analysis, yet the source and formation process of individual organic particles may be quite different due to the diversity of chemical composition and mixing state in single particles. Here we present the observation results of chemical composition and mixing state of carbonaceous single particles at an urban site in Guangzhou. The carbonaceous particles accounted for 74.6% of the total detected single particles, and were grouped into four types including elemental carbon-aged (EC-aged), elemental and organic carbon (ECOC), organic carbon-rich (OC-rich) and secondary ions-rich (SEC) particles. The formation of EC-aged particles was closely associated with the absorption of organics onto fresh EC particles from primary sources, and the further enrichment of organics in EC-aged particles resulted in the production of ECOC particles. In the daytime OC-rich and SEC particles were mainly produced from the photochemical reactions, while in the nighttime their sharp increases were found along with the enrichment of nitrate and organic nitrogen fragments, suggesting the heterogeneous formation of nitrate and organic nitrogen in OC-rich and SEC particles. The production rates of carbonaceous particles were also investigated in an episodic event, and the EC-aged particles showed the highest production rate compared to the other carbonaceous particles both in the daytime and nighttime, suggesting a significant role of EC in the formation and aging process of carbonaceous particles. The results from this work have revealed different formation processes and production rates of carbonaceous particles due to their diversity in mixing state, providing further insights into the formation mechanisms of OA in field studies.

Keywords: single particles; mixing state; carbonaceous particles; photochemical production; elemental carbon.